Cooperative Control in Complex Multi-Agent Networks Facing Information Constraints

Hui Liu

The research described in this dissertation has been carried out at the Faculty of Mathematics and Natural Sciences, University of Groningen, The Netherlands. The author acknowledges the financial support from the university and the faculty for her Bernoulli Scholarship.

This dissertation has been completed in partial fulfillment of the requirements of the Dutch Institute of Systems and Control (DISC) for graduate study.

Published by *Ipskamp Drukkers B.V.*, Enschede, The Netherlands

RIJKSUNIVERSITEIT GRONINGEN

Cooperative Control in Complex Multi-Agent Networks Facing Information Constraints

Proefschrift

ter verkrijging van het doctoraat in de
Wiskunde en Natuurwetenschappen
aan de Rijksuniversiteit Groningen
op gezag van de
Rector Magnificus, dr. E. Sterken,
in het openbaar te verdedigen op
dinsdag 3 december 2013
om 9.00 uur

door

Hui Liu

geboren op 6 oktober 1983
te Hubei, China

Promotores:	Prof. dr. ir. M. Cao
	Prof. dr. ir. J.M.A. Scherpen
Beoordelingscommissie:	Prof. dr. C. De Persis
	Prof. dr. Y. Hong
	Prof. dr. H.L. Trentelman

ISBN (book): 978-90-367-6650-0
ISBN (e-book): 978-90-367-6651-7

Contents

Acknowledgments

This thesis could not have been written without the support of many people to whom I am very grateful. First of all, I give special thanks to my promoter and supervisor Ming Cao, who provided me with the opportunity to pursue a PhD degree with the University of Groningen. I especially thank him for the freedom, guidance, support, and patience that he gave me during my PhD research. In the occasions when I was lost and almost felt hopeless, he always had good suggestions and gave me confidence to continue. I thank my promoter Jacquelien Scherpen for providing a pleasant and inspirational working environment for our group. I am also grateful to her for carefully reading my thesis and providing me a lot of valuable comments to improve the quality of this thesis.

I deeply thank Claudio De Persis who also has provided his active guidance over the past four years. I learned a lot from him on nonsmooth analysis and output regulation theory which are important to my thesis work. I am extremely grateful for his help, encouragement, patience, and constructive suggestions when I was stuck.

I am grateful to my reading committee members Prof. Claudio De Persis, Prof. Yiguang Hong, and Prof. Harry Trentelman. They took many hours to read my thesis, provided lots of valuable comments, and spent time to attend my defense.

During my PhD research, I have also received a lot of support from other research associates besides the group in Groningen. I thank Prof. Jun-an Lu who supervised me and helped me a lot when I studied at Wuhan University, China. I deeply thank him for encouraging me to study abroad and to broaden my view of the world. I am especially grateful to Prof. Jinhu Lü at Chinese Academy of Sciences, China, for his advice on my research and life. I am very grateful to Dr. Chai Wah Wu at IBM T. J. Watson Research Center, USA, for his input and nice suggestions that contributed to Chapter 6 of this thesis. Thanks go to Prof. Wei Ren at the University of California, Riverside, USA, Prof. Guangming Xie and Prof. Zhisheng Duan both from Peking University, China, for their discussions on my research project and

sharing their valuable academic experience with me.

While writing this thesis, I have been proud to be a member of the Discrete Technology & Production Automation (DTPA) research group at the University of Groningen. The group has grown in size and seen many changes over the years. Many thanks go to my former and present colleagues during all these four years. Especially, I thank Sebastian Trip for translating the summary of this thesis into Dutch, thank Hector Garcia de Marina Peinado for our nice cooperation on formation control and his help with experiments with E-pucks, and thank James Riehl for his help with my written English. I am grateful to Ruiyue Ouyang, Chen Wang, Weiguo Xia, Shuo Zhang, Fan Zhang, Tao Liu, Liu Liu, Chunyan Zhang, and Jianlei Zhang for their help with my life here and for spare time we spent together on the weekends. I am very grateful to my favorite officemates Dustano del Puerto Flores, Desti Alkano, and Hector for our good times and the short talks we had during many tea breaks. Many thanks go to Bayu Jayawardhana, Mauricio Munos Arias, Daniel Alonzo Dirksz, Gunn Larsen, James, Sebastian, Ewoud Vos, Matin Jafarian, Shodhan Rao, Robert Huisman, Pim van den Dool, Sietse Achterop, Herman Kuis, Marko Seslija, Xiaofeng Liu, Jieqiang Wei, Pouria Ramazi, Manuel Mazo, Nima, Tjardo Scholten, Jasper Boomer, and Bao Nguyen for their friendship. I also thank the secretaries, Frederika Fokkens, Karen Meyer, and Annette Korringa, for helping me out with lots of things and the university bureaucracy.

I express my gratitude for the help of my friends who stand by me all the time, including Yanping Zhao, Juan Chen, Xiaoqun Wu, Qunjiao Zhang, Junchan Zhao, and Zhong Luo. I especially thank Yanping and Zhong for the many conversations we had in reflecting upon our lives and work.

I am especially grateful for the friendship of Anita Verhoeven. I was invited to her home many times, and enjoyed the time and love she shared with me. I especially thank the wonderful meals she served and her kindness to show me around to enjoy traditional festival celebrations in The Netherlands and accompany me to many nice places around Groningen. All of these were very impressive and enjoyable, and helped me to know more about the Dutch and their country!

Last but not least, special thanks go to my husband Zengyang for his love and support. I am grateful for his decision to pursue his PhD degree also in Groningen which makes my life here happier and more comfortable. I also thank my other family members for their understanding and support for years.

Hui Liu
Groningen
October, 2013

Chapter 1

Introduction

This thesis takes a theoretic point of view on synchronization and formation-keeping in groups of interacting autonomous agents. The focus is cooperative control of complex multi-agent networks facing information constraints, such as quantized information, uncertainties in agents' dynamics, and local knowledge on network topologies. When agents have to communicate in order to coordinate, we look into quantization effects on synchronization of multi-agent systems. We also look into controlling triangular formations of autonomous mobile agents in finite time using coarse measurements. When agents are governed by different dynamics, we study cooperation in heterogeneous linear systems with uncertain parameters aiming at synchronizing and trajectory tracking. When focusing on the effects of network topologies, we investigate adaptively allocating coupling strengths based on local topological information to guarantee global complete synchronization in complex dynamical networks.

1.1 Cooperative control

In the past two decades, cooperative control of autonomous multiple agent systems has drawn more and more attention in many disciplines, including engineering (Bullo et al. 2009, Kumar et al. 2005, Ren and Beard 2008), computer science (Bertsekas and Tsitsiklis 1997), biology (Couzin et al. 2005), social science (Hegselmann and Krause 2002), and so on. The mobile agents that are under study are usually autonomous with computation, communication and sensing capabilities. The goal of the team is to achieve prescribed collective behaviors provided that each agent uses only local information (Bai et al. 2011). Such local information may be positions, velocities, and directions obtained from sensing or communication between neighboring agents.

The key characteristic of cooperative control is local availability of information (Shamma 2007). The distributed control laws make use of local information available only to some agents. A *centralized* control system usually has a central decision-maker that has access to the information gathered by all the agents. In compari-

son, the distributed approach does not require such a powerful central decision-maker with the tradeoff that it makes the computation more complicated. However, distributed control strategies find their growing applications in complex networked systems of information constraints, such as limited sensing range, limited bandwidth in communication, and potentially large scales of systems (Ren and Beard 2008). In addition, distributed information processing may lead to interesting and appealing collective behaviors, such as intelligent self-organization, robustness to system component failures, and flexibility to environment or communication changes (Shamma 2007).

The objectives in cooperative control of distributed multi-agent coordination include agreement, flocking or swarming, formation keeping, intelligent transportation, distributed optimization, and distributed estimation and sensing, etc. We discuss below several tasks in cooperative control that are related to the work in this thesis.

Agreement. The agreement problem is also called the consensus or synchronization problem in different contexts. In such a problem, the goal of a group of interacting agents is to drive agents' variables of interest (such as the heading angles of vehicles, the positions or velocities of robots, and the phases of oscillators, etc.) to a common value. The pioneering work (Bertsekas and Tsitsiklis 1997, Jadbabaie et al. 2003, Cao et al. 2008) has studied consensus in Vicsek's model and its variations facing time-varying topologies using distributed updating laws. More recently, significant research progress has been made in terms of how to coordinate the motions of teams of autonomous mobile agents (Bullo et al. 2009, Kumar et al. 2005, Ren and Beard 2008). In parallel, synchronization in complex dynamical networks has been intensively studied in the last two decades (Wu and Chua 1995, Wu 2007, Lü, Yu, Chen and Cheng 2004, Wang and Chen 2002). The studies in this field focus on synchronization phenomena in networks of coupled dynamical systems.

Formation keeping. The objective is to stabilize the shape of a formation of mobile agents to prescribed desired one. Some approach to formation stabilization requires that each mobile agent is equipped with a compass such that all the agents share a common sense of direction (Lin et al. 2004). Some others do not make such a requirement, and only assume that each mobile agent knows its neighbors' relative distances and directions in its local coordinates (Smith et al. 2006, Cao and Morse 2007, Cao et al. 2007, Cao and Morse 2010). The differences in the local coordinates of the mobile agents significantly complicate formation stabilization, since control laws involving Euclidean norms of relative distances result in nonlinearity and multiple equilibrium manifolds of the coupled agent systems. The formation stabilization problem has been studied using rigid graph theory (Krick et al. 2009, Anderson et al. 2008).

Trajectory tracking. In the tracking problem, usually leaders' information (such as the tracking references) is only available to a small portion of agents. Distributed control laws are proposed using local interaction of agents among themselves and the references according to the given communication graphs. The tracking can be realized globally provided that the leader has directed paths to its follower agents (Ren and Beard 2008, Mei, Ren and Ma 2011).

1.2 Information constraints in the control of multi-agent networks

This thesis focuses on cooperative control in complex multi-agent networks facing information constraints. The motivation of taking into account the information constraints in cooperative multi-agent systems is discussed in this section.

Generally speaking, there are two components requiring special attention in the framework of cooperative control: agent dynamics governing the self-motions of agents and interaction terms between agents subject to communication constraints. The complexity of the agent dynamics (Wieland 2011) may range from simple linear integrator dynamics to higher order integrator dynamics to nonlinear dynamics, and to heterogenous dynamics with uncertainties. The complexity of the interaction includes local interaction topologies due to limited communication links or limited sensing ranges, static or dynamical coupling strategies, and imperfect information exchange that suffers from effects of quantization, time-delays, package dropouts, etc. This thesis addresses the information constraints rooted in both agent dynamics and interaction, in the framework of cooperative control of multi-agent networks. In particular, we consider the information constraints from the three aspects listed below.

1.2.1 Heterogeneities and uncertainties

Uncertainties are commonly used in system models, which usually arise from the unknown components and imprecise measurements that contribute to the differences between the real systems and the models. However, even small errors in the models' parameters may make the controlled systems behave quite different from expectations. Thus it is important to design controllers to stabilize the systems and make them robust against their parameter uncertainties. Furthermore, when we consider a multi-agent system with parameter uncertainties, it may be too restrictive to assume that the agents are with identical uncertainties. Hence, it is of practical importance to study cooperative control in heterogeneous multi-agent systems with

parameter uncertainties.

1.2.2 Quantization and coarse information

In real applications, agents in a cooperative control system are equipped with communication or sensing devices. Thus they might be constrained by their limited communication or sensing capabilities. Agents sometimes cannot acquire their neighbors' information through realtime sensing, but rely on digital communication to obtain the needed information in its quantized form. In some other cases, coarse sensors are applied due to cost considerations. The coarsely quantized information to be used in control is usually described by a sign function that returns finite values.

1.2.3 Local and global network topologies

Since cooperative control is based on the interaction among agents, network topologies play an important role in the coordination of agents. The eigenvalues of the Laplacian matrix of the network under study are important for the synchronization problems. They can measure the synchronization thresholds of complex dynamical networks (Wu 2007), and indicate the convergence speed of consensus-type linear models. However, the eigenvalues of the Laplacian matrix can be calculated in analytic forms only for simple network topologies such as complete graphs, star graphs, etc. It is rarely possible to obtain analytical estimation for the eigenvalues for more complicated networks. Neither is it straightforward to tell anything about the eigenvalues from information about local topologies. So it is challenging to estimate the eigenvalues determined by global properties using flexibly local topological features of the network.

1.3 Outline and contributions

This thesis is structured as follows.

Chapter 2 gives some basics on algebraic graph theory and some important definitions and theorems for nonsmooth analysis. It is the preliminary for the thesis work.

Chapter 3 studies synchronized motions of multi-agent systems with quantization in information exchange. For a team of multiple agents governed by second-order dynamics, it answers how different quantizers affect the performances of consensus-type schemes to achieve synchronized collective motion. It is shown that when different types of quantizers are used for the exchange of relative position and

velocity information between neighboring agents, different collective behaviors appear.

- Under the chosen logarithmic quantizers and with symmetric neighbor relationships, we prove that the agents' velocities and positions get synchronized asymptotically.

- Under the chosen symmetric uniform quantizers and with symmetric neighbor relationships, the agents' velocities converge to the same value asymptotically while the differences of their positions converge to a bounded set. It has also been shown that when the uniform quantizers are not symmetric, the agents' velocities may grow unbounded.

Chapter 4 studies the performances of the gradient-based formation-control strategies for teams of autonomous mobile agents when the agents' range measurements are coarse. The triangular formation stabilization problem is considered without the restriction that the agents share a common compass. Since the dynamics of the resulting closed-loop system are discontinuous, Filippov solutions to nonsmooth dynamical systems are introduced.

- Similar to the existing stability results for triangular formations with precise range measurements, we prove that under coarse range measurements, the convergence to the desired formation is almost global except for initially collinearly positioned formations.

- More importantly, we are able to make stronger statements that the convergence takes place within finite time and that the settling time can be determined by the geometric information of the initial shape of the formation.

Chapter 5 studies the synchronization and trajectory tracking problem in teams of heterogeneous agents. It is impossible to completely synchronize the full states of heterogeneous agents. However, it is possible to synchronize the partial states (outputs) of those heterogeneous agents through decentralized output regulation. We consider the problem in which N heterogeneous linear systems with parameter uncertainties aim at tracking one or more reference signals generated by given exosystems. We consider information constraints that not all the agents can get direct access to the exosystems. Decentralized robust controllers are designed to track the prescribed reference signals in the following two steps:

- Reconstruct reference signals via local interaction of the systems among themselves and the exosystems in accordance with the given communication graph.

- Decentralized robust controllers that use the reconstructed reference signals are designed applying the internal model principle. It has been shown that there exist decentralized controllers which achieve the desired regulation task in the presence of large but bounded uncertainties in the systems' models.

Chapter 6 studies how to synchronize a network of diffusively coupled oscillators via allocating coupling strengths according to the topological structure of the network. We consider undirected and directed networks, respectively, as follows:

- Using spectral graph theory and especially its graph comparison techniques, we propose new methodologies to allocate coupling strengths to guarantee global complete synchronization in complex undirected networks. The key step is that all the eigenvalues of the Laplacian matrix associated with a given network can be estimated by utilizing flexibly topological features of the network. The proposed methodologies enable the construction of different coupling-strength combinations in response to different knowledge about subnetworks.

- We further extend the allocation method to the case of directed networks. For large directed networks that can be decomposed into a set of smaller strongly connected components, we apply the methodology at the local level to improve computational efficiency.

Chapter 7 concludes the thesis and provides recommendations for possible future research.

1.4 List of publications

Conference proceedings:

- Hui Liu, Hector Garcia de Marina, Ming Cao, *"Controlling triangular formation of autonomous agents in finite-time using coarse measurements"*, Submitted to the 2014 IEEE International Conference on Robotics and Automation.

- Hui Liu, Ming Cao, Chai Wah Wu, *"Graph comparison and its application in network synchronization"*, in Proceedings of European Control Conference 2013, Zürich, Switzerland, 3809-3814, July 17th-19th, 2013.

- Hui Liu, Ming Cao, Chai Wah Wu, *"New spectral graph theoretic conditions for synchronization in directed complex networks"*, in Proceedings of the 2013 IEEE International Symposium on Circuits and Systems, Special Session: Advances in complex networks - theories & applications, Beijing, China, 2307-2310, May 19th-23rd, 2013.

- Claudio De Persis, Hui Liu, Ming Cao, *"Robust decentralized output regulation for uncertain heterogeneous systems"*, in Proceedings of the 2012 American Control Conference, Montréal, Canada, 5214-5219, June 27th-29th, 2012.

- Hui Liu, Ming Cao, Claudio De Persis, *"Quantization effects on synchronization of mobile agents with second-order dynamics"*, in Proceedings of the 18th IFAC World Congress, Milano, Italy, 2376-2381, August 28th-September 2nd, 2011.

- Claudio De Persis, Hui Liu, Ming Cao, *"Control of one-dimensional guided formations using coarsely quantized information"*, in Proceedings of the 49th IEEE Conference on Decision and Control, Atlanta, USA, 2257-2262, December 2010.

Journal papers in preparation:

- Hui Liu, Ming Cao, et al., *"Formation control of autonomous agents in finite-time using coarse measurements"*.

- Hui Liu, Ming Cao, Chai Wah Wu, *"Coupling strength allocation for synchronization in directed complex networks using spectral graph theory"*.

Journal publications:

- Hui Liu, Ming Cao, Chai Wah Wu, *"Coupling strength allocation for synchronization in complex networks using spectral graph theory"*, IEEE Transactions on Circuits and Systems-I, regular paper, to appear.

- Hui Liu, Claudio De Persis, Ming Cao, *"Robust decentralized output regulation with single or multiple reference signals for uncertain heterogeneous systems"*, International Journal of Robust and Nonlinear Control, under review.

- Hui Liu, Ming Cao, Claudio De Persis, *"Quantization effects on synchronized motion of teams of mobile agents with second-order dynamics"*, Systems and Control Letters, 61(12), 1157-1167, 2012.

- Hui Liu, Juan Chen, Jun-an Lu, and Ming Cao, *"Generalized Synchronization of Complex Dynamical Networks via Adaptive Coupling Strengths"*, Physica A, 389: 1759-1770, 2010.

Chapter 2

Preliminaries

This chapter introduces notations used in the thesis, and tools from algebraic graph theory and nonsmooth analysis.

2.1 Notations

$\mathbb{R}$	field of real numbers
$\mathbb{R}^n$	vector space of $n \times 1$ real vectors
$\mathbb{R}^{m \times n}$	space of $m \times n$ real matrices
$\mathbb{G}$	graph
$\otimes$	Kronecker product
$\lhd$	partial order
$\mathbf{0}_n$	$n \times 1$ column vector of all zeros
$\mathbf{1}_n$	$n \times 1$ column vector of all ones
$F[\cdot]$	the Filippov set-valued map
co	convex hull
$\lambda_i(A)$	the ith eigenvalue of matrix A
$\mathrm{diag}\{a_1, \ldots, a_n\}$	diagonal matrix with diagonal entries a_1 to a_n
$\mathrm{diag}\{A_1, \ldots, A_n\}$	diagonal matrix with diagonal entries A_1 to A_n
sgn	sign function
$\overline{S}$	the closure of set S
$\langle \cdot, \cdot \rangle$	the inner product
$\|\|x\|\|$	Euclidean norm of a real vector x
$\|\|x\|\|_\infty$	∞-norm of a real vector x
$\nabla f(x)$	gradient of function f at x
$\partial f(x)$	generalized gradient of function f at x
$f'(x, \nu)$	directional derivative of f at x in direction ν
$f^0(x, \nu)$	generalized directional derivative of f at x in direction ν

The Kronecker product of an n by m matrix A and a p by q matrix B is the np by

mq matrix $A \otimes B$ defined by

$$A \otimes B = \begin{pmatrix} a_{11} B & a_{12} B & \dots & a_{1m} B \\ a_{21} B & a_{22} B & \dots & a_{2m} B \\ \vdots & \vdots & \ddots & \vdots \\ a_{n1} B & a_{n2} B & \dots & a_{nm} B \end{pmatrix}.$$

For a matrix $A \in \mathbb{R}^{n \times n}$, we say $A > 0$ (resp. $A \geq 0$) if $x^T Ax$ is positive (resp. non-negative) for all nonzero $x \in \mathbb{R}^n$.

2.2 Algebraic graph theory

This section introduces some useful definitions and results from algebraic graph theory. In particular, it focuses on results about the Laplacian matrices and connectivity of graphs which are useful for studying synchronization in multi-agent systems and networks of coupled oscillators. The notations and terminologies are adopted from (Godsil and Royle 2001, Wu 2007).

Graphs

Graphs are frequently used to model connection relationships between any two objects in some domain. In this thesis, we use graphs to describe the interaction relationships among the agents in a multi-agent network. A graph $\mathbb{G} = (\mathcal{V}, \mathcal{E})$ consists of a set of vertices $\mathcal{V}$ and a set of edges $\mathcal{E}$. We take $\mathcal{V} = \{1, \ldots, N\}$, where N is the number of vertices of the graph. The edge set $\mathcal{E} \subseteq \mathcal{V} \times \mathcal{V}$, i.e., $\mathcal{E} \subseteq \{(i, j) : i, j \in \mathcal{V}\}$. If the two vertices of an edge are the same, we call this edge a self-loop. A *simple* graph is a graph with no self-loops and no multiple edges between the same pair of distinct vertices. We focus on simple graphs in this thesis.

A *directed* graph is a graph where each edge in $\mathcal{E}$ is denoted by an ordered pair of vertices. Let i and j be two vertices, then (i, j) denotes an edge which starts at vertex i and ends at vertex j. A *directed path* from i to j is a sequence of edges $(v_0, v_1), (v_1, v_2), \ldots, (v_{k-1}, v_k)$ in $\mathcal{E}$ such that $v_0 = i$ and $v_k = j$. A path with no repeated vertices is called a *simple path*. We only consider simple paths in the thesis.

An *undirected* graph is a graph where the edges in $\mathcal{E}$ are denoted by unordered pairs of vertices, i.e., $(i, j) \in \mathcal{E}$ if and only if $(j, i) \in \mathcal{E}$. An undirected graph can be considered as a directed graph by associating each undirected edge between vertices i and j as two directed edges between i and j with opposite orientations. Thus undirected graphs can be considered as special directed graphs.

Connected graphs

An undirected graph is *connected* if there is a path between any pair of vertices. A directed graph is *strongly connected* if for any pair of vertices (i, j) where $j \neq i$, there is a directed path from i to j. A *directed tree* on n vertices is a directed graph with $n - 1$ edges which has a root vertex such that there is a directed path from the root vertex to every other vertex. A *spanning directed tree* of graph $\mathbb{G}$ is a subgraph which is a directed tree with the same vertex set and a selection of edges of $\mathbb{G}$.

Adjacency and Laplacian matrices

Given a graph $\mathbb{G}$, the associated *adjacency matrix* $A = [a_{ij}]_{N\times N}$ is defined as follows: the entry $a_{ij} = 1$ if $(j, i) \in \mathcal{E}$ and 0 otherwise. Since we only focus on graphs with no self-loops in this thesis, we can set the entries $a_{ii} = 0$ for $i = 1, 2, \ldots, N$. The *in-degree* of a vertex in a directed graph is the number of edges ending at the vertex, and the *out-degree* of a vertex is defined to be the number of edges starting at the vertex. Let $d_i^{(in)}$ denote the in-degree of vertex i, and $d_i^{(out)}$ the out-degree. Then one has $d_i^{(in)} = \sum_{j\neq i} a_{ij}$, $d_i^{(out)} = \sum_{j\neq i} a_{ji}$. We say vertex i is balanced if its in-degree equals its out-degree. If all the vertices in a directed graph $\mathbb{G}$ are balanced, then $\mathbb{G}$ is said to be *balanced*. If graph $\mathbb{G}$ is undirected, one has $a_{ij} = a_{ji}$ for all $1 \leqslant i, j \leqslant N$.

The in-degree matrix $\Delta \in \mathbb{R}^{N\times N}$ is a diagonal matrix with the in-degrees $d_i^{(in)}$ being its diagonal entries. The Laplacian matrix of graph $\mathbb{G}$ is the matrix $L = \Delta - A$.

Example: The graph shown in Fig. 2.1(a) is undirected. The graph shown in Fig. 2.1(b) is directed and strongly connected. The adjacency matrices of the two graphs are, respectively,

$$\begin{pmatrix} 0 & 1 & 0 & 1 \\ 1 & 0 & 1 & 0 \\ 0 & 1 & 0 & 1 \\ 1 & 0 & 1 & 0 \end{pmatrix} \quad \text{and} \quad \begin{pmatrix} 0 & 0 & 0 & 1 \\ 1 & 0 & 0 & 0 \\ 0 & 1 & 0 & 0 \\ 0 & 0 & 1 & 0 \end{pmatrix}.$$

The Laplacian matrices of the two graphs are, respectively,

$$\begin{pmatrix} 2 & -1 & 0 & -1 \\ -1 & 2 & -1 & 0 \\ 0 & -1 & 2 & -1 \\ -1 & 0 & -1 & 2 \end{pmatrix} \quad \text{and} \quad \begin{pmatrix} 1 & 0 & 0 & -1 \\ -1 & 1 & 0 & 0 \\ 0 & -1 & 1 & 0 \\ 0 & 0 & -1 & 1 \end{pmatrix}.$$

Incidence matrix

For an undirected graph $\mathbb{G}$, we can assign an orientation to each edge in $\mathbb{G}$. We use $\mathbb{G}^\sigma$ to denote the oriented graph determined by a specified orientation σ. The incidence matrix $D = D(\mathbb{G}^\sigma) = [d_{ij}]$ of an oriented graph $\mathbb{G}^\sigma$ is the $\{0, 1, -1\}$ matrix with rows and columns indexed by the vertices and edges of $\mathbb{G}$, respectively, such that $d_{ij} = 1$ if vertex i is the head of edge j, $d_{ij} = -1$ if vertex i is the tail of edge j, and 0 otherwise. If graph $\mathbb{G}$ has N vertices and m edges, the incidence matrix of $\mathbb{G}^\sigma$ has order $N \times m$. We have $D\,D^T = L$ (Godsil and Royle 2001, Section 8.3).

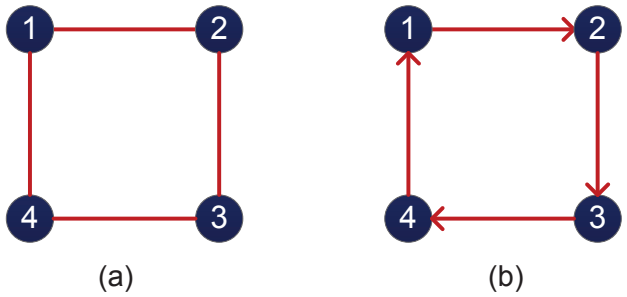

Figure 2.1: *Two simple graphs: (a) An undirected graph, (b) A directed graph.*

Several typical undirected graphs

Now we introduce several typical undirected graphs. An *undirected complete graph* is a graph in which every pair of distinct vertices are connected by a unique undirected edge. The complete graph on N vertices is denoted by $\mathbb{K}_N$. $\mathbb{K}_N$ has $N(N-1)/2$ edges, and each vertex has the degree $N-1$. The *undirected star graph* $\mathbb{S}_N$ consists of a single central vertex with degree $N-1$ and $N-1$ other vertices with degree 1. The *undirected path graph* $\mathbb{P}_N$ is the graph with the vertex set $\{1,\dots,N\}$ where i is adjacent to $i+1$ for $1 \leqslant i \leqslant N-1$. The *undirected ring graph* $\mathbb{R}_N$ is the connected graph with the vertex set $\{1,\dots,N\}$ where every vertex has exactly two neighbors. Fig. 2.2 shows these graphs when $N=6$.

Weighted graphs

If we consider weights on the edges of graph $\mathbb{G}$, the weighted graph can be described by $\mathbb{G}=(\mathcal{V},\mathcal{E},\varepsilon)$ with the vertex set $\mathcal{V}$, the edge set $\mathcal{E}$, and the weight function $\varepsilon:\mathcal{E}\to\mathbb{R}$. Let ε_{ij} be the weight on edge (j,i), then the adjacency matrix for the weighted graph is $A^{(w)}=[a_{ij}^{(w)}]_{N\times N}$, where the entry $a_{ij}^{(w)}=\varepsilon_{ij}$ if $(j,i)\in\mathcal{E}$ and 0 otherwise. The weighted degree matrix $D^{(w)}\in\mathbb{R}^{N\times N}$ is defined to be the diagonal matrix with entries $\sum_{j\neq i}\varepsilon_{ij}$ for $i=1,\dots,N$. The Laplacian matrix of the weighted graph $\mathbb{G}$ is the matrix $L^{(w)}=D^{(w)}-A^{(w)}$.

2.3 Nonsmooth analysis

In this section, we introduce some important results on nonsmooth systems. The notation and terminology is mainly taken from (Clarke 1983, Cortés 2008a).

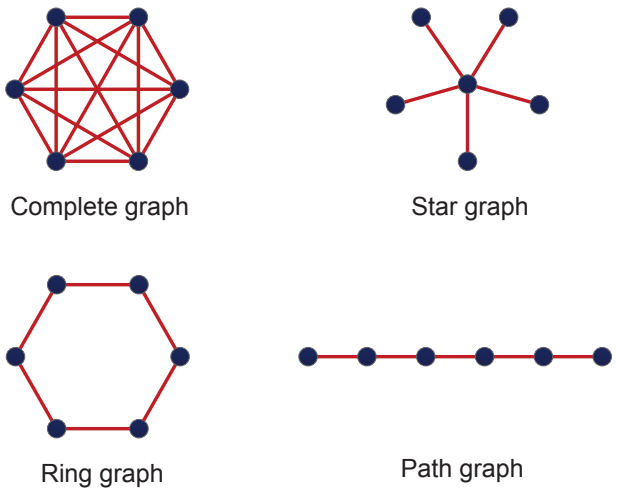

Figure 2.2: *Some typical undirected graphs with $N = 6$ vertices.*

For a differential equation

$$\dot{x}(t) = X(x(t)) \tag{2.1}$$

where $X : \mathbb{R}^d \to \mathbb{R}^d$ is measurable but discontinuous, the existence of a continuously differentiable solution is not guaranteed. In this paper, we adopt the Filippov solution (Cortés 2008a).

Definition 2.1 *Let $\mathfrak{B}(\mathbb{R}^d)$ denote the collection of all subsets of $\mathbb{R}^d$. The Filippov set-valued map $F[X] : \mathbb{R}^d \to \mathfrak{B}(\mathbb{R}^d)$ is defined by*

$$F[X](x) \triangleq \bigcap_{\delta>0} \bigcap_{\mu(\mathcal{S})=0} \overline{\text{co}}\{X(\mathbf{B}(x,\delta)\backslash\mathcal{S})\}, \qquad x \in \mathbb{R}^d$$

where $\mathcal{S}$ is the set of x at which $X(x)$ is discontinuous, $\mathbf{B}(x,\delta)$ is the open ball of radius δ centered at x, $\overline{\text{co}}$ denotes the convex closure, and $\bigcap_{\mu(\mathcal{S})=0}$ denotes the intersection over all sets $\mathcal{S}$ of Lebesgue measure zero.

Filippov solutions are then defined to be those absolutely continuous curves, which satisfy the differential inclusion of the form

$$\dot{x}(t) \in F[X](x). \tag{2.2}$$

The Filippov set-valued map obeys the following rule.

Lemma 2.1 (Cortés 2008a) *If $X_1, X_2 : \mathbb{R}^d \to \mathbb{R}^m$ are locally bounded at $x_0 \in \mathbb{R}^d$, then*
(a) sum rule: $F[X_1 + X_2](x_0) \subseteq F[X_1](x_0) + F[X_2](x_0)$,
(b) product rule: $F[(X_1, X_2)^T](x_0) \subseteq F[X_1](x_0) \times F[X_2](x_0)$,
for which the equality signs hold when either X_1 or X_2 is continuous at x_0.

A sufficient condition for the existence of the Filippov solution is given as follows.

Lemma 2.2 (Cortés 2008a) *Assume $X : \mathbb{R}^d \to \mathbb{R}^d$ is measurable and locally essentially bounded, i.e. bounded in any bounded neighborhood of every point of definition excluding the sets of measure zero. Then for all $x_0 \in \mathbb{R}^d$, there exists a Filippov solution to (2.1) with the initial condition $x(0) = x_0$.*

We also use the following notions of the generalized directional derivative and generalized gradient.

Definition 2.2 (Clarke 1983) *Assume $f : \mathbb{R}^d \to \mathbb{R}$ is locally Lipschitz near any given point $x \in \mathbb{R}^d$. Then the generalized directional derivative of f at x in the direction $\nu \in \mathbb{R}^d$ is defined by*

$$f^0(x;\nu) \triangleq \limsup_{\substack{y \to x, \\ t \downarrow 0}} \frac{f(y + t\nu) - f(y)}{t},$$

where y is a vector in $\mathbb{R}^d$ and t is a positive number.

Definition 2.3 (Clarke 1983) *If $f : \mathbb{R}^d \to \mathbb{R}$ is locally Lipschitz, its generalized gradient is defined by*

$$\partial f(x) \triangleq \mathrm{co}\{\lim_{i \to \infty} \nabla f(x_i) : x_i \to x,\ f^{'}(x_i) \text{ exists}\},$$

where co *denotes the convex hull, and $f^{'}(x_i)$ is the derivative of f at $x_i \in \mathbb{R}^d$.*

The relationship between the generalized directional derivative and generalized gradient can be summarized as follows.

Lemma 2.3 (Clarke 1983) *Assume $f : \mathbb{R}^d \to \mathbb{R}$ is locally Lipchitz near x. Then for every direction $\nu \in \mathbb{R}^d$, we have*

$$f^0(x;\nu) = \max\{\langle \zeta, \nu \rangle : \zeta \in \partial f(x)\},$$

where $\langle \cdot, \cdot \rangle$ denotes the inner product.

The definition of regular functions is based on the notion of right directional derivative $f^{'}(x;\nu) = \lim_{t \downarrow 0} \frac{1}{t}(f(x + t\nu) - f(x))$.

Definition 2.4 (Clarke 1983) *A function $f : \mathbb{R}^d \to \mathbb{R}$ is said to be regular at $x \in \mathbb{R}^d$ if for all $\nu \in \mathbb{R}^d$, the right directional derivative $f^{'}(x;\nu)$ exists and $f^{'}(x;\nu) = f^0(x;\nu)$.*
We say that function $f : \mathbb{R}^d \to \mathbb{R}$ is a regular function, if it is regular everywhere in its domain.

There are sufficient conditions for a function to be regular.

Lemma 2.4 (Clarke 1983) *(i) If $f : \mathbb{R}^d \to \mathbb{R}$ is continuously differentiable at x, then f is regular at x.*
(ii) If $\{f_i : \mathbb{R}^d \to \mathbb{R}\}$, $i = 1, \ldots, m$, is a finite family of regular functions, each of which is regular at x, then for any nonnegative scalars λ_i, $\sum_{i=1}^m \lambda_i f_i(x)$ is regular at x.

The following chain rule is useful for the calculations of derivatives of Lyapunov functions.

Lemma 2.5 (Shevitz and Paden 1994) *Let $x(\cdot)$ be a Filippov solution to $\dot{x} = X(x)$ on an interval containing t, and $V : \mathbb{R}^d \to \mathbb{R}$ be a Lipschitz and regular function. Then $V(x(t))$ is absolutely continuous and $\frac{d}{dt} V(x(t))$ exists almost everywhere*

$$\frac{d}{dt} V(x(t)) \in \dot{\tilde{V}}(x), \qquad \text{for a.e. } t \geqslant 0\,,$$

where

$$\dot{\tilde{V}}(x) = \bigcap_{\zeta \in \partial V(x(t))} \zeta^T F[X](x)\,.$$

Another definition of the set-valued derivative of Lyapunov function was introduced in (Bacciotti and Ceragioli 1999). The set-valued derivative of Lyapunov function V with respect to the differential inclusion $\dot{x} \in F[X](x)$ is defined by

$$\dot{\overline{V}}(x) = \{a \in \mathbb{R} : \exists \nu \in F[X](x) \text{ such that } p \cdot \nu = a\,, \forall p \in \partial V(x)\}. \tag{2.3}$$

In the case V is differentiable at x, one has $\dot{\overline{V}}(x) = \{\nabla V(x) \cdot \nu : \nu \in F[X](x)\}$. Analogous to Lemma 2.5, the following lemma characterizes the derivative of V:

Lemma 2.6 (Bacciotti and Ceragioli 1999) *Let $x(\cdot)$ be a solution of the differential inclusion (2.2) and let $V : \mathbb{R}^d \to \mathbb{R}$ be a locally Lipschitz continuous and regular function. Then $\frac{d}{dt} V(x(t))$ exists almost everywhere and $\frac{d}{dt} V(x(t)) \in \dot{\overline{V}}(x)$ for a.e. t.*

In the following we introduce the invariant principle that is applicable to discontinuous differential equations.

Lemma 2.7 (Cortés 2008a, Theorem 2) *Let $V : \mathbb{R}^d \to \mathbb{R}$ be a locally Lipschitz continuous and regular function. Let $S \subset \mathbb{R}^d$ be compact and strongly invariant for the differential inclusion (2.2), and assume that $\max \dot{\overline{V}}(x) \leqslant 0$ for each $x \in S$. Then, all solutions $x : [0, \infty) \to \mathbb{R}^d$ of (2.2) starting at S converge to the largest weakly invariant set M contained in*

$$\overline{S \cap \{x \in \mathbb{R}^d : 0 \in \dot{\overline{V}}(x)\}}.$$

Moveover, if the set M consists of a finite number of points, then the limit of each solution starting in S exists and is an element of M.

Chapter 3

Synchronization for Coupled Agents with Quantized Information

In this chapter, we study how different quantizers affect the performances of consensus-type schemes to achieve synchronized collective motion, for a team of mobile agents governed by second-order dynamics. It is shown that when different types of quantizers are used for the exchange of relative position and velocity information between neighboring agents, different collective behaviors appear. Under the chosen logarithmic quantizers and with symmetric neighbor relationships, we prove that the agents' velocities and positions get synchronized asymptotically. We show that under the chosen symmetric uniform quantizers and with symmetric neighbor relationships, the agents' velocities converge to the same value while the differences of their positions converge to a bounded set. We also show that when the uniform quantizers are not symmetric, the agents' velocities may grow unbounded. Through simulations we present richer undesirable system behaviors when different logarithmic and uniform quantizers are used. Such different quantization effects underscore the necessity for a careful selection of quantization strategies, especially for multi-agent systems with higher-order agent dynamics. The results presented in this chapter are published in (Liu et al. 2011, Liu et al. 2012).

3.1 Introduction

Recently significant research efforts have been made to study how to coordinate the motion of teams of mobile autonomous agents (Kumar et al. 2005). One popular approach is to use consensus-type algorithms to guide a team of agents to coincide with one another moving with the same velocity under the conditions that the relative position and/or relative velocity information is shared locally among agents and no agent is isolated from the rest of the team (Olfati-Saber et al. 2007, Ren and Beard 2008, Yu et al. 2010a). Since agents might be constrained by their limited sensing capabilities, they sometimes cannot acquire their neighboring agents' information through realtime sensing, but rely on digital communication to obtain the needed information in its quantized form. This has motivated a growing number

of research activities studying how to design effective coordination control strategies using quantized information (Kashyap et al. 2007, Nedic et al. 2009, Frasca et al. 2009, Carli et al. 2010, De Persis et al. 2010, Ceragioli et al. 2011, Liu et al. 2011, You and Xie 2011, Chen, Lewis and Xie 2011, De Persis and Jayawardhana 2012).

Agents governed by second-order dynamics as double-integrators are widely used for modeling mobile autonomous agents especially when the research focus is on the collective team dynamics instead of detailed individual agent dynamics (Ren 2008). Multi-agent systems with second-order agent dynamics can have dramatically different collective behavior than those with first-order agent dynamics even when agents are coupled together in similar manners (Yu et al. 2010b). However, while various quantized consensus schemes have been proposed for multi-agent systems with first-order agent dynamics (Frasca et al. 2009, Ceragioli et al. 2011), less is known about the quantization effects on the consensus-type algorithms for motion coordination in systems with higher-order agent dynamics. Recently some interesting sufficient and/or necessary conditions have been constructed for synchronizing coupled double integrators without quantization (Ren 2008, Yu et al. 2010b). In a more recent paper (De Persis and Jayawardhana 2012), higher-order passive nonlinear systems under quantized measurements are considered, but the coordination task considered there is different and its results cannot be applied directly to the problem considered here.

In this chapter, we utilize the control laws that have been used in (Ren 2008), but study their performances when quantized information is used. Then a new set of tools including new forms of Lyapunov functions are developed accordingly to deal with the challenges in analysis for the discontinuity on the right-hand side of the system equations as a result of quantization. We find in this chapter that when logarithmic quantizers are used in the proposed coordination scheme and the neighbor relationships are symmetric, the agents' velocities and positions get synchronized asymptotically. When the chosen symmetric uniform quantizers are used instead of the logarithmic quantizers, the agents' velocities converge to the same value asymptotically, while the differences of the agents' positions converge to a bounded set as time goes to infinity. In comparison, when the chosen uniform quantizers are asymmetric, the agents' velocities might keep increasing and become unbounded. We also indicate through simulations that richer undesirable system behavior may appear under asymmetric neighbor relationships, e.g. the agents' positions may never become the same. Some of such undesirable behaviors are inherently associated with the higher-order agent dynamics. Hence, it is emphasized that when choosing quantization schemes for agents with higher-order dynamics, in order to achieve desired motion coordination, appropriate quantizers have to be picked carefully.

The rest of this chapter is organized as follows. In Section 3.2, the quantized

control for motion synchronization is discussed for systems of agents governed by second-order dynamics and the uniform and logarithmic quantizers are defined. The analysis for systems with the chosen logarithmic and uniform quantizers are discussed in Sections 3.3 and 3.4 respectively. We provide some additional simulation results in Section 3.5 for the case when the neighbor relationships are not symmetric.

3.2 Motion coordination for agents with second-order dynamics

We consider a team of $N > 0$ autonomous agents, each of which is governed by the following second-order dynamics

$$\begin{cases} \dot{r}_i = v_i \\ \dot{v}_i = u_i \qquad i = 1, \ldots, N, \end{cases} \tag{3.1}$$

where $r_i, v_i \in \mathbb{R}^n$ denote the position and the velocity of agent i respectively and u_i is agent i's control input. The goal for designing distributed control laws u_i is to synchronize the motions of the N agents in such a way that the velocities and positions of all the agents become the same asymptotically and thus they move together as a single entity. Such a motion coordination problem has been studied before (Ren 2008, Yu et al. 2010b), and the solution that has been proposed is to use a consensus-type scheme

$$u_i = -\sum_{j \in \mathcal{N}_1(i)} (r_i - r_j) - \sum_{j \in \mathcal{N}_2(i)} (v_i - v_j)\,, \tag{3.2}$$

where $\mathcal{N}_1(i)$ (resp. $\mathcal{N}_2(i)$) denotes the set of agent i's neighbors in the graph $\mathbb{G}_1$ (resp. $\mathbb{G}_2$) that describes the neighbor relationships in terms of whether the position (resp. velocity) information can be exchanged between a pair of agents. We use a_{ij} and b_{ij}, $1 \leqslant i, j \leqslant N$, to denote the elements of the adjacency matrices of $\mathbb{G}_1$ and $\mathbb{G}_2$ respectively; in other words, a_{ij} (resp. b_{ij}) equals one if j is a neighbor of i in $\mathbb{G}_1$ (resp. $\mathbb{G}_2$) and zero otherwise. The entries $a_{ii} = 0, b_{ii} = 0$ for all $i = 1, \ldots, N$.

In the rest of the chapter unless we clarify otherwise, we assume that $\mathbb{G}_1$ and $\mathbb{G}_2$ are undirected and fixed. Note that in the context of distributed control, each agent only has access to the *relative* position or velocity information, i.e. no global coordinate system is available. It has been shown in (Ren 2008) that when $\mathbb{G}_1$ and $\mathbb{G}_2$ are connected, the control law (3.2) can achieve the control goal effectively.

In this chapter, we consider the scenario where for each agent, the relative position and velocity information of its neighbors is acquired through digital communi-

cation. Hence, if we continue to use the consensus-type coordination strategy (3.2), we have the control signals in the following form

$$u_i = -\sum_{j\in\mathcal{N}_1(i)} \mathbf{q}(r_i - r_j) - \sum_{j\in\mathcal{N}_2(i)} \mathbf{q}(v_i - v_j)\,, \tag{3.3}$$

where $\mathbf{q} : \mathbb{R}^n \to \mathbb{R}^n$ denotes the vector quantizer of choice. Here we have assumed that all the agents have been installed with identical quantizers.

Remark 3.1 *In the literature, when quantizers are applied to agents with* first-order *dynamics, different information has been quantized. For example, in (Nedic et al. 2009) the quantization takes place after the relative positions have been summed up, namely*

$$u_i = -\mathbf{q}\left(\sum_{j\in\mathcal{N}_1(i)} (r_i - r_j)\right);$$

in (Ceragioli et al. 2011) the absolute *position information in some global coordinate system is quantized, namely*

$$u_i = -\sum_{j\in\mathcal{N}_1(i)} \Big(\mathbf{q}(r_i) - \mathbf{q}(r_j)\Big).$$

In (Dimarogonas and Johansson 2010), the relative position information is quantized in a similar way as what we have done in (3.3) for first-order agent dynamics. Thus the coordination task is different.

In this chapter, we consider the following three types of quantizers. The *symmetric uniform quantizer* that we consider is a map $q_u : \mathbb{R} \to \mathbb{R}$ such that

$$q_u(x) = \delta_u \left(\left\lfloor \frac{x}{\delta_u} \right\rfloor + \frac{1}{2}\right), \tag{3.4}$$

where δ_u is a positive number and $\lfloor a \rfloor$, $a \in \mathbb{R}$, denotes the greatest integer that is less than or equal to a. The uniform quantizer (3.4) is similar to the one used in (Carli et al. 2010, Dimarogonas and Johansson 2010), with the difference that the definition at 0 is different.
The *asymmetric uniform quantizer* that we consider (Johansson et al. 2005) is a map $q_u^* : \mathbb{R} \to \mathbb{R}$ such that

$$q_u^*(x) = \delta_u \left\lfloor \frac{x}{\delta_u} \right\rfloor. \tag{3.5}$$

The *logarithmic quantizer* that we use (Carli et al. 2010) is an odd map $q_l : \mathbb{R} \to \mathbb{R}$ such that

$$q_l(x) = \begin{cases} e^{q_u(\ln x)} & \text{when } x > 0; \\ 0 & \text{when } x = 0; \\ -e^{q_u(\ln(-x))} & \text{when } x < 0. \end{cases} \tag{3.6}$$

Note that for the uniform quantizers, the quantization error is always bounded by δ_u, namely $|q_u(x) - x| \leqslant \delta_u$ or $|q_u^*(x) - x| \leqslant \delta_u$ for all $x \in \mathbb{R}$. Note also that for the logarithmic quantizer, it holds that

$$x\, q_l(x) \geqslant 0, \text{ for all } x \in \mathbb{R}, \tag{3.7}$$

and the equality sign holds if and only if $x = 0$; the quantization error for the logarithmic quantizer is bounded by $|q_l(x) - x| \leqslant \delta_l\, |x|$, where the parameter δ_l is determined by $\delta_l = 1 - e^{-\delta_u}$.

The above definitions of scalar-valued uniform and logarithmic quantizers can be easily generalized to their counterparts of vector-valued quantizers. Take the logarithmic quantizer as an example. For any $x = \begin{bmatrix} x_1 & \dots & x_n \end{bmatrix}^T \in \mathbb{R}^n$, we define the vector logarithmic quantizer $\mathbf{q}_l(\cdot) : \mathbb{R}^n \to \mathbb{R}^n$ to be $\mathbf{q}_l(x) \triangleq \begin{bmatrix} q_l(x_1) & \dots & q_l(x_n) \end{bmatrix}^T$. One can easily check that $\langle x, \mathbf{q}_l(x) \rangle \geqslant 0$ and the equality sign holds if and only if $x = 0$.

The main purpose of the chapter is to show different quantization effects on the performances of the consensus-type coordination algorithms (3.3). Because of the discontinuity of the quantized signals, we will make use of nonsmooth analysis of differential equations to proceed.

3.3 Main results

Because of the discontinuity of the quantized signals, we consider Filippov solutions (r, v) to the equations (3.1) and (3.3), where $r \triangleq \begin{bmatrix} r_1^T & \dots & r_N^T \end{bmatrix}^T$ and $v \triangleq \begin{bmatrix} v_1^T & \dots & v_N^T \end{bmatrix}^T$. In other words, we consider absolutely continuous functions (r, v) such that

$$\dot{v}_i \in F[u_i] \subseteq -\sum_{j \in \mathcal{N}_1(i)} F[\mathbf{q}(r_i - r_j)] - \sum_{j \in \mathcal{N}_2(i)} F[\mathbf{q}(v_i - v_j)], \tag{3.8}$$

where we have used Lemma 2.1 to deduce the relationship between the sets.

Now we take another look at the set-valued map $F[\cdot]$ in equation (3.8). For all $x_0 \in \mathbb{R}^n$, let $\mathbf{q}(x_0^-) \triangleq \lim_{x \uparrow x_0} \mathbf{q}(x)$ and $\mathbf{q}(x_0^+) \triangleq \lim_{x \downarrow x_0} \mathbf{q}(x)$. We use the notation

$$\tilde{r}_{ij} \triangleq r_i - r_j$$

for $i \neq j$. If $\mathbf{q}(\cdot)$ is continuous at $\tilde{r}_{ij}$, then it follows that $F[\mathbf{q}(\tilde{r}_{ij})] = \mathbf{q}(\tilde{r}_{ij})$. If on the other hand $\mathbf{q}(\cdot)$ is discontinuous at $\tilde{r}_{ij}$, then $F[\mathbf{q}(\tilde{r}_{ij})] = [\mathbf{q}(\tilde{r}_{ij}^-), \mathbf{q}(\tilde{r}_{ij}^+)]$ where for $x = \begin{bmatrix} x_1 & \dots & x_n \end{bmatrix}^T \in \mathbb{R}^n$, $[\mathbf{q}(x^-), \mathbf{q}(x^+)]$ is defined to be $[q(x_1^-), q(x_1^+)] \times [q(x_2^-), q(x_2^+)] \times \cdots \times [q(x_n^-), q(x_n^+)]$.

The main result of the chapter is to show different quantization effects on the performances of the consensus-type coordination algorithms (3.3). We first study logarithmic quantizers.

3.3.1 Synchronized motion using logarithmic quantizers

When the logarithmic quantizer is used, one can show that the distributed control law that we are using can still cause the motions of all the agents to get synchronized.

Theorem 3.1 *Assume the graphs $\mathbb{G}_1$ and $\mathbb{G}_2$ are connected and the logarithmic quantizers $\mathbf{q}_l(\cdot)$ are used in the control (3.3). Then, any Filippov solution (r, v) to the system (3.1) and (3.3), is such that the positions of all the agents converge to $\frac{1}{N}\sum_{j=1}^N r_j(0) + \frac{t}{N}\sum_{j=1}^N v_j(0)$ as $t \to \infty$, and the velocities of all the agents converge to $\frac{1}{N}\sum_{j=1}^N v_j(0)$ as $t \to \infty$.*

To prove this theorem, we first need to prove a few facts. In order to proceed, note that $\mathbf{q}_l(\cdot)$ is monotonic, so it is integrable. So we can define the potential function $W(\cdot) : \mathbb{R}^n \to \mathbb{R}$ for $\tilde{r}_{ij}$

$$W(\tilde{r}_{ij}) = \int_0^{\tilde{r}_{ij}} \mathbf{q}_l(x)dx\,, \tag{3.9}$$

where $W(\tilde{r}_{ij})$ is the line integral from 0 to $\tilde{r}_{ij}$. It is easy to check that $W(\tilde{r}_{ij}) \geqslant 0$ and the equality sign holds if and only if $\tilde{r}_{ij} = 0$. Let $\mathcal{S}$ denote the set of all discontinuous points of $\mathbf{q}_l$, and then for any $z \in \mathcal{S}$, $\lim_{\tilde{r}_{ij}\uparrow z} W'(\tilde{r}_{ij}) \neq \lim_{\tilde{r}_{ij}\downarrow z} W'(\tilde{r}_{ij})$. So $W(\tilde{r}_{ij})$ is not differentiable with respect to $\tilde{r}_{ij}$ at any point in $\mathcal{S}$. Using the generalized gradient defined in Definition 2.3, one has

$$\frac{\partial W(\tilde{r}_{ij})}{\partial \tilde{r}_{ij}} = \begin{cases} \mathbf{q}_l(\tilde{r}_{ij}) & \tilde{r}_{ij} \in R^n \backslash \mathcal{S}, \\ \{Q^* : Q^* \in [\mathbf{q}_l(\tilde{r}_{ij}^-), \mathbf{q}_l(\tilde{r}_{ij}^+)]\} & \tilde{r}_{ij} \in \mathcal{S}. \end{cases} \tag{3.10}$$

We define the kinetic energy function for the velocity v_i to be

$$U(v_i) = \frac{1}{2} v_i^T v_i\,. \tag{3.11}$$

We first prove the following result.

Lemma 3.1 *$W(\cdot)$ is regular everywhere.*

Proof: From Definition 2.4, it suffices to prove that $W^{'}(z;\nu) = W^{0}(z;\nu)$ for all $\nu = \begin{bmatrix}\nu_1 & \cdots & \nu_n\end{bmatrix}^T \in \mathbb{R}^n$ and $z = \begin{bmatrix}z_1 & \cdots & z_n\end{bmatrix}^T \in \mathbb{R}^n$. The definitions of $W^{0}(z;\nu)$ and $W^{'}(z;\nu)$ have been given in Lemma 2.3 and Definition 2.4 respectively. Since $W^{'}(z;\nu) = W^{0}(z;\nu)$ holds trivially for $z \notin \mathcal{S}$, we only need to consider the case when $z \in \mathcal{S}$.

From the definition of $W(\cdot)$, one has

$$W(z) = \int_0^z \mathbf{q}_l(x)dx = \sum_{k=1}^{n} \int_0^{z_k} q_l(x)dx\,.$$

From Lemma 2.3 it follows that

$$\begin{aligned} W^{0}(z;\nu) &= \max\{\langle\zeta,\nu\rangle : \zeta \in \partial W(z)\} \\ &= \max\left\{\sum_{k=1}^{n} \zeta_k\,\nu_k : \zeta_k \in \frac{\partial W}{\partial z_k}\right\} \\ &= \sum_{k=1}^{n} \max\left\{\zeta_k\,\nu_k : \zeta_k \in \frac{\partial W}{\partial z_k}\right\}, \end{aligned} \tag{3.12}$$

and the last equality follows from the fact that the sets, which ζ and ν take their values from, are rectangular. Since $q_l(z_k^-) < q_l(z_k^+)$, for each k one has

$$\max\left\{\zeta_k\,\nu_k : \zeta_k \in \frac{\partial W}{\partial z_k}\right\} = q_l(z_k^+)\,\nu_k \tag{3.13}$$

when $\nu_k > 0$ and

$$\max\left\{\zeta_k\,\nu_k : \zeta_k \in \frac{\partial W}{\partial z_k}\right\} = q_l(z_k^-)\,\nu_k \tag{3.14}$$

when $\nu_k < 0$. On the other hand, the directional derivative of $W(z)$ is

$$\begin{aligned} W^{'}(z;\nu) &= \lim_{t\downarrow 0} \frac{W(z+t\nu) - W(z)}{t} \\ &= \lim_{t\downarrow 0} \frac{\int_z^{z+t\nu} \mathbf{q}_l(x)\,dx}{t} \\ &= \lim_{t\downarrow 0} \frac{1}{t} \sum_{k=1}^{n} \int_{z_k}^{z_k+t\nu_k} q_l(x)dx. \end{aligned} \tag{3.15}$$

Since

$$\lim_{t\downarrow 0} \frac{1}{t} \int_{z_k}^{z_k+t\nu_k} q_l(x)dx = q_l(z_k^+)\,\nu_k \tag{3.16}$$

when $\nu_k > 0$ and

$$\lim_{t\downarrow 0} \frac{1}{t} \int_{z_k}^{z_k+t\nu_k} q_l(x)dx = q_l(z_k^-)\,\nu_k, \tag{3.17}$$

when $\nu_k < 0$, we know

$$\lim_{t\downarrow 0} \frac{1}{t} \int_{z_k}^{z_k+t\nu_k} q_l(x)dx = \max\left\{ \zeta_k\,\nu_k : \zeta_k \in \frac{\partial W}{\partial z_k} \right\}, \quad \text{for all } k = \{1, \cdots, n\}. \tag{3.18}$$

Combining (3.12), (3.15) and (3.18), we arrive at $W^{'}(z;\nu) = W^0(z;\nu)$ for all ν. □

Note that $F[\mathbf{q}_l(r_i - r_j)]$ represents the set that is given by the interval $[\mathbf{q}_l(\tilde{r}_{ij}^-), \mathbf{q}_l(\tilde{r}_{ij}^+)]$. We now prove a property of the set-valued map.

Lemma 3.2 *It holds that* $r_i^T\, F[\mathbf{q}_l(r_i - r_j)] = -r_i^T\, F[\mathbf{q}_l(r_j - r_i)]$, *for all* $i \neq j$.

Proof: Since $\mathbf{q}_l(\cdot)$ is an odd function, one has $\mathbf{q}_l(r_i - r_j) + \mathbf{q}_l(r_j - r_i) = \mathbf{0}$. Then we have $r_i^T\, F[\mathbf{q}_l(r_i - r_j)] = r_i^T\, F[-\mathbf{q}_l(r_j - r_i)] = -r_i^T\, F[\mathbf{q}_l(r_j - r_i)]$. □

We can further derive some relationships between the positions and velocities of the agents.

Lemma 3.3 *It holds that*

$$\sum_{i=1}^{N} \sum_{j\in\mathcal{N}_1(i)} r_i^T\, F[\mathbf{q}_l(r_i - r_j)] = \frac{1}{2} \sum_{i=1}^{N} \sum_{j\in\mathcal{N}_1(i)} (r_i - r_j)^T\, F[\mathbf{q}_l(r_i - r_j)] \tag{3.19}$$

and

$$\sum_{i=1}^{N} \sum_{j\in\mathcal{N}_2(i)} v_i^T\, F[\mathbf{q}_l(v_i - v_j)] = \frac{1}{2} \sum_{i=1}^{N} \sum_{j\in\mathcal{N}_2(i)} (v_i - v_j)^T\, F[\mathbf{q}_l(v_i - v_j)]. \tag{3.20}$$

Proof: We only prove (3.20). The equality (3.19) can be proved in a similar manner. It suffices to prove that $\sum_{i=1}^N \sum_{j=1}^N b_{ij}\, v_i^T\, F[\mathbf{q}_l(v_i - v_j)] = \frac{1}{2} \sum_{i=1}^N \sum_{j=1}^N b_{ij}\, (v_i - v_j)^T\, F[\mathbf{q}_l(v_i - v_j)]$. Then

$$\begin{aligned} & \frac{1}{2} \sum_{i=1}^{N} \sum_{j=1}^{N} b_{ij}\, (v_i - v_j)^T\, F[\mathbf{q}_l(v_i - v_j)] \\ = \; & \frac{1}{2} \sum_{i=1}^{N} \sum_{j=1}^{N} b_{ij}\, v_i^T\, F[\mathbf{q}_l(v_i - v_j)] - \frac{1}{2} \sum_{i=1}^{N} \sum_{j=1}^{N} b_{ij}\, v_j^T\, F[\mathbf{q}_l(v_i - v_j)] \end{aligned}$$

$$
\begin{aligned}
&= \frac{1}{2}\sum_{i=1}^{N}\sum_{j=1}^{N} b_{ij}\, v_i^T\, F[\mathbf{q}_l(v_i - v_j)] - \frac{1}{2}\sum_{j=1}^{N}\sum_{i=1}^{N} b_{ji}\, v_i^T\, F[\mathbf{q}_l(v_j - v_i)] \\
&= \frac{1}{2}\sum_{i=1}^{N}\sum_{j=1}^{N} b_{ij}\, v_i^T\, F[\mathbf{q}_l(v_i - v_j)] + \frac{1}{2}\sum_{i=1}^{N}\sum_{j=1}^{N} b_{ij}\, v_i^T\, F[\mathbf{q}_l(v_i - v_j)] \\
&= \sum_{i=1}^{N}\sum_{j=1}^{N} b_{ij}\, v_i^T\, F[\mathbf{q}_l(v_i - v_j)],
\end{aligned}
$$

where we have used the fact that $b_{ij} = b_{ji}$ for undirected graph $\mathbb{G}_2$ and Lemma 3.2. □

The following result, in which v and r are mixed, can be proved in a similar manner.

Lemma 3.4 *It holds that*

$$
\sum_{i=1}^{N}\sum_{j=1}^{N} a_{ij}\, v_i^T\, F[\mathbf{q}_l(r_i - r_j)] = \frac{1}{2}\sum_{i=1}^{N}\sum_{j=1}^{N} a_{ij}\, (v_i - v_j)^T\, F[\mathbf{q}_l(r_i - r_j)]. \tag{3.21}
$$

In order to prove the convergence result in Theorem 3.1, we rewrite the system dynamics (3.1) and (3.3) into

$$
\begin{cases}
\dot{\tilde{r}}_{ij} = v_i - v_j, \qquad j \neq i \\
\dot{v}_i = -\sum_{j=1}^{N} a_{ij}\mathbf{q}_l\,(\tilde{r}_{ij}) - \sum_{j=1}^{N} b_{ij}\mathbf{q}_l\,(v_i - v_j),
\end{cases} \tag{3.22}
$$

using the new set of states

$$
\tilde{r}_{12}, \tilde{r}_{13}, \ldots, \tilde{r}_{1N}, \ldots, \tilde{r}_{N1}, \tilde{r}_{N2} \ldots, \tilde{r}_{N,N-1}, v_1, \ldots, v_N.
$$

Then in what follows, we will carry out our analysis on solutions to (3.22) and in fact we will prove the convergence of $\tilde{r}_{ij}(t)$ and $v_i(t) - v_j(t)$.

Proof of Theorem 3.1: Consider the following candidate Lyapunov function that is defined using the potential functions defined in (3.9) and (3.11) respectively

$$
V(\tilde{r}, v) = \frac{1}{2}\sum_{i=1}^{N}\sum_{j=1}^{N} a_{ij}\, W(\tilde{r}_{ij}) + \sum_{i=1}^{N} U(v_i), \tag{3.23}
$$

where $\tilde{r} = [\tilde{r}_{12}^T, \ldots, \tilde{r}_{1N}^T, \ldots, \tilde{r}_{N,N-1}^T]^T$ and $v = [v_1^T, \ldots, v_N^T]^T$. From Lemma 3.1 we know that $W(\tilde{r}_{ij})$ is regular. Then in view of Lemma 2.4, it follows that

$\sum_{i=1}^{N}\sum_{j=1}^{N} W(\tilde{r}_{ij})$ is also regular. Furthermore, $U(v_i)$ is continuously differentiable, so $V(\tilde{r}, v)$ is regular. In addition,

$$\frac{\partial V(\tilde{r}, v)}{\partial \tilde{r}_{ij}} = \frac{\partial W(\tilde{r}_{ij})}{\partial \tilde{r}_{ij}}, \tag{3.24}$$

where $\frac{\partial W(\tilde{r}_{ij})}{\partial \tilde{r}_{ij}}$ are given in (3.10), and

$$\frac{\partial V(\tilde{r}, v)}{\partial v_i} = v_i . \tag{3.25}$$

Then the generalized gradient of $V(\tilde{r}, v)$ has the form

$$\begin{aligned} \partial V(\tilde{r}, v) = \Bigg[& \left(\frac{\partial V(\tilde{r}, v)}{\partial \tilde{r}_{12}}\right)^T, \left(\frac{\partial V(\tilde{r}, v)}{\partial \tilde{r}_{13}}\right)^T, \ldots, \\ & \left(\frac{\partial V(\tilde{r}, v)}{\partial \tilde{r}_{N-1,N}}\right)^T, v_1^T, v_2^T, \ldots, v_N^T \Bigg]^T . \end{aligned} \tag{3.26}$$

Applying Lemma 2.5, one has

$$\frac{d}{dt} V(\tilde{r}, v) \in \dot{\tilde{V}}(\tilde{r}, v), \qquad \text{a.e. for } t \geqslant 0,$$

which can be further computed by

$$\begin{aligned} \dot{\tilde{V}}(\tilde{r}, v) &= \bigcap_{\xi \in \partial V(\tilde{r}, v)} \xi^T \left[\dot{\tilde{r}}_{12}^T, \dot{\tilde{r}}_{13}^T, \ldots, \dot{\tilde{r}}_{N,N-1}^T, F^T[\dot{v}_1], F^T[\dot{v}_2], \ldots, F^T[\dot{v}_N]\right]^T \\ &= \bigcap_{\xi_{ij} \in \frac{\partial V(\tilde{r}, v)}{\partial \tilde{r}_{ij}}} \left(\frac{1}{2}\sum_{i=1}^{N}\sum_{j=1}^{N} a_{ij}\, \xi_{ij}^T (v_i - v_j) + \sum_{i=1}^{N} v_i^T F[\dot{v}_i]\right). \end{aligned}$$

Using (3.24) to rewrite the intersection condition and (3.8) to replace $\dot{v}$, we have

$$\begin{aligned} \dot{\tilde{V}}(\tilde{r}, v) \subseteq \bigcap_{\xi_{ij} \in \frac{\partial W(\tilde{r}_{ij})}{\partial \tilde{r}_{ij}}} \Bigg(& \frac{1}{2}\sum_{i=1}^{N}\sum_{j=1}^{N} a_{ij}\, \xi_{ij}^T (v_i - v_j) \\ & - \sum_{i=1}^{N}\sum_{j=1}^{N} a_{ij} v_i^T F[\mathbf{q}_l(\tilde{r}_{ij})] \\ & - \sum_{i=1}^{N}\sum_{j \in \mathcal{N}_2(i)} v_i^T F[\mathbf{q}_l(v_i - v_j)] \Bigg). \end{aligned}$$

From Lemma 3.4, we can further deduce

$$\begin{aligned}
\dot{\tilde{V}}(\tilde{r},v) \quad \subseteq \quad & \bigcap_{\xi_{ij}\in\frac{\partial W(\tilde{r}_{ij})}{\partial \tilde{r}_{ij}}} \Bigg(\frac{1}{2}\sum_{i=1}^{N}\sum_{j=1}^{N} a_{ij}\,\xi_{ij}^{T}\,(v_i - v_j) \\
& -\frac{1}{2}\sum_{i=1}^{N}\sum_{j=1}^{N} a_{ij}(v_i-v_j)^{T}\,F[\mathbf{q}_l(\tilde{r}_{ij})] \quad -\sum_{i=1}^{N}\sum_{j\in\mathcal{N}_2(i)} v_i^{T}\,F[\mathbf{q}_l(v_i-v_j)] \Bigg) \\
= \quad & \bigcap_{\xi_{ij}\in\frac{\partial W(\tilde{r}_{ij})}{\partial \tilde{r}_{ij}}} \Bigg(\frac{1}{2}\sum_{i=1}^{N}\sum_{j=1}^{N} a_{ij}(v_i-v_j)^{T}\xi_{ij} \\
& -\frac{1}{2}\sum_{i=1}^{N}\sum_{j=1}^{N} a_{ij}(v_i-v_j)^{T}\,[\mathbf{q}_l(\tilde{r}_{ij}^{-}),\mathbf{q}_l(\tilde{r}_{ij}^{+})] \Bigg) \\
& -\sum_{i=1}^{N}\sum_{j\in\mathcal{N}_2(i)} v_i^{T}\,F[\mathbf{q}_l(v_i-v_j)] \\
= \quad & \bigcap_{\xi_{ij}\in[\mathbf{q}_l(\tilde{r}_{ij}^{-}),\mathbf{q}_l(\tilde{r}_{ij}^{+})]} \frac{1}{2}\sum_{i=1}^{N}\sum_{j=1}^{N} a_{ij}(v_i-v_j)^{T}\ \times \\
& \qquad [-\mathbf{q}_l(\tilde{r}_{ij}^{+})+\xi_{ij}, -\mathbf{q}_l(\tilde{r}_{ij}^{-})+\xi_{ij}] \\
& -\sum_{i=1}^{N}\sum_{j\in\mathcal{N}_2(i)} v_i^{T}\,F[\mathbf{q}_l(v_i-v_j)].
\end{aligned}$$

Since

$$\bigcap_{\xi_{ij}\in[\mathbf{q}_l(\tilde{r}_{ij}^{-}),\mathbf{q}_l(\tilde{r}_{ij}^{+})]} [-\mathbf{q}_l(\tilde{r}_{ij}^{+})+\xi_{ij}, -\mathbf{q}_l(\tilde{r}_{ij}^{-})+\xi_{ij}] = \{\mathbf{0}\},$$

and in view of Lemma 3.3, one has

$$\begin{aligned}
\frac{d}{dt}\,V(\tilde{r},v) \in \dot{\tilde{V}}(\tilde{r},v) &\subseteq -\sum_{i=1}^{N}\sum_{j\in\mathcal{N}_2(i)} v_i^{T}\,F[\mathbf{q}_l(v_i-v_j)] \\
&= -\frac{1}{2}\sum_{i=1}^{N}\sum_{j\in\mathcal{N}_2(i)} (v_i-v_j)^{T}\,F[\mathbf{q}_l(v_i-v_j)]\,.
\end{aligned} \tag{3.27}$$

This implies that $\frac{d}{dt}\,V(\tilde{r},v)\leqslant 0$. Thus, $V(\tilde{r},v)\leqslant V(\tilde{r}(0),v(0))$, which further implies that both $\tilde{r}(t)$ and $v(t)$ are bounded. Now we apply LaSalle's invariance principle (Cortés 2008a, Theorem 2) to show the convergence of solutions to (3.22). Define

$\mathcal{S} \triangleq \{(\tilde{r}, v) | V(\tilde{r}, v) \leqslant V(\tilde{r}(0), v(0))\}$ and $\mathcal{E} \triangleq \{(\tilde{r}, v) | 0 \in \dot{\tilde{V}}(\tilde{r}, v)\}$. Note that from (3.27) and the connectivity of $\mathbb{G}_2$, $\mathcal{E} = \{(\tilde{r}, v) | v_i = v_j, \ \forall i \neq j\}$. The solutions to (3.22) converge to the largest weakly invariant set $\mathcal{M}$ contained in $\mathcal{S} \cap \mathcal{E}$. Consider a solution to (3.22) that evolves in this set for all $t \geqslant 0$. It satisfies

$$\begin{cases} \dot{\tilde{r}}_{ij} = \mathbf{0}, & j \neq i \\ \dot{v}_i = -\sum_{j=1}^{N} a_{ij} \mathbf{q}_l(\tilde{r}_{ij}) & \forall \, i, j = 1, \cdots, N. \end{cases} \tag{3.28}$$

Hence, the solutions to (3.22) converge to a set of points $(\tilde{r}, v)$ such that every $\tilde{r}_{ij}$ remains constant and all the velocities v_i are equal.

Following (Arcak 2007, De Persis 2011), to proceed further in the proof, we use D_1 to denote the incidence matrix associated with the graph $\mathbb{G}_1$ and introduce the variable $z \triangleq (D_1^T \otimes I_n) r$ to denote the vector of the relative positions between neighboring agents where $\otimes$ denotes the Kronecker product. Since $\mathbb{G}_1$ is connected, $\tilde{r}$ is constant if and only if z is constant. Moreover, in view of (3.3), the second equation in (3.28) can be written in a compact form

$$\dot{v} = -(D_1 \otimes I_n) \mathbf{q}_l(z).$$

Hence, a solution to (3.28) such that $\tilde{r}$ is constant and $v_i = v_j$ for all i, j in the coordinates (z, v) satisfies

$$\begin{cases} \dot{z} = \mathbf{0}, \\ \dot{v} = -(D_1 \otimes I_n) \mathbf{q}_l(z) \end{cases} \tag{3.29}$$

and is such that $z = (D_1^T \otimes I_n) r$ is constant and $(D_1^T \otimes I_n) v = \mathbf{0}$, i.e. all the velocities are the same. Consider a solution to system (3.29) and define $\tilde{v} \triangleq (D_1^T \otimes I_n) v$. We have $\dot{\tilde{v}} \in -(D_1^T \otimes I_n)(D_1 \otimes I_n) F[\mathbf{q}_l(z)]$. For a solution to (3.29) to remain in a set where $z = (D_1^T \otimes I_n) r$ is constant and $\tilde{v} = \mathbf{0}$, it must be true that

$$\mathbf{0} \in -(D_1^T \otimes I_n)(D_1 \otimes I_n) F[\mathbf{q}_l(z)] \quad = -(D_1^T D_1 \otimes I_n) F[\mathbf{q}_l(z)].$$

Let $w \in F[\mathbf{q}_l(z)]$ be such that $\mathbf{0} = (D_1^T D_1 \otimes I_n) w$. Then $y \triangleq (D_1 \otimes I_n) w$ belongs to $\ker(D_1^T \otimes I_n)$, i.e. $(D_1^T \otimes I_n) y = \mathbf{0}$. Then $y^T y = y^T (D_1 \otimes I_n) w = 0$. Hence, $(D_1 \otimes I_n) w = \mathbf{0}$ with $w \in F[\mathbf{q}_l(z)]$. Since $z = (D_1^T \otimes I_n) r$, from $(D_1 \otimes I_n) w = \mathbf{0}$ one obtains that $r^T (D_1 \otimes I_n) w = 0 = z^T w$. Since $w \in F[\mathbf{q}_l(z)]$ and $\mathbf{q}_l$ is the logarithmic quantizer, we know $z^T w = 0$ implies necessarily that $z = \mathbf{0}$. Hence a weakly invariant set for (3.29) where $z = (D_1^T \otimes I_n) r$ remains constant and $(D_1^T \otimes I_n) v = \mathbf{0}$ is such that $z = \mathbf{0}$.

In view of the second equation of (3.29), this also implies that $\dot{v} = \mathbf{0}$. Considering the trajectories of $(\tilde{r}, v)$, we conclude that the solutions converge to a set $\mathcal{M}$ where $\tilde{r} = 0$, $(D_1^T \otimes I_n)v = \mathbf{0}$ and $\dot{v} = \mathbf{0}$.
One can further calculate the asymptotic positions and velocities for all the agents. On one hand, one can check that for any solution (r, v), $(\mathbf{1}_N \otimes I_n)^T \dot{v} = \mathbf{0}$ a.e. for $t \geqslant 0$, namely $\sum_{i=1}^N \dot{v}_i = \mathbf{0}$. Hence, one has $\sum_{i=1}^N v_i = \sum_{i=1}^N v_i(0)$. Combining with the fact that $v_i = v_j = \bar{v}$ on $\mathcal{M}$, we know that $\bar{v} = \frac{1}{N}\sum_{i=1}^N v_i(0)$, for all $i = 1, 2, \cdots, N$. So any solution $v_i(t)$ tends to $\frac{1}{N}\sum_{i=1}^N v_i(0)$ as $t \to +\infty$. On the other hand, on $\mathcal{M}$, $\dot{r}_i = \bar{v} = \frac{1}{N}\sum_{i=1}^N v_i(0)$, and hence $r_i(t) = \frac{1}{N}\sum_{j=1}^N r_j(0) + \frac{t}{N}\sum_{j=1}^N v_j(0)$, for all $i = \{1, 2, \cdots, N\}$. We conclude that any solution $(\tilde{r}, v)$ is such that $r_i \to \frac{1}{N}\sum_{j=1}^N r_j(0) + \frac{t}{N}\sum_{j=1}^N v_j(0)$ as $t \to +\infty$. □

Remark 3.2 *In the proof of Theorem 3.1, from $0 \in \dot{\tilde{V}}(\tilde{r}, v)$ it is shown that $v_i = v_j, \forall i \neq j$, which implies that the velocities of all the agents get synchronized precisely. However, if we use a logarithmic quantizer with finite quantization levels towards the origin, such as*

$$q_l(x) = \begin{cases} e^{q_u(\ln x)} & \text{when } x > \delta; \\ 0 & \text{when } x \in [-\delta, \delta]; \\ -e^{q_u(\ln(-x))} & \text{when } x < -\delta, \end{cases} \tag{3.30}$$

where $\delta \in \mathbb{R}$ is a positive constant, the convergence result for velocities will be different. In fact, a slight modification of the proof leads to the conclusion that $v_i - v_j \in [-\delta, \delta]\mathbf{1}_n, \forall j \in \mathcal{N}_2(i), i = 1, \ldots, N$; in other words, the norms $||v_i - v_j||$ of the relative velocities between neighboring agents are bounded from above by the constant $\sqrt{n}\delta$.

Theorem 3.1 can be illustrated through simulations. We consider a team of 4 agents whose neighbor relationship graphs $\mathbb{G}_1$ and $\mathbb{G}_2$ are taken to be the same as shown in the upper left corner of Figure 3.1.

We take $n = 2$ and let $\delta_u = 1, \delta_l = 1 - e^{-1}$. Each coordinate of the initial positions are chosen randomly from $(0, 30)$ while those of the initial velocities from $(0, 10)$. Figures 3.2 (a) and (b) illustrate the evolutions of the positions and velocities of the four agents in their x-coordinates respectively.

3.3.2 Synchronized motion using uniform quantizers

When uniform quantizers (3.4) are used, one achieves a form of roughly synchronized motion, i.e., the differences of the agents' positions converging to a bounded set. For simplicity, we suppose that the undirected graphs $\mathbb{G}_1$ and $\mathbb{G}_2$ are the same and use a common symbol $\mathbb{G}$. Let $L \in \mathbb{R}^{N\times N}$ denote the Laplacian matrix of the

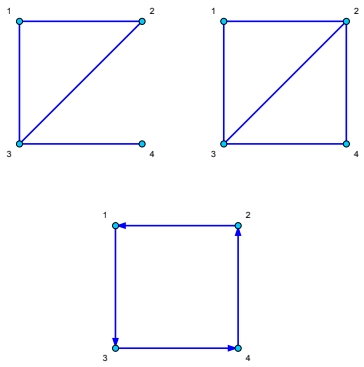

Figure 3.1: *Some graphs for different communication topologies.*

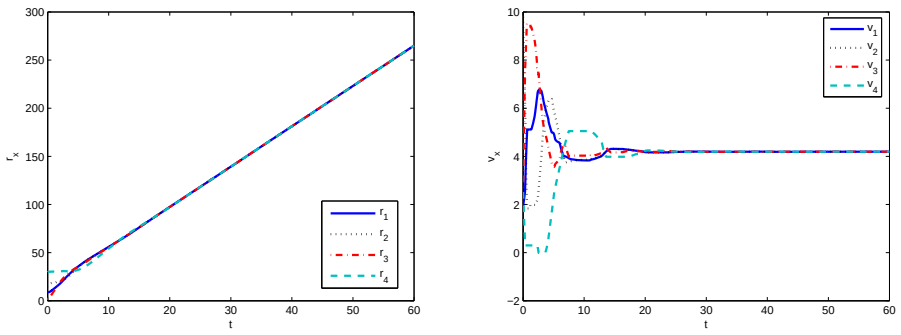

(a) $r_i(t)$, $i = 1, 2, 3, 4$. (b) $v_i(t)$, $i = 1, 2, 3, 4$.

Figure 3.2: *Evolutions of $r_i(t)$ and $v_i(t)$ with the logarithmic quantizers.*

graph $\mathbb{G}$ and $D \in \mathbb{R}^{N\times m}$ the corresponding incidence matrix, where m is the number of edges in $\mathbb{G}$.

Theorem 3.2 *Assume the graph $\mathbb{G}$ is connected and that the uniform quantizers $\mathbf{q}_u(\cdot)$ in (3.4) are used in the control law (3.3). Then any Filippov solution (r, v) to the system (3.1) and (3.3) is such that*
a) the velocities v of all the agents converge to $\frac{1}{N}\sum_{j=1}^{N} v_j(0)$;
b) the distances $||r_i - r_j||$ between all pairs of neighboring agents are upper bounded by $\sqrt{n}\delta_u$ when $t \to \infty$;

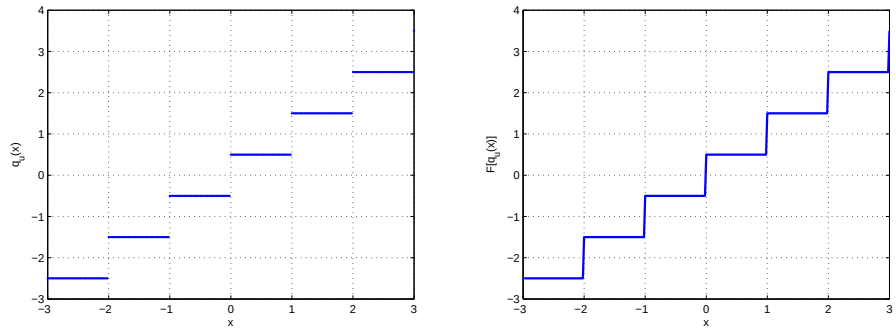

Figure 3.3: *Visualization of the map $q_u(\cdot)$ in (3.4) and the set-valued map $F[q_u(\cdot)]$, when $\delta_u = 1$.*

c) the positions of all the agents converge to the set

$$\mathcal{R} = \{r \in \mathbb{R}^{Nn} : ||r - (\mathbf{1}_N \otimes I_n) r_{avg})|| \leqslant \sqrt{\frac{mn}{\lambda_2(L)}}\, \delta_u\}\,,$$

where $r_{avg} = \frac{1}{N} \sum_{i=1}^{N} r_i(0) + \frac{t}{N} \sum_{i=1}^{N} v_i(0)$.

To prove this theorem, we first need a few facts. The following is straightforward to prove:

Lemma 3.5 *For the incidence matrix $D \in \mathbb{R}^{N\times m}$ associated with the graph $\mathbb{G}$, the null space of $D^T D$ is the null space of D.*

Moreover, we have the following Lemma (see e.g. Lemma 1 in (Ceragioli et al. 2011)).

Lemma 3.6 *For any $x \in \mathbb{R}^N$, one has $x^T Lx \geqslant \lambda_2(L)||x - \frac{\mathbf{1}\mathbf{1}^T}{N} x||^2$, where $\mathbf{1} \in \mathbb{R}^N$ is the vector of all ones and λ_2 is the algebraic connectivity.*

In the following, we analyze a few properties of the uniform quantizer (3.4). First we represent the map $q_u(\cdot)$ and the set-valued map $F[q_u(\cdot)]$ in Figure 3.3. This will be helpful in our analysis. From the definition of the uniform quantizer (3.4), one has the following lemma.

Lemma 3.7 *a) For $x \in \mathbb{R}$ and $|x| \leqslant \delta_u$, it holds that*

$$x(F[q_u(x)] + F[q_u(0)]) \subseteq [0, +\infty). \tag{3.31}$$

b) For $x \in \mathbb{R}$ and $|x| > \delta_u$, it holds that

$$x(F[q_u(x)] + F[q_u(0)]) \subseteq (0, +\infty). \tag{3.32}$$

Proof: We use Figure 3.3 to help our analysis.
a) If $x = 0$, it follows that $x(F[q_u(x)] + F[q_u(0)]) = \{0\}$.
If $0 < x < \delta_u$, it follows that $F[q_u(x)] = \{\frac{\delta_u}{2}\}$. Then $F[q_u(x)] + F[q_u(0)] = [0, \delta_u]$, since $F[q_u(0)] = [-\frac{\delta_u}{2}, \frac{\delta_u}{2}]$. Thus one has that every element in the set $x(F[q_u(x)] + F[q_u(0)])$ is nonnegative.
Similarly one proves that if $-\delta_u < x < 0$, then $F[q_u(x)] + F[q_u(0)] = [-\delta_u, 0]$. Thus one has that every element in the set $x(F[q_u(x)] + F[q_u(0)])$ is nonnegative.
If $x = \delta_u$ or $x = -\delta_u$, similar arguments work as well. Hence, we conclude that (3.31) holds if $|x| \leqslant \delta_u$.
b) If $x > \delta_u$, it follows that $F[q_u(x)] \subseteq [\frac{3\,\delta_u}{2}, +\infty)$. Then $F[q_u(x)] + F[q_u(0)] \subseteq [\delta_u, +\infty)$, since $F[q_u(0)] = [-\frac{\delta_u}{2}, \frac{\delta_u}{2}]$. Thus one has that any element in the set $x(F[q_u(x)] + F[q_u(0)])$ is strictly positive. In the same way one can prove (3.32) if $x < -\delta_u$. Now we conclude that (3.32) holds if $|x| > \delta_u$. □

Now we are ready to prove the synchronization of the systems of second-order agent dynamics with uniform quantizers.
Proof of Theorem 3.2: We use the variable $z = (D^T \otimes I_n)r$ to denote the vector of the relative positions between neighboring agents. Then we rewrite (3.1) and (3.3) into the compact form

$$\begin{cases} \dot{z} = (D^T \otimes I_n)v \\ \dot{v} = -(D \otimes I_n)\mathbf{q}_u(z) - (D \otimes I_n)\mathbf{q}_u((D^T \otimes I_n)v)\,. \end{cases} \tag{3.33}$$

We use the Lyapunov function

$$V(z, v) = \sum_{k=1}^{m} \sum_{j=1}^{n} \int_0^{z_{kj}} q_u(s)ds + \sum_{i=1}^{N} U(v_i)$$

where $U(v_i) = \frac{1}{2} v_i^T v_i$. The function is convex and when computed along the solutions to (3.33) it satisfies $\frac{d}{dt} V(z(t), v(t)) \in \dot{\overline{V}}(z(t), v(t))$ a.e. for $t \geqslant 0$, where the set-valued derivative $\dot{\overline{V}}(z, v)$ can be computed similarly as in Lemma 1 in (De Persis 2011), and is given by

$$\dot{\overline{V}}(z, v) = \{a \in \mathbb{R} : \exists w \in F[\mathbf{q}_u((D^T \otimes I_n)v)] \,\text{s.t.}\, a = -v^T(D \otimes I_n)w\}.$$

Following the convention (Bacciotti and Ceragioli 1999) let $\max \dot{\overline{V}}(z, v) = -\infty$ if $\dot{\overline{V}}(z, v) = \varnothing$. By definition of $F[\mathbf{q}_u((D^T \otimes I_n)v)]$ this implies that $\frac{d}{dt} V(z, v) \subseteq$

$(-\infty, 0]$ and that $\mathbf{0} \in \dot{\overline{V}}(z, v)$ necessarily implies $(D^T \otimes I_n)v = \mathbf{0}$, i.e. $v = \text{span}\{\mathbf{1} \otimes I_n\}$. We conclude that the solutions converge to a subset of the largest weakly invariant set where $v = \text{span}\{\mathbf{1} \otimes I_n\}$. On this invariant set the system evolves according to

$$\begin{cases} \dot{z} = \mathbf{0} \\ \dot{v} = -(D \otimes I_n)\mathbf{q}_u(z) - (D \otimes I_n)\mathbf{q}_u((D^T \otimes I_n)v) \end{cases}$$

and the solutions must satisfy the differential inclusion

$$\begin{pmatrix} \dot{z} \\ \dot{v} \end{pmatrix} \in \begin{pmatrix} \mathbf{0} \\ -(D \otimes I_n)F[\mathbf{q}_u(z)] - (D \otimes I_n)F[\mathbf{q}_u(\mathbf{0})] \end{pmatrix}. \tag{3.34}$$

Consider the solution to system (3.34), which evolves in the largest weakly invariant set where $(D^T \otimes I_n)v \equiv \mathbf{0}$. One has $(D^T \otimes I_n)\dot{v} \equiv \mathbf{0}$. From (3.34), it follows that $(D^T \otimes I_n)\dot{v} \in -(D^T D \otimes I_n)(F[\mathbf{q}_u(z)] + F[\mathbf{q}_u(0)])$ and also

$$\mathbf{0} \in -(D^T D \otimes I_n)\left(F[\mathbf{q}_u(z)] + F[\mathbf{q}_u(0)]\right).$$

Applying Lemma 3.5, one has

$$\mathbf{0} \in -(D \otimes I_n)\left(F[\mathbf{q}_u(z)] + F[\mathbf{q}_u(0)]\right).$$

And multiplying on the right by r^T, one further obtains

$$0 \in -z^T\left(F[\mathbf{q}_u(z)] + F[\mathbf{q}_u(\mathbf{0})]\right). \tag{3.35}$$

The latter in combination with Lemma 3.7 shows that $||z||_\infty \leqslant \delta_u$. Thus, the solutions (z, v) converge to the set where $||z||_\infty \leqslant \delta_u$, $(D^T \otimes I_n)v = \mathbf{0}$.
As to the further calculation of asymptotic velocities of all the agents, one can follow the argument of the last part of the proof of Theorem 3.1. And we have that any solution $v_i(t)$ tends to $\frac{1}{N}\sum_{i=1}^{N} v_i(0)$ as $t \to +\infty$. Now we calculate the asymptotic positions of all the agents. From $||z||_\infty \leqslant \delta_u$, one has

$$||r_i - r_j|| \leqslant \sqrt{n}\delta_u\,, \tag{3.36}$$

where $i = \{1, \cdots, N\}$ and j is a neighbor of i. Note that $z = (D^T \otimes I_n)r \in \mathbb{R}^{mn}$. Then one has

$$||(D^T \otimes I_n)r|| = ||z|| \leqslant \sqrt{mn}\,||z||_\infty \leqslant \sqrt{mn}\delta_u.$$

From Lemma 3.6, one has

$$\begin{aligned} ||r - (\frac{\mathbf{1}_N \mathbf{1}_N^T}{N} \otimes I_n)r||^2 &\leqslant \frac{1}{\lambda_2(L)}\, r^T (L \otimes I_n) r \\ &= \frac{1}{\lambda_2(L)}\, r^T (DD^T \otimes I_n) r \\ &= \frac{1}{\lambda_2(L)}\, ||(D^T \otimes I_n) r||^2 \\ &\leqslant \frac{mn}{\lambda_2(L)}\, \delta_u^2 \,, \end{aligned}$$

that is,

$$||r - (\frac{\mathbf{1}_N \mathbf{1}_N^T}{N} \otimes I_n)r|| \leqslant \sqrt{\frac{mn}{\lambda_2(L)}}\, \delta_u. \tag{3.37}$$

Furthermore, $\sum_{i=1}^N \dot{r}_i(t) = \sum_{i=1}^N v_i(t) = \sum_{i=1}^N v_i(0)$, and hence the average position of all the agents can be calculated by

$$r_{avg} \triangleq \frac{1}{N} \sum_{i=1}^N r_i(t) = \frac{1}{N} \sum_{i=1}^N r_i(0) + \frac{t}{N} \sum_{i=1}^N v_i(0). \tag{3.38}$$

Then in combination with (3.37), we have

$$||r - (\mathbf{1}_N \otimes I_n) r_{avg})|| \leqslant \sqrt{\frac{mn}{\lambda_2(L)}}\, \delta_u \,. \tag{3.39}$$

We conclude that the asymptotic positions of all the agents converge to the set $\mathcal{R} = \{r \in \mathbb{R}^{Nn} : ||r - (\mathbf{1}_N \otimes I_n) r_{avg})|| \leqslant \sqrt{\frac{mn}{\lambda_2(L)}}\, \delta_u\}$, where $r_{avg} = \frac{1}{N} \sum_{i=1}^N r_i(0) + \frac{t}{N} \sum_{i=1}^N v_i(0)$. □

Remark 3.3 *In the proof it is shown that $(D^T \otimes I_n)v = \mathbf{0}$, which means that the velocities of all the agents accurately achieve synchronization. However, if we use a different uniform quantizer, such as the one used in (Frasca et al. 2009, Ceragioli et al. 2011):*

$$q_u(x) = \delta_u \left\lfloor \frac{x}{\delta_u} + \frac{1}{2} \right\rfloor , \tag{3.40}$$

instead of the uniform quantizer in (3.4), the convergence result for velocities will be different. In fact, a slight variation of the proof shows that $(D^T \otimes I_n)v \in [-\frac{\delta_u}{2}, \frac{\delta_u}{2}]\mathbf{1}_{mn}$, i.e. the norm $||v_i - v_j||$ of the relative velocity between neighbors is bounded by the constant $\frac{\sqrt{n}}{2}\delta_u$.

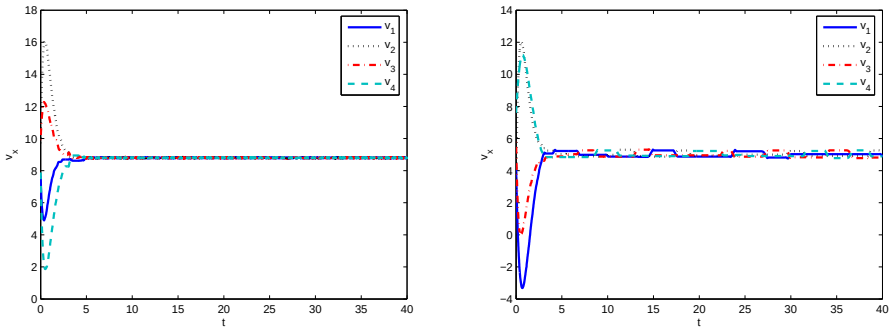

(a) $v_i(t)$, $i = 1, 2, 3, 4$. (b) $v_i(t)$, $i = 1, 2, 3, 4$.

Figure 3.4: $v_i(t)$ *under the uniform quantizers (3.4) and (3.40) respectively.*

Theorem 3.2 and Remark 3.3 can be illustrated through simulations. We take the neighbor relationship graphs $\mathbb{G}_1$ and $\mathbb{G}_2$ both to be the graph on the upper right of Figure 3.1. We set $\delta_u = 1$ and initialize the system in the same way as what we have done for the simulation of the system with the logarithmic quantizer. We show the results in Figure 3.4. When the uniform quantizer (3.4) is adopted, the agents' velocities converge [1] to the average value, as shown in Figure 3.4(a). When the uniform quantizer (3.40) is adopted, the agents' velocities converge to a bounded set with the diameter less than 1, shown in Figure 3.4(b). The results in Figure 3.4 are consistent with the different convergence results in Theorem 3.2 and Remark 3.3.

While the steady-state performances of the consensus-type coordination algorithm is satisfactory when the above quantizers are chosen, we show in the next section that this is not the case if uniform quantizers are used differently.

3.4 Undesirable steady-state dynamics using asymmetric quantizers

In this section, we consider the effects of asymmetric uniform quantizers (3.5) on the consensus-type scheme (3.3). We first use two examples to demonstrate that when the uniform quantizers (3.5) are utilized for the controllers (3.3), some undesirable

[1] Namely, every Filippov solution converges to a set where velocities synchronize. However, chattering with very small amplitudes (less than 0.05 in the shown simulation run) takes place in steady states. This is due to sliding modes along the synchronized manifolds of velocities.

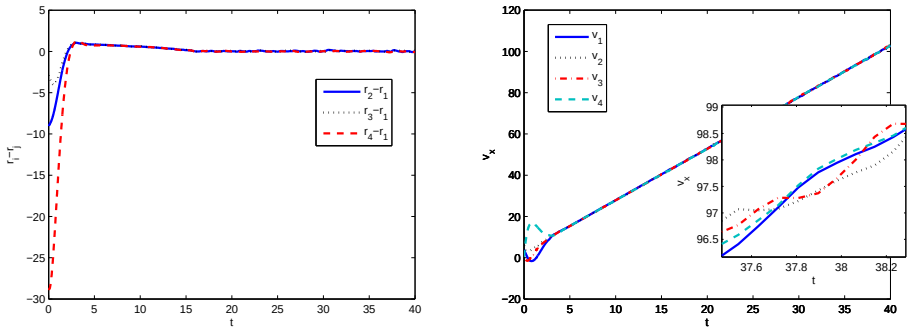

(a) $r_i(t) - r_1(t)$, $i = 2, 3, 4$. (b) $v_i(t)$, $i = 1, 2, 3, 4$.

Figure 3.5: *Synchronized motion with unbounded agent velocities with the uniform quantizers (3.5).*

steady-state behaviors may arise for the multi-agent systems (3.1). In the first example, we show that, although the agents may get synchronized in the sense that they move with almost the same velocity and almost the same time-varying position asymptotically, the agents' velocities grow unbounded, which cannot happen in reality. In the second case, we show an even worse case when the agents' positions never coincide with one another.

We take the neighbor relationship graphs $\mathbb{G}_1$ and $\mathbb{G}_2$ both to be the graph on the upper right of Figure 3.1. We set $\delta_u = 1$ and initialize the system in the same way as what we have done for the simulation of the system with the logarithmic quantizer in Section 3.3. We show the simulation results in Figure 3.5. It is clear that as the system evolves, the agents' positions become the same, their velocities keep oscillating around the time-varying average velocity of the whole group $\frac{1}{N}\sum_{i=1}^{N} v_i(t)$. Obviously, as indicated by Figure 3.5(b), the agents' velocities grow unbounded as t increases.

Next we show that the steady states of the system can be even more undesirable, namely the agents' positions always differ from one another. Towards this end, we take the neighbor relationship graphs $\mathbb{G}_1$ and $\mathbb{G}_2$ both to be the graph on the upper left of Figure 3.1. We keep all the other setting the same as before. The simulated system dynamics are shown in Figure 3.6. It is clear that the agents' positions do not become the same while their velocities oscillate around the average velocity $\frac{1}{N}\sum_{i=1}^{N} v_i(t)$ and become unbounded. In particular, in Figure 3.6(a) the values of r_1, r_2, and r_3 become the same for almost every t and r_4 keeps a distance of 1 from the rest.

Now we explain the observed behavior in Figure 3.5(b) and Figure 3.6(b). We consider again the Filippov solutions to system (3.1) and (3.3) with the chosen uniform quantizer. To simplify the discussion, here we focus on the case when the positions r_i and the velocities v_i, $i = 1, \cdots, N$, are scalars. The analysis can be extended straightforwardly to the higher dimensional case. From the definition for the uniform quantizer in (3.5), we know that

$$F[q_u^*(r_i - r_j)] + F[q_u^*(r_j - r_i)] = q_u^*(r_i - r_j) + q_u^*(r_j - r_i) = -\delta_u \tag{3.41}$$

when $r_i - r_j \neq k\delta_u$, where k are integers, and

$$\begin{aligned} &F[q_u^*(r_i - r_j)] + F[q_u^*(r_j - r_i)] \\ &= [(k-1)\delta_u, k\delta_u] + [-(k+1)\delta_u, -k\delta_u] \\ &= -\delta_u\,[0, 2] \end{aligned} \tag{3.42}$$

when $r_i - r_j = k\delta_u$. From (3.42), we have

$$\begin{aligned} \sum_{i=1}^{N}\sum_{j=1}^{N} a_{ij} F[q_u^*(r_i - r_j)] &= \frac{1}{2}\sum_{i=1}^{N}\sum_{j=1}^{N} a_{ij}\, F[q_u^*(r_i - r_j)] + \frac{1}{2}\sum_{j=1}^{N}\sum_{i=1}^{N} a_{ji}\, F[q_u^*(r_j - r_i)] \\ &= \frac{1}{2}\sum_{i=1}^{N}\sum_{j=1}^{N} a_{ij}\, F[q_u^*(r_i - r_j)] + \frac{1}{2}\sum_{i=1}^{N}\sum_{j=1}^{N} a_{ij}\, F[q_u^*(r_j - r_i)] \\ &= \frac{1}{2}\sum_{i=1}^{N}\sum_{j=1}^{N} a_{ij}\, \{F[q_u^*(r_i - r_j)] + F[q_u^*(r_j - r_i)]\} \\ &= -\frac{1}{2}\sum_{i=1}^{N}\sum_{j=1}^{N} a_{ij}\delta_u\,[0, 2]\,. \end{aligned}$$

Then in combination with (3.8), we have

$$\begin{aligned} \sum_{i=1}^{N} \dot{v}_i \in &-\sum_{i=1}^{N}\sum_{j=1}^{N} a_{ij}\, F[q_u^*(r_i - r_j)] - \sum_{i=1}^{N}\sum_{j=1}^{N} b_{ij}\, F[q_u^*(v_i - v_j)] \\ &= \frac{1}{2}\sum_{i=1}^{N}\sum_{j=1}^{N} a_{ij}\delta_u\,[0, 2] + \frac{1}{2}\sum_{i=1}^{N}\sum_{j=1}^{N} b_{ij}\delta_u\,[0, 2] \end{aligned} \tag{3.43}$$

Now we claim that $\sum_{i=1}^{N} \dot{v}_i$ is always positive whenever there is at least one pair of $\hat{i}$ and $\hat{j}$, $1 \leqslant \hat{i}, \hat{j} \leqslant N$, such that $r_{\hat{i}} - r_{\hat{j}} \neq k_1\delta_u$ or $v_{\hat{i}} - v_{\hat{j}} \neq k_2\delta_u$ for any integers k_1 and k_2. This is because for such a pair of $\hat{i}$ and $\hat{j}$, it follows from (3.41) and (3.43) that

$$\sum_{i=1}^{N} \dot{v}_i \in \left\{\frac{1}{2}\sum_{i=1}^{N}\sum_{j=1}^{N} a_{ij} - 1\right\}\delta_u\,[0, 2] + \frac{1}{2}\sum_{i=1}^{N}\sum_{j=1}^{N} b_{ij}\delta_u\,[0, 2] + \delta_u \tag{3.44}$$

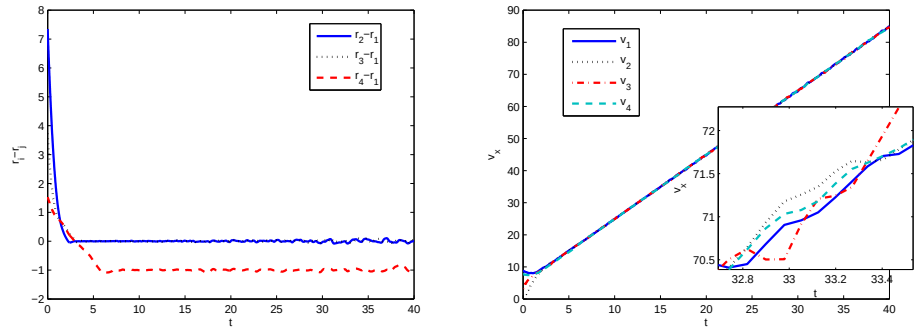

(a) $r_i(t) - r_1(t)$, $i = 2, 3, 4$. (b) $v_i(t)$, $i = 1, 2, 3, 4$.

Figure 3.6: *Agents evolving with different positions and increasing velocities with the uniform quantizers (3.5).*

when $r_{\hat{i}} - r_{\hat{j}} \neq k_1\delta_u$ and

$$\sum_{i=1}^{N} \dot{v}_i \in \frac{1}{2}\sum_{i=1}^{N}\sum_{j=1}^{N} a_{ij}\delta_u\,[0,2] + \left\{\frac{1}{2}\sum_{i=1}^{N}\sum_{j=1}^{N} b_{ij} - 1\right\}\delta_u\,[0,2] + \delta_u \tag{3.45}$$

when $v_{\hat{i}} - v_{\hat{j}} \neq k_2\delta_u$. So in either case, $\sum_{i=1}^{N} \dot{v}_i$ is always positive since the first and second terms of (3.44) and (3.45) are always nonnegative and the third terms are always positive. This gives one of the reasons that the agents' velocities may grow unbounded as t increases.

3.5 More complicated behaviors resulting from network topologies

Up to now, we have assumed that both $\mathbb{G}_1$ and $\mathbb{G}_2$ are undirected. In this section, we show through simulations that when $\mathbb{G}_1$ and $\mathbb{G}_2$ are directed, more undesirable system behaviors may arise. In (Yu et al. 2010b), some necessary and sufficient conditions based on directed neighbor relationship graphs have been constructed for reaching consensus in multi-agent systems with second-order agent dynamics without quantization. However, those conditions are not applicable to the case with quantization. We use again an example to illustrate this.

We take both $\mathbb{G}_1$ and $\mathbb{G}_2$ to be the directed ring shown on the bottom of Figure 3.1, which is balanced and contains a directed spanning tree (Cao et al. 2008). The other simulation conditions are set to be the same as in the simulation in Section 3.3.

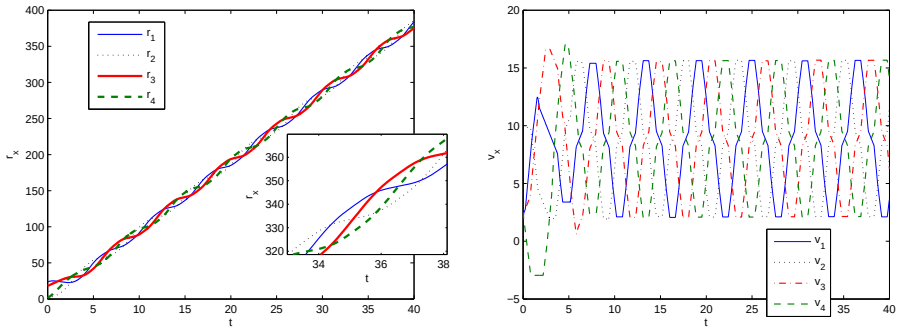

(a) $r_i(t)$, $i = 1, 2, 3, 4$. (b) $v_i(t)$, $i = 1, 2, 3, 4$.

Figure 3.7: *Oscillating behavior when $\mathbb{G}_1$ and $\mathbb{G}_2$ are directed rings with the logarithmic quantizers.*

Although the logarithmic quantizers are used, neither the agents' positions $r_i(t)$ nor their velocities $v_i(t)$ can be synchronized, which keep oscillating as shown in Figure 3.7 (a) and (b) respectively. Note that the same system without quantization satisfies the conditions stipulated in Theorem 1 of (Yu et al. 2010b) and thus can get synchronized. So conditions for synchronized motions with directed $\mathbb{G}_1$ and $\mathbb{G}_2$ need to be further investigated in the future.

3.6 Concluding remarks

We have shown the effects of different quantizers on the steady-state behavior of teams of mobile agents with second-order dynamics. We have studied the performances of the chosen logarithmic and uniform quantizers respectively. It has been emphasized that for coordinating agents with higher-order dynamics, the quantization effects of various quantizers are different and undesirable system behavior, e.g. oscillations, may happen even when the same system without quantization is stable.

It is of interest to look into more different quantization schemes. We are also interested in understanding how different non-standard solutions to nonsmooth systems can be used in the analysis of the quantization effects. More coordination strategies other than the consensus-type algorithms will be studied in the future to obtain more general conclusions about the quantization effects on coordination tasks in multi-agent systems in general.

Chapter 4

Formation Control for Mobile Agents using Coarse Measurements

The chapter studies the performances of the popular gradient-based formation control strategies for teams of autonomous agents when the agents' range measurements are coarse. Since the dynamics of the resulting closed-loop system are discontinuous, Filippov solutions of non-smooth dynamical systems are introduced. Similar to the existing stability results for triangular formations with precise range measurements, we prove that under coarse range measurements, the convergence to the desired formation is almost global except for initially collinearly positioned formations. More importantly, we are able to make stronger statements that the convergence takes place within finite time and that the settling time can be determined by the geometric information of the initial shape of the formation. Simulation and experimental results are provided to illustrate the theoretical analysis. The results presented in this chapter have been submitted for publication (Liu et al. n.d.).

4.1 Introduction

Cooperative control for teams of autonomous robots has been extensively studied in the last decade (Bullo et al. 2009, Fink et al. 2013). One typical coordination task is formation keeping in which a team of mobile agents is required to move collaboratively so that the overall team manoeuvres as a whole with a prescribed formation shape (Anderson et al. 2008, Krick et al. 2009, Cao et al. 2011, Grocholsky et al. 2008, Stump et al. 2009, Turpin et al. 2012). The biggest challenge in such formation-keeping tasks is that each agent has only limited local information about its neighboring agents while the success of the team tasks can only be evaluated globally. Various ideas have been proposed to address this challenge (Krick et al. 2009, Smith et al. 2006). In particular, controlling triangular formations has been identified to be the benchmark case, since these formations are small enough to allow global stability analysis while still exhibiting interesting behaviors inherently related to the rigidity properties of a formation (Cao and Morse 2011).

However, most of the existing work assumes that the agents are able to obtain the precise information about the relative positions of their neighboring agents. In this chapter, we look into the more challenging case when the range measurements are carried out by coarse sensing. In practice, agents can sense the directions of their neighboring agents through bearing sensors, such as acoustic or infrared sensors, which have a range of low-price choices (Quigley et al. 2010). But it is more expensive to acquire precise distance information through range sensors, such as laser sensors (Guo et al. 2009). This motivates researchers to look into the scenarios when range measurements are acquired in their quantized forms (Frasca et al. 2009, Ceragioli et al. 2011, Liu et al. 2012). To maximally reduce the requirements for sensing and computation capabilities, existing work (Cortés 2006, Chen, Lewis and Xie 2011, De Persis et al. 2010) has attempted to deduce theoretical stability results for formation control or consensus problems in simplified settings when controllers use coarsely quantized information.

Along this line of research, in this chapter we propose the gradient-based formation control strategy for a team of autonomous agents when agents' range measurements are coarse. We focus on cyclic triangular formations since it is the building block for controlling bigger formations and allows rigorous global stability analysis. The formation control strategy utilizing coarsely quantized range measurements has the additional advantage in application that the agents' velocities become normalized and computations are thus greatly simplified. However, since the continuous-time model describing the resulting behavior of the overall system is non-smooth, we have to apply tools from non-smooth analysis to analyze the performances of the controllers. We are able to prove the convergence results using the Lyapunov function method, and show the set of feasible initial positions of the agents to achieve prescribed triangular formations. Compared with the convergence results in (Cao and Morse 2011), a much stronger statement is proven that finite time convergence can be achieved, which is especially appealing if one wants to apply similar control strategies to larger formations in practice.

The rest of the chapter is organized as follows. Our research problem is formulated in Section 4.2. Then in Section 4.3, we provide the convergence analysis results using tools from nonsmooth analysis. Furthermore we prove the finite-time convergence in Section 4.4. Experimental and numerical examples are given in Section 4.5 to illustrate our theoretical analysis. In Section 4.6, we make concluding remarks and suggest possible extensions of this work.

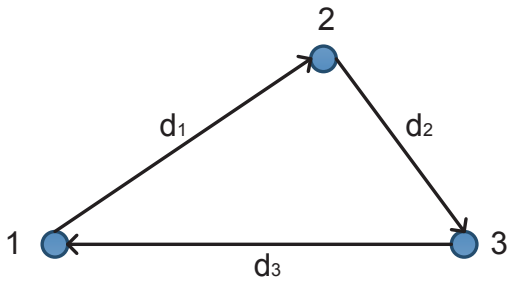

Figure 4.1: *Clockwise triangular formation.*

4.2 Problem formulation

We consider a formation in the plane consisting of three autonomous agents labeled by 1, 2, and 3, shown in Fig 4.1. For $i \in \{1, 2, 3\}$, we write $[i]$ for the label of agent i's leader where $[1] = 2$, $[2] = 3$ and $[3] = 1$. We assume that the desired distance between agents i and $[i]$ is d_i; here the d_i are positive numbers which satisfy the triangle inequalities:

$$d_1 < d_2 + d_3\,, \quad d_2 < d_1 + d_3\,, \quad d_3 < d_1 + d_2\,. \tag{4.1}$$

Note that there are two distinct triangular formations which satisfy the desired distance constraints. The first is shown in Fig. 4.1 and referred to as a clockwise triangle. The second, called a counterclockwise triangle, is the triangle which results when the triangle shown in Fig. 4.1 is flipped over.

We write x_i for the Cartesian coordinate vector of agent i in some fixed global coordinate system in the plane. In (Cao et al. 2007), Cao et al have studied how to control three autonomous agents to achieve a prescribed triangular formation, for which the agents' dynamics are described by

$$\begin{aligned}
\dot{x}_1 &= -(x_1 - x_2)(||x_1 - x_2||^2 - d_1^2)\,,\\
\dot{x}_2 &= -(x_2 - x_3)(||x_2 - x_3||^2 - d_2^2)\,,\\
\dot{x}_3 &= -(x_3 - x_1)(||x_3 - x_1||^2 - d_3^2)\,.
\end{aligned} \tag{4.2}$$

In their setting, it is assumed that for $i \in \{1, 2, 3\}$, agent i can measure precisely the relative position $x_i - x_{[i]}$ of agent $[i]$ in its own coordinate system. It has been proved that under such gradient-based control laws, system (4.2) can be stabilized almost globally to an equilibrium corresponding to the triangular formation with

the desired shape. However, in this chapter we investigate the much more challenging scenario where each agent cannot measure precisely the relative distances. To be more specific, we assume that in the three-agent system shown in Fig. 4.1, agent i can sense the direction $\frac{x_{[i]}-x_i}{||x_{[i]}-x_i||}$ of its non-collocated leader $[i]$ in its own local coordinates through a bearing sensor, and measure whether the relative distance is greater or less than the desired distance through a crude range sensor. Let the sign function $\text{sgn}(\cdot) : \mathbb{R} \to \mathbb{R}$ be defined by

$$\text{sgn}(a) = \begin{cases} +1 & a > 0; \\ 0 & a = 0; \\ -1 & a < 0. \end{cases} \tag{4.3}$$

Then the agents' coarse measurements about the range $x_i - x_{[i]}$ are in the form of the trinary value $\text{sgn}(||x_i - x_{[i]}|| - d_i)$. With such measurements, we investigate the performance of the gradient-based control law corresponding to (4.2) and obtain the new set of equations describing the system's dynamics

$$\begin{aligned} \dot{x}_1 &= -\frac{(x_1 - x_2)}{||x_1 - x_2||} \text{sgn}(||x_1 - x_2|| - d_1)\,, \\ \dot{x}_2 &= -\frac{(x_2 - x_3)}{||x_2 - x_3||} \text{sgn}(||x_2 - x_3|| - d_2)\,, \\ \dot{x}_3 &= -\frac{(x_3 - x_1)}{||x_3 - x_1||} \text{sgn}(||x_3 - x_1|| - d_3)\,. \end{aligned} \tag{4.4}$$

Let

$$z_i \triangleq x_i - x_{[i]}, \qquad e_i \triangleq ||z_i|| - d_i\,, \tag{4.5}$$

for $i = 1, 2, 3$. And let

$$x = \begin{bmatrix} x_1 \\ x_2 \\ x_3 \end{bmatrix}, \quad z = \begin{bmatrix} z_1 \\ z_2 \\ z_3 \end{bmatrix}, \quad e = \begin{bmatrix} e_1 \\ e_2 \\ e_3 \end{bmatrix}. \tag{4.6}$$

Then system (4.4) is defined on the set

$$\mathcal{X} = \left\{ x \in \mathbb{R}^6 : ||x_i - x_{[i]}|| > 0, \text{ for all } i = 1, 2, 3 \right\}.$$

Let $\mathcal{X}^c$ be the complement of $\mathcal{X}$ in $\mathbb{R}^6$, i.e.,

$$\mathcal{X}^c = \mathbb{R}^6 \backslash \mathcal{X} = \left\{ x \in \mathbb{R}^6 : ||x_i - x_{[i]}|| = 0, \text{ for some } i = 1, 2, 3 \right\}.$$

Now we study the stability of system (4.4). Towards this end, we first rewrite the dynamics (4.4) using z_i, and study the stability of the resulting z-system

$$\begin{aligned}
\dot{z}_1 &= -\frac{z_1}{||z_1||}\,\mathrm{sgn}(||z_1|| - d_1) + \frac{z_2}{||z_2||}\,\mathrm{sgn}(||z_2|| - d_2)\,, \\
\dot{z}_2 &= -\frac{z_2}{||z_2||}\,\mathrm{sgn}(||z_2|| - d_2) + \frac{z_3}{||z_3||}\,\mathrm{sgn}(||z_3|| - d_3)\,, \\
\dot{z}_3 &= -\frac{z_3}{||z_3||}\,\mathrm{sgn}(||z_3|| - d_3) + \frac{z_1}{||z_1||}\,\mathrm{sgn}(||z_1|| - d_1)\,,
\end{aligned} \tag{4.7}$$

which is defined on the set

$$\mathcal{Z} = \left\{ z \in \mathbb{R}^6 : ||z_i|| > 0, \text{ for all } i = 1, 2, 3 \right\} .$$

Let $\mathcal{Z}^c$ be the complement of $\mathcal{Z}$ in $\mathbb{R}^6$, i.e.,

$$\mathcal{Z}^c = \mathbb{R}^6 \backslash \mathcal{Z} = \left\{ z \in \mathbb{R}^6 : ||z_i|| = 0, \text{ for some } i = 1, 2, 3 \right\} .$$

Obviously, the set $\mathcal{Z}$ is open and connected. One can easily check that $x \in \mathcal{X}$ if and only if $z \in \mathcal{Z}$. It turns out that the z-system (4.7) is easier to work with for convergence analysis, which we will present in detail in the next section. However, to study the system's dynamics, we need to first specify what we mean by the solutions to the system. Since the vector fields on the right-hand sides of (4.4) and (4.7) are discontinuous, we consider Filippov solutions.

First we use Lemma 2.2 to show the existence of the Filippov solutions to system (4.4) and system (4.7). Since the Euclidean norms of the right-hand sides of (4.7) are upper bounded by 2 on $\mathcal{Z}$, the conditions in Lemma 2.2 are satisfied and thus the Filippov solutions to (4.7) exist when $z \in \mathcal{Z}$. So the Filippov solution to (4.7) exists for all $t \geqslant 0$ when the system is well defined. One can use similar arguments to show that the Filippov solution to (4.4) also exists for all $t \geqslant 0$ when $x \in \mathcal{X}$. In the next section, we present the convergence analysis for the Filippov solutions to the z-system.

4.3 Convergence analysis

Let $g(z)$ be the vector field on the right-hand side of (4.7). We consider the differential inclusions $\dot{z} \in F[g(z)]$ of system (4.7), where $F[\cdot]$ is the set-valued map corresponding to the Filippov solutions.

Let $\mathcal{N}$ be the set of points in $\mathbb{R}^6$ corresponding to agent positions in the plane which are collinear, namely

$$\mathcal{N} \triangleq \left\{ z : \mathrm{rank} \begin{bmatrix} z_1 & z_2 & z_3 \end{bmatrix} < 2, z_1 + z_2 + z_3 = 0 \right\} . \tag{4.8}$$

One can easily see that the positions of the three agents x_1, x_2, x_3 are collinear if and only if z_1, z_2, z_3 are collinear.

Note that $\mathcal{N}$ is a closed manifold containing the set $\mathcal{Z}^c$. Now we show that if a solution to (4.7) starts outside of $\mathcal{N}$ and thus in $\mathcal{Z}$ at $t = 0$, it remains outside of $\mathcal{N}$ for all $t > 0$; in other words, the evolution of the z-system is well defined when $z(0) \notin \mathcal{N}$.

Lemma 4.1 *If a solution to (4.7) starts outside of $\mathcal{N}$ at $t = 0$, it cannot converge to $\mathcal{Z}^c$ for any $t > 0$.*

Proof: We prove by contradiction. Suppose the contrary is true. Then for some $z(0) \notin \mathcal{N}$, there exists a $T > 0$, which can approach infinity, such that $z(t)$ approaches $\mathcal{Z}^c$ as t approaches T. It is straightforward to check that $\det\begin{bmatrix} z_1 & z_2 \end{bmatrix} = -\det\begin{bmatrix} z_1 & z_3 \end{bmatrix}$. This and the definition of $\mathcal{N}$ in (4.8) imply that

$$\mathcal{N} = \left\{ z : \det\begin{bmatrix} z_1 & z_2 \end{bmatrix} = 0 \right\} . \tag{4.9}$$

So the assumption about T implies that

$$\lim_{t \to T} \det\begin{bmatrix} z_1 & z_2 \end{bmatrix} = 0. \tag{4.10}$$

Furthermore, from the definition for $\mathcal{Z}^c$, we know that $\lim_{t \to T} ||z_i(t)|| = 0$ for some $i \in \{1, 2, 3\}$. Without loss of generality, we take $i = 1$. Then for any δ satisfying $0 < \delta \ll \min\{d_1, d_2, d_3\}$, there exists a finite $t_1 < T$ such that $||z_1(t)|| \leqslant \delta$ for all $t > t_1$. Now for any $t_1 < t < T$, we consider two cases:
Case 1: $||z_2(t)|| \geqslant 3\delta$ and $||z_3(t)|| \geqslant 3\delta$. In this case, we have

$$\begin{aligned} & -\left(\frac{\text{sgn}(e_1(t))}{||z_1(t)||} + \frac{\text{sgn}(e_2(t))}{||z_2(t)||} + \frac{\text{sgn}(e_3(t))}{||z_3(t)||} \right) \\ > \; & \frac{1}{\delta} - \frac{1}{||z_2(t)||} - \frac{1}{||z_3(t)||} \\ \geqslant \; & \frac{1}{\delta} - \frac{1}{3\delta} - \frac{1}{3\delta} = \frac{1}{3\delta} . \end{aligned}$$

Case 2: $||z_2(t)|| < 3\delta$ or $||z_3(t)|| < 3\delta$. Then we have

$$-\left(\frac{\text{sgn}(e_1(t))}{||z_1(t)||} + \frac{\text{sgn}(e_2(t))}{||z_2(t)||} + \frac{\text{sgn}(e_3(t))}{||z_3(t)||} \right) > \frac{1}{\delta} + \frac{1}{3\delta} + \frac{1}{4\delta} > \frac{1}{3\delta} .$$

In either case, we always have

$$-\left(\frac{\text{sgn}(e_1(t))}{||z_1(t)||} + \frac{\text{sgn}(e_2(t))}{||z_2(t)||} + \frac{\text{sgn}(e_3(t))}{||z_3(t)||} \right) > \frac{1}{3\delta} \qquad \text{for } t_1 < t < T. \tag{4.11}$$

Now we look more carefully at the evolution of system (4.7). Let $\mathcal{D}$ denote the set of all the discontinuity points of its right-hand side

$$\mathcal{D} \triangleq \{z : e_1\, e_2\, e_3 = 0\}\ .$$

Then along any solution to (4.7), one has

$$\frac{d}{dt}\det\begin{bmatrix} z_1 & z_2\end{bmatrix} = -\left(\frac{\mathrm{sgn}e_1}{||z_1||} + \frac{\mathrm{sgn}e_2}{||z_2||} + \frac{\mathrm{sgn}e_3}{||z_3||}\right)\det\begin{bmatrix} z_1 & z_2\end{bmatrix} \tag{4.12}$$

when $z \notin \mathcal{D}$; and

$$\frac{d}{dt}\det\begin{bmatrix} z_1 & z_2\end{bmatrix} \in -\left(\frac{F[\mathrm{sgn}e_1]}{||z_1||} + \frac{F[\mathrm{sgn}e_2]}{||z_2||} + \frac{F[\mathrm{sgn}e_3]}{||z_3||}\right)\det\begin{bmatrix} z_1 & z_2\end{bmatrix} \tag{4.13}$$

when $z \in \mathcal{D}$. Note that

$$\det\begin{bmatrix} z_1(t) & z_2(t)\end{bmatrix} = e^{-\int_{t_1}^{t}\left(\frac{\mathrm{sgn}e_1(s)}{||z_1(s)||}+\frac{\mathrm{sgn}e_2(s)}{||z_2(s)||}+\frac{\mathrm{sgn}e_3(s)}{||z_3(s)||}\right)ds}\det\begin{bmatrix} z_1(t_1) & z_2(t_1)\end{bmatrix} \tag{4.14}$$

for $t \geqslant t_1$ because of (4.12) and (4.13). Hence,

$$\det\begin{bmatrix} z_1(t) & z_2(t)\end{bmatrix} > e^{\frac{t-t_1}{3\delta}}\det\begin{bmatrix} z_1(t_1) & z_2(t_1)\end{bmatrix}\ ,$$

for all $t \in (t_1, T)$. On the other hand,

$$\det\begin{bmatrix} z_1(t_1) & z_2(t_1)\end{bmatrix} = e^{-\int_{0}^{t_1}\left(\frac{\mathrm{sgn}e_1(s)}{||z_1(s)||}+\frac{\mathrm{sgn}e_2(s)}{||z_2(s)||}+\frac{\mathrm{sgn}e_3(s)}{||z_3(s)||}\right)ds}\det\begin{bmatrix} z_1(0) & z_2(0)\end{bmatrix}\ .$$

and $\det\begin{bmatrix} z_1(0) & z_2(0)\end{bmatrix}$ is bounded away from below from zero since $z(0)$ starts outside of $\mathcal{N}$. Thus, $\det\begin{bmatrix} z_1(t_1) & z_2(t_1)\end{bmatrix}$ is also bounded away from below from zero. Therefore, $\det\begin{bmatrix} z_1(t) & z_2(t)\end{bmatrix} > \det\begin{bmatrix} z_1(t_1) & z_2(t_1)\end{bmatrix}$ is bounded from below from zero for any $t \in (t_1, T)$, which contradicts (4.10). This completes the proof. □

To show system (4.7) is well defined, it remains to be shown that it is so when $z(0) \in \mathcal{N} \cap \mathcal{Z}$.

Lemma 4.2 *If a solution to (4.7) starts in $\mathcal{N} \cap \mathcal{Z}$, it remains in $\mathcal{N} \cap \mathcal{Z}$ for all $t > 0$.*

Proof: One can easily check that $\mathcal{N}$ is positively invariant since if $\det\begin{bmatrix} z_1 & z_2\end{bmatrix} = 0$ at $t = 0$, then $\det\begin{bmatrix} z_1 & z_2\end{bmatrix} = 0$ for all $t > 0$ from (4.12) and (4.13). So for a solution starting in $\mathcal{N} \cap \mathcal{Z}$, it remains in $\mathcal{N}$, and thus z_1, z_2 and z_3 remain collinear. For this reason, one can always use the coordinate transformation aligning the coordinate axis with $\mathcal{N}$ to write z_1, z_2, z_3 into scalars. To simplify notations, we still use z_i to denote the resulting scalars and rewrite (4.7) into

$$\begin{aligned}
\dot{z}_1 &= -\mathrm{sgn}(z_1)\,\mathrm{sgn}(|z_1| - d_1) + \mathrm{sgn}(z_2)\,\mathrm{sgn}(|z_2| - d_2)\,,\\
\dot{z}_2 &= -\mathrm{sgn}(z_2)\,\mathrm{sgn}(|z_2| - d_2) + \mathrm{sgn}(z_3)\,\mathrm{sgn}(|z_3| - d_3)\,,\\
\dot{z}_3 &= -\mathrm{sgn}(z_3)\,\mathrm{sgn}(|z_3| - d_3) + \mathrm{sgn}(z_1)\,\mathrm{sgn}(|z_1| - d_1)\,.
\end{aligned} \tag{4.15}$$

For any $i = 1, 2, 3$, if $0 < |z_i| < d_i$, then the derivative of z_i^2 along a solution to (4.15) is

$$\frac{d\, z_i^2}{dt} \in \left\{ |z_i| \left(1 + \text{sgn} z_i \cdot \text{sgn} z_{[i]} \cdot \gamma_{[i]}\right) : \quad \gamma_{[i]} \in [-1, 1] \right\}.$$

So if there exists a t^* such that $0 < |z_i(t^*)| < d_i$, then $|z_i(t)| \geqslant |z_i(t^*)|$ for $t > t^*$ whenever $|z_i(t)| < d_i$. Hence, $|z_i|$ cannot approach 0 for any t. □

From Lemmas 4.1 and 4.2, we have shown that system (4.7) is well defined. We summarize it as follows.

Proposition 4.1 *If a solution to (4.7) starts in $\mathcal{Z}$, it remains in $\mathcal{Z}$ for all $t > 0$.*

The set of the equilibrium points of the z-system (4.7) is the union of the two sets $\mathcal{E}$ and $\mathcal{M}$ defined as follows

$$\mathcal{E} \triangleq \{z : e_1 = e_2 = e_3 = 0\} \text{ and} \tag{4.16}$$

$$\mathcal{M} \triangleq \left\{ z : \frac{z_1}{||z_1||}\text{sgn}\, e_1 = \frac{z_2}{||z_2||}\text{sgn}\, e_2 = \frac{z_3}{||z_3||}\text{sgn}\, e_3 \right\}.$$

One can check that $\mathcal{M}$ is a subset of $\mathcal{N}$. Using similar arguments as those to prove Lemma 2 in (Cao et al. 2007), one can prove the following lemma for the sets $\mathcal{N}$ and $\mathcal{E}$.

Lemma 4.3 (Cao et al. 2007) *$\mathcal{N}$ and $\mathcal{E}$ are disjoint sets.*

Obviously, $\mathcal{N}$ and $\mathcal{E}$ are closed sets. In addition, $\mathcal{M}$ and $\mathcal{E}$ are also disjoint sets since $\mathcal{M} \subset \mathcal{N}$. That $\mathcal{N}$ might be the place where the triangular formation will fail is further underscored by the fact that $\mathcal{N}$ is an invariant manifold; in other words, formations which are initially collinear, remain collinear forever. This is true since if $\det\begin{bmatrix} z_1 & z_2 \end{bmatrix} = 0$ at $t = 0$, then $\det\begin{bmatrix} z_1 & z_2 \end{bmatrix} = 0$ for all $t > 0$ as shown in (4.12) and (4.13).

4.3.1 Lyapunov-function based analysis

The main result in this chapter that we want to prove is as follows.

Theorem 4.1 *All the Filippov solutions to system (4.7) starting outside of $\mathcal{N}$, converges to a finite limit in $\mathcal{E}$. Furthermore, the convergence is achieved within finite time.*

The set of points $\mathbb{R}^6 \backslash \mathcal{N}$ consists of two disjoint sets, one for which $\det\begin{bmatrix} z_1 & z_2 \end{bmatrix} > 0$ and the other for which $\det\begin{bmatrix} z_1 & z_2 \end{bmatrix} < 0$. Once this theorem is proved, it will be easy to verify that formations starting at positions such that $\det\begin{bmatrix} z_1 & z_2 \end{bmatrix} < 0$, converge to the positively oriented triangular formations in $\mathcal{E}$ whereas formations starting at points such that $\det\begin{bmatrix} z_1 & z_2 \end{bmatrix} > 0$, converge to the corresponding negatively oriented triangular formation in $\mathcal{E}$.

The proof of Theorem 4.1 involves several steps. First we focus on the convergence and later on check the convergence speed. To begin with, we introduce some notations. We use $\langle \cdot, \cdot \rangle : \mathbb{R}^n \times \mathbb{R}^n \mapsto \mathbb{R}$ to denote the inner product, and $\theta(a, b)$ the angle between any two vectors $a, b \in \mathbb{R}^2$. For the two vectors $z_i, z_{[i]}$, one has the fact that $\cos\, \theta(z_i, z_{[i]}) = \frac{\langle z_i\, , z_{[i]} \rangle}{||z_i|| \cdot ||z_{[i]}||}$.

Theorem 4.2 *All the Filippov solutions to system (4.7) are bounded and converge globally to the set $\mathcal{E} \cup \mathcal{M}$.*

Proof: We choose the candidate Lyapunov function

$$V(z(t)) = \frac{1}{4}\left((||z_1||^2 - d_1^2)^2 + (||z_2||^2 - d_2^2)^2 + (||z_3||^2 - d_3^2)^2\right) . \tag{4.17}$$

When $z(t) \notin \mathcal{D}$,

$$\begin{aligned}
& \frac{d}{dt} V(z(t)) \\
= & \sum_{i=1}^{3} (||z_i||^2 - d_i^2) z_i^T \left(-\frac{z_i}{||z_i||} \operatorname{sgn}(||z_i|| - d_i) + \frac{z_{[i]}}{||z_{[i]}||} \operatorname{sgn}(||z_{[i]} - d_{[i]}||) \right) \\
= & -\sum_{i=1}^{3} |\, ||z_i||^2 - d_i^2| \cdot\, ||z_i||\, \left(1 - \frac{\langle z_i, z_{[i]} \rangle}{||z_i|| \cdot ||z_{[i]}||} \operatorname{sgn}(||z_i|| - d_i) \operatorname{sgn}(||z_{[i]}|| - d_{[i]}) \right) \\
\leqslant & \; 0
\end{aligned}$$

with the equality sign holds if and only if $\frac{z_1}{||z_1||}\operatorname{sgn}(||z_1|| - d_1) = \frac{z_2}{||z_2||}\operatorname{sgn}(||z_2|| - d_2) = \frac{z_3}{||z_3||}\operatorname{sgn}(||z_3|| - d_3)$.

When $z(t) \in \mathcal{D}$, one has $\frac{d}{dt} V(z(t)) \in \dot{\overline{V}}(z(t))$, where the set-valued derivative $\dot{\overline{V}}(z(t))$ is given by $\dot{\overline{V}}(z(t)) = \{\langle \nabla V(z), \nu \rangle, \nu \in F[g(z)]\}$, and the column vector $\nabla V(z)$ is the gradient of $V(z)$.

If $z \in \mathcal{E} \subset \mathcal{D}$, then $\nabla V(z) = \mathbf{0}$ and therefore $\dot{\overline{V}}(z(t)) = \{0\}$; if on the other hand, $z \in \mathcal{D} \backslash \mathcal{E}$, then there must exist at least one i such that $||z_i|| - d_i = 0$ and at least one

$j \neq i$ such that $||z_j|| - d_j \neq 0$. Denote the label of the remaining agent by k. Then

$$\begin{aligned}\langle \nabla V(z), \nu \rangle &= (||z_k||^2 - d_k^2) z_k^T \left(-\frac{z_k}{||z_k||} \gamma_k + \frac{z_j}{||z_j||} \operatorname{sgn}(||z_j|| - d_j) \right) \\ &\quad + (||z_j||^2 - d_j^2) z_j^T \left(-\frac{z_j}{||z_j||} \operatorname{sgn}(||z_j|| - d_j) + \frac{z_i}{||z_i||} \gamma_i \right)\end{aligned}$$

where $\gamma_i \in [-1, 1]$ and $\gamma_k \in [-1, 1]$. In particular, γ_k can be reduced to $\operatorname{sgn}(||z_k|| - d_k)$ if $||z_k|| - d_k \neq 0$. The above inequality can be further written into

$$\begin{aligned}\langle \nabla V(z), \nu \rangle &= -| \, ||z_k||^2 - d_k^2| \cdot ||z_k|| \left(1 - \frac{\langle z_k, z_j \rangle}{||z_k|| \cdot ||z_j||} \gamma_k \operatorname{sgn}(||z_j|| - d_j) \right) \\ &\quad -| \, ||z_j||^2 - d_j^2| \cdot ||z_j|| \left(1 - \frac{\langle z_j, z_i \rangle}{||z_j|| \cdot ||z_i||} \gamma_i \operatorname{sgn}(||z_j|| - d_j) \right) \\ &\leqslant 0\end{aligned}$$

with the equality sign holds if and only if $\frac{z_j}{||z_j||} \operatorname{sgn}(||z_j|| - d_j) = \frac{z_i}{||z_i||} \gamma_i = \frac{z_k}{||z_k||} \gamma_k$ and $z \in \mathcal{N} \cap \mathcal{D}$.

Summarizing the discussion so far, we have shown that for all $z \in \mathcal{Z}$, $\max \dot{\overline{V}}(z(t)) \leqslant 0$, and that $0 \in \dot{\overline{V}}(z(t))$ if and only if $z \in \mathcal{E} \cup \overline{\mathcal{M}}$. Hence, for all $t \geqslant 0$, we have $V(z(t))$ is non-increasing and satisfies $0 \leqslant V(z(t)) \leqslant V(z(0))$. In view of V's definition, the z_i are bounded for all $t \geqslant 0$. Furthermore, applying LaSalle's invariance principle for differential inclusions (Bacciotti and Ceragioli 1999, Cortés 2008a, Cortés 2008b), any solution to the differential inclusion converges to the largest weakly invariant set in the closure of $\mathcal{E} \cup \mathcal{M}$. Since $\mathcal{E} \cup \mathcal{M}$ is the set of equilibria of (4.7), we know $\mathcal{E} \cup \mathcal{M}$ is weakly invariant. So we arrive at the conclusion that any solution $z(t)$ of the differential inclusion $\dot{z} \in F[g(z)]$ is bounded and converges to the equilibrium set $\mathcal{E} \cup \mathcal{M}$. □

In fact, one can make a stronger claim about the boundedness of z_i.

Lemma 4.4 *It holds that*

$$||z_i|| \leqslant d_i + \sqrt{2} \, [V(z(0))]^{\frac{1}{4}}, \quad \textit{for } i = 1, 2, 3,$$

where V is defined in (4.17).

Proof: Since $V(z(t)) \leqslant V(z(0))$, we know that $\frac{1}{4} \sum_{i=1}^{3} (||z_i||^2 - d_i^2)^2 \leqslant V(z(0))$. It implies $\frac{1}{4} (||z_i||^2 - d_i^2)^2 \leqslant V(z(0))$ for $i = 1, 2, 3$. Then, $||z_i||^2 \leqslant d_i^2 + 2[V(z(0))]^{1/2}$. Using the fact that the inequality $a + b \leqslant (\sqrt{a} + \sqrt{b})^2$ holds for any nonnegative numbers a and b, we conclude that $||z_i|| \leqslant d_i + \sqrt{2}[V(z(0))]^{1/4}$. □

Since for any $z \in \mathcal{M}$, it holds that $\dot{z} = 0$, we know $\mathcal{M}$ is an invariant manifold; moreover along any trajectory in $\mathcal{M}$, the three agents move at the same constant

velocity. Thus x_1, x_2, x_3 could drift to infinity together while the $||x_i - x_{[i]}||$ still converge to some finite positive numbers. So although as we have proved, the solutions to (4.7) are always bounded, those to (4.4) are not necessarily so. Examples to show such cases will be provided in the simulation section.

Since the largest weakly invariant set $\mathcal{E} \cup \mathcal{M}$ contains the set $\mathcal{M}$ on which the three agents are collinear, it is of interest to characterize those initial conditions under which the asymptotic relative positions of the agents converge to the set $\mathcal{M}$. We will do so in the next subsection.

4.3.2 Different steady states depending on initial conditions

We now turn to the problem of showing that all trajectories starting outside of $\mathcal{N}$ must be bounded away from $\mathcal{M}$, even in the limit as $t \to \infty$. In view of (4.9) and (4.14), it must be true that any trajectory starting outside of $\mathcal{N}$ cannot enter $\mathcal{N}$ {and therefore $\mathcal{M}$} in finite time. It remains to be shown that any such trajectory cannot approach $\mathcal{M}$ even in the limit as $t \to \infty$. To prove this, we need several facts.

Lemma 4.5 (Cao et al. 2007) *It holds that*

$$\mathcal{N} = \mathcal{N}_1 \cup \mathcal{N}_2 \cup \mathcal{N}_3$$

where $\mathcal{N}_i = \{x : x \in \mathcal{N}, ||z_i|| = ||z_{[i]}|| + ||z_{[[i]]}||\}$ *for* $i = 1, 2, 3$.

With Lemma 4.5 at hand, it is possible to write

$$\mathcal{M} = \mathcal{M}_1 \cup \mathcal{M}_2 \cup \mathcal{M}_3$$

where $\mathcal{M}_i = \mathcal{N}_i \cap \mathcal{M}$.

Lemma 4.6 *For any* $x \in \mathcal{M}$,

$$\frac{sgne_1}{||z_1||} + \frac{sgne_2}{||z_2||} + \frac{sgne_3}{||z_3||} \leqslant 0\,.$$

Proof: We will prove this lemma for the case when $x \in \mathcal{M}_1$. Similar arguments work as well when $x \in \mathcal{M}_2$ or $x \in \mathcal{M}_3$. Since $x \in \mathcal{M}_1$, we know that $||z_1|| = ||z_2|| + ||z_3||$. Note that $||z_i|| \neq 0$ for $i = 1, 2, 3$. From the definition of $\mathcal{M}$, we have $e_i \neq 0$ for all $i \in \{1, 2, 3\}$. Since $\frac{z_1}{||z_1||}\text{sgn}e_1 = \frac{z_2}{||z_2||}\text{sgn}e_2$ and $||z_1|| > ||z_2||$, it follows that $\frac{|\text{sgn}e_1|}{||z_1||} \leqslant \frac{|\text{sgn}e_2|}{||z_2||}$. Because of the definition of $\mathcal{M}_1$, we know that z_1 is pointing to the opposite direction with respect to that of z_2 and z_3, which implies $\text{sgn}e_1 \cdot \text{sgn}e_2 \leqslant 0$ and $\text{sgn}e_1 \cdot \text{sgn}e_3 \leqslant 0$. Now suppose $e_1 \leqslant 0$. Then $e_2 \geqslant 0$ and $e_3 \geqslant 0$, which imply that $||z_1|| \leqslant d_1$, $||z_2|| \geqslant d_2$ and $||z_3|| \geqslant d_3$. Consequently $d_1 \geqslant ||z_1|| = ||z_2|| + ||z_3|| \geqslant$

$d_2 + d_3$ which contradicts the triangle inequality $d_1 < d_2 + d_3$. Hence, it must be true that $e_1 \geqslant 0, e_2 \leqslant 0, e_3 \leqslant 0$. In view of the fact $\frac{|\text{sgn}e_1|}{||z_1||} \leqslant \frac{|\text{sgn}e_2|}{||z_2||}$, we know $\frac{\text{sgn}e_1}{||z_1||} + \frac{\text{sgn}e_2}{||z_2||} + \frac{\text{sgn}e_3}{||z_3||} \leqslant \frac{\text{sgn}e_3}{||z_3||} \leqslant 0$. □

Now we are ready to show that any trajectory starting outside of $\mathcal{N}$, cannot approach $\mathcal{M}$ in the limit as $t \to \infty$. Suppose the opposite is true, namely that $x(t)$ is a trajectory starting outside of $\mathcal{N}$ which approaches $\mathcal{M}$ as $t \to \infty$. Then in view of (4.14), (4.9), and the fact that $\mathcal{M} \subset \mathcal{N}$,

$$\lim_{t\to\infty} |\det \begin{bmatrix} z_1 & z_2 \end{bmatrix}| = 0\,. \tag{4.18}$$

We show that this is false in the following. In view of Lemma 4.6, there must be an open set $\mathcal{V}$ containing $\mathcal{M}$ on which the equality in Lemma 4.6 continues to hold. In view of Lemma 4.3 and the fact that $\mathcal{M} \subset \mathcal{N}$, it is possible to choose $\mathcal{V}$ small enough so that in addition to the preceding, $\mathcal{V}$ and $\mathcal{E}$ are disjoint. In order to have $x(t)$ approaching $\mathcal{M}$, it must be true that there exists some finite time t^* such that $x(t) \in \mathcal{V}$ for $t \in [t^*, \infty)$. This implies that $\frac{\text{sgn}e_1}{||z_1||} + \frac{\text{sgn}e_2}{||z_2||} + \frac{\text{sgn}e_3}{||z_3||} \leqslant 0$ for $t > t^*$. In view of (4.14), $\det \begin{bmatrix} z_1(t) & z_2(t) \end{bmatrix} \geqslant \det \begin{bmatrix} z_1(t^*) & z_2(t^*) \end{bmatrix}$ for $t > t^*$. But

$$\det \begin{bmatrix} z_1(t^*) & z_2(t^*) \end{bmatrix} = e^{-\int_0^{t^*} \left(\frac{\text{sgn}e_1(s)}{||z_1(s)||} + \frac{\text{sgn}e_2(s)}{||z_2(s)||} + \frac{\text{sgn}e_3(s)}{||z_3(s)||} \right) ds} \det \begin{bmatrix} z_1(0) & z_2(0) \end{bmatrix}\,.$$

Moveover, $\det \begin{bmatrix} z_1(0) & z_2(0) \end{bmatrix} > 0$ since z starts outside of $\mathcal{N}$. Therefore

$$\det \begin{bmatrix} z_1(t) & z_2(t) \end{bmatrix} \geqslant \det \begin{bmatrix} z_1(t^*) & z_2(t^*) \end{bmatrix} > 0$$

for $t > t^*$, which contradicts (4.18). This completes the proof of Theorem 4.1. □

We have proved that trajectories starting outside of $\mathcal{N}$ cannot approach $\mathcal{M}$. On the other hand, any trajectory starting inside of $\mathcal{N}$ will be in $\mathcal{N}$ for $t > 0$ and must approach $\mathcal{M}$ in particular. This can be easily proved by exploiting the fact that $\dot{V} < 0$ at all points in $\mathcal{N}$ which are not in $\mathcal{M}$. Therefore, combing with Theorem 4.2, we have achieved the following proposition.

Proposition 4.2 *(a) All the Filippov solutions to system (4.7) starting outside of $\mathcal{N}$ converge to $\mathcal{E}$.*
(b) All the Filippov solutions to system (4.7) starting inside of $\mathcal{N}$ stay in this invariant set for $t > 0$, and converge to $\mathcal{M}$.

In the next section, we look into the convergence speed of the converging process just analyzed.

4.4 Finite-time convergence

In the previous section, we have shown that all trajectories starting outside of $\mathcal{N}$ converge to $\mathcal{E}$. In this section, we will prove that the convergence is achieved in finite time. We first prove some useful facts.

Lemma 4.7 *Let $\varrho(t) \triangleq \max_{i\in\{1,2,3\}} |\cos\theta(z_i(t), z_{[i]}(t))|$. If $z(0) \notin \mathcal{N}$, then there exists a positive constat $\bar{\varrho} < 1$ such that $\varrho(t) \leqslant \bar{\varrho}$ for all $t \geqslant 0$.*

Proof: Let σ_1 be defined by $\sigma_1 \triangleq \max_{z\in\mathcal{E}, i\in\{1,2,3\}} |\cos\theta(z_i, z_{[i]})|$. From Proposition 4.2(a) we know that $\lim_{t\to\infty} \varrho(t) = \sigma_1 < 1$, which implies that for the fixed number $\frac{1-\sigma_1}{2} > 0$, there exists a finite time $T > 0$ such that for all $t > T$, $|\varrho(t) - \sigma_1| < \frac{1-\sigma_1}{2}$. It further implies $\varrho(t) \leqslant \frac{1+\sigma_1}{2} < 1$ for all $t > T$. Since $\varrho(t)$ is continuous, one can consider $\sigma_2 \triangleq \max_{0\leqslant t\leqslant T} \varrho(t)$. We now prove by contradiction that $\sigma_2 < 1$. Suppose there exists $0 \leqslant t_1 \leqslant T$ such that $\varrho(t_1) = 1$. It follows then that z_1, z_2, z_3 are collinear at $t = t_1$ and thus $z(t_1) \in \mathcal{N}$, which in combination with the fact that $\mathcal{N}$ is positively invariant, contradicts the result in Proposition 4.2(a), that z approaches $\mathcal{E}$. Hence, let $\bar{\varrho} = \max\{\frac{1+\sigma_1}{2}, \sigma_2\}$, then we have $\rho(t) \leqslant \bar{\varrho} < 1$ for all $t \geqslant 0$. □

Lemma 4.8 *If $z(0) \notin \mathcal{N}$, then it follows that*

$$||z_i(t)|| \geqslant \min\{d_i, ||z_i(0)||\}\,, \tag{4.19}$$

for all $t \geqslant 0$ and $i = 1, 2, 3$.

Proof: Let $V_i(z(t)) = \frac{1}{4}(||z_i||^2 - d_i^2)^2$, for $i = 1, 2, 3$. We consider the derivative of $V_1(z(t))$ along the Filippov solutions to (4.7), and have that $\frac{d}{dt} V_1(z(t)) \in \dot{\overline{V_1}}(z(t))$ where $\dot{\overline{V_1}}(z(t)) = \{\langle \nabla V_1(z), \nu\rangle, \nu \in F[g(z)]\}$. Moreover,

$$\langle \nabla V_1(z), \nu\rangle = -|\,||z_1||^2 - d_1^2|\;||z_1||\left(1 - \cos\theta(z_1, z_2)\,\gamma_1\gamma_2\right)$$

where $\gamma_1, \gamma_2 \in [-1, 1]$. From Lemma 4.7, one has $|\cos\theta(z_1, z_2)| < 1$ for all $t > 0$. Thus, we have $\frac{d}{dt} V_1(z(t)) \leqslant 0$ and $\frac{d}{dt} V_1(z(t)) = 0$ if and only if $||z_1|| = d_1$. Therefore $V_1(z(t))$ decreases monotonously to zero as $t \to \infty$. Then we have $||z_1(t)|| \geqslant ||z_1(0)||$ when $||z_1(0)|| \leqslant d_1$ and $||z_1(t)|| \geqslant d_1$ when $||z_1(0)|| \geqslant d_1$. So we have proved the conclusion for $i = 1$. Using similar arguments for V_2 and V_3, one can prove the cases for $i = 2$ and 3. □

We will need the following theorem on the finite-time stability of differential inclusion.

Theorem 4.3 (Moulay and Perruquetti 2005, Proposition 5) *Let $\mathcal{Y}$ be an open set of $\mathbb{R}^n$ containing the origin and H a set valued function on $\mathcal{Y}$ that defines the differential inclusion*

$$\dot{y} \in H(y), \qquad y \in \mathcal{Y} \tag{4.20}$$

and satisfies $0 \in H(0)$. If there exists a continuously differential Lyapunov function V that satisfies the differential ineqaulity

$$\langle \nabla V(y), \nu \rangle \leqslant -r(V(y)), \tag{4.21}$$

for all $y \in \mathcal{Y}$ and all $\nu \in H(y)$, where $r : \mathbb{R}_{\geqslant 0} \to \mathbb{R}_{\geqslant 0}$ is continuous and satisfies $r(0) = 0$ such that for all $\epsilon > 0$

$$\int_0^{\epsilon} \frac{dz}{r(z)} < +\infty, \tag{4.22}$$

then the origin of (4.20) is finite time stable and for any Filippov solution with the initial condition y_0, the settling time $T(y_0)$ satisfies $T(y_0) \leqslant \int_0^{V(y_0)} \frac{dz}{r(z)}$.

Now we prove the main result on finite-time convergence.

Theorem 4.4 *All the Filippov solutions to the z-system (4.7) starting outside of $\mathcal{N}$ reach $\mathcal{E}$ in finite time, for which the settling time is $T_s = \frac{\sqrt{V(z(0))}}{d\,(1-\bar{\varrho})}$, where V is defined in (4.17), $d = \min\{d_1, d_2, d_3, ||z_1(0)||, ||z_2(0)||, ||z_3(0)||\}$, and $\bar{\varrho}$ is defined in Lemma 4.7.*

Proof: For the $V(z(t))$ defined in (4.17), we have that for each $\nu \in F[g(z)]$,

$$\begin{aligned} \langle \nabla V(z), \nu \rangle &= \sum_{i=1}^{3} (||z_i||^2 - d_i^2) z_i^T \left(-\frac{z_i}{||z_i||}\gamma_i + \frac{z_{[i]}}{||z_{[i]}||}\gamma_{[i]} \right) \\ &= -\sum_{i=1}^{3} |\,||z_i||^2 - d_i^2| \cdot ||z_i|| \, \left[1 - \cos\theta(z_i, z_{[i]}) \cdot \gamma_i\, \gamma_{[i]}\right] \end{aligned}$$

where $\gamma_i \in [-1, 1]$ for $i = 1, 2, 3$. In particular, γ_i reduce to $\mathrm{sgn}(||z_i|| - d_i)$ if $||z_i|| - d_i \neq 0$. From Lemma 4.7 we know that $|\cos\theta(z_i, z_{[i]})| \leqslant \bar{\varrho}$ since $z(0) \notin \mathcal{N}$. From Lemma 4.8, one has $||z_i|| \geqslant d$. Combining the two inequalities, we have

$$\langle \nabla V(z), \nu \rangle \leqslant -d\,(1 - \bar{\varrho}) \cdot \sum_{i=1}^{3} |\,||z_i||^2 - d_i^2|\,.$$

Using the fact that for any real numbers a_1, a_2 and a_3, $|a_1| + |a_2| + |a_3| \geqslant (a_1^2 + a_2^2 + a_3^2)^{1/2}$, we know that

$$\langle \nabla V(z), \nu \rangle \leqslant -2d\,(1 - \bar{\varrho}) \cdot [V(z)]^{1/2}\,, \tag{4.23}$$

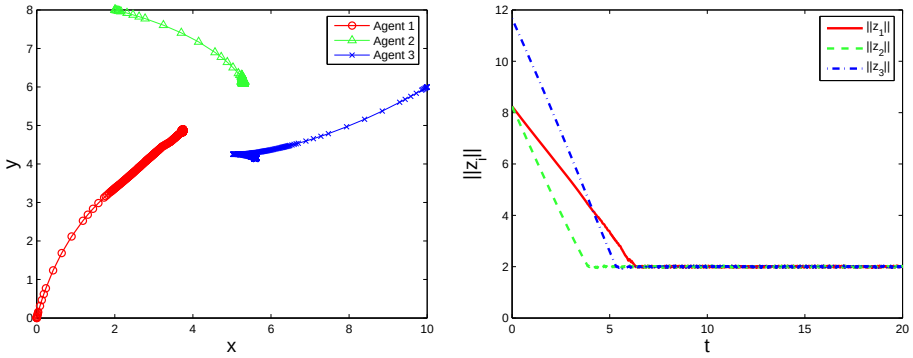

(a) (b)

Figure 4.2: *Three agents whose dynamics are described by (4.4) converge to the formation with the prescribed shape. (a) shows the trajectories of the three agents in the plane. (b) shows the pairwise distances of the three agents.*

for all $\nu \in F[g(z)]$. Let $r(s) \triangleq 2d\,(1-\bar{\varrho})\,s^{1/2}$. Note that $V(z)|_{z\in\mathcal{E}} = 0$ and every $z \in \mathcal{E}$ is an equilibrium of system (4.7). From Theorem 4.3, we know that the solutions to system (4.7) reach the equilibrium set $\mathcal{E}$ in finite time with the settling time $T_s \leqslant \int_0^{V(z(0))} \frac{ds}{r(s)} = \frac{\sqrt{V(z(0))}}{d\,(1-\bar{\varrho})}$. □

4.5 Simulations and experiments

First we give a numerical example to illustrate the correctness of Theorem 4.1. We consider the three agents in the two dimensional plane with the initial positions $(0,0), (2,8), (10,6)$. The initial positions are not collinear. The prescribed distances are $d_1 = d_2 = d_3 = 2$. Fig. 4.2(a) shows the trajectories of the three agents in the plane according to the evolution of system (4.4). Fig. 4.2(b) shows the relative distances between the three agents, in which these distances converge to d_1, d_2, d_3 in finite time.

Now we give another numerical example to illustrate the conclusions in Proposition 4.2(b). We choose the initial positions for the three agents to be the collinear positions $(0,1), (4.5,1), (7,1)$. The other settings are chosen to be the same as in the previous example. Fig. 4.3 shows the simulation results. Fig. 4.3(a) illustrates that the three agents drift to infinity and move at the same velocity eventually. From Fig. 4.3(b), one can see that the three agents fail to achieve the desired formation, and their positions remain collinear for all t.

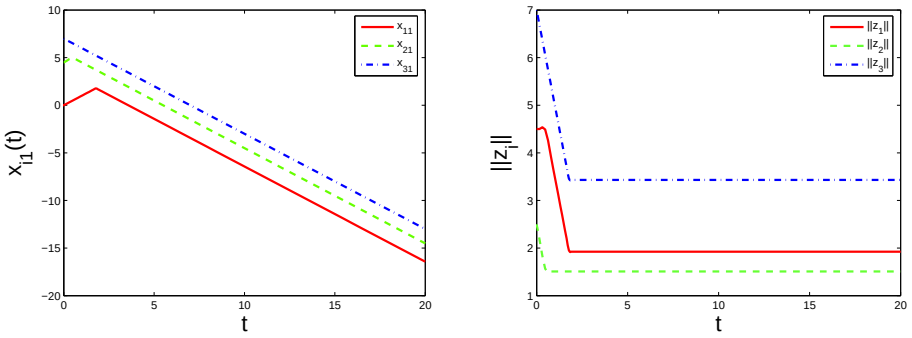

(a) (b)

Figure 4.3: *Evolutions of the positions and the pairwise distances of the three agents. It is shown that agents starting in collinear positions remain so.*

Finally, we test the formation convergence result in Theorem 4.1 using E-pucks (Mondada et al. 2009). The experimental setup consists of three wheeled E-puck robots in a 2D area of 2.6×2 meters. Each robot is identified by a datamatrix as a marker on its top as shown in Fig. 4.4. The robot's reference point in the position of its lower right corner and the orientation of the marker are recognized by a vision algorithm running at a PC employing a webcam placed above the testing area. Since an E-puck is usually modeled by a unicycle, we apply feedback linearization about its reference point to obtain the single-integrator model for simpler controller implementation. Therefore, we control the shape formed by the three reference points of the robots. The whole image of the testing area is covered by 1600×1200 pixels, where the distance between two consecutive horizontal or vertical pixels corresponds approximately to 1.6mm. The PC runs a real time process computing the relative vectors between the robots from the vision algorithm, then it computes the control inputs determined by (4.4). Note that although the control inputs for the robots are computed by the PC, this does not change the distributed nature of the proposed control algorithm since we are not modifying (4.4) in any way. The communication takes place when sending the commands from the PC to the E-pucks in order to move their wheels. These commands are obtained after applying the feedback linearization, which gives the required linear and angular velocities to the robots, and this information is translated to common (linear velocity) and differential (angular velocity) commands to the wheels of the robots. The communication is done via Bluetooth at the fixed frequency of 20Hz. In order to make the experiments faster, the selected constant speed has been chosen to be 17 pixels/sec or

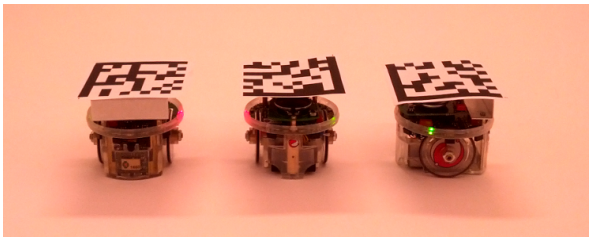

Figure 4.4: *Three wheeled E-pucks with datamatrices as markers on their tops.*

equivalently 2.72cm/sec.

We consider an equilateral triangle with side length being 250 pixels as the prescribed shape. Chattering might be occur when the three robots are close to the target formation since in practice the argument in the sign function of (4.4) cannot be zero due to noise in sensors or floating point number representation. In order to prevent the chattering, if the absolute error for e_i is smaller than the threshold of 8 pixels (1.3cm), then we set the control input to 0.

By using the proposed controllers, the three robots converge to the desired formation as it is shown in Figure 4.5. The observed settling time is 31 seconds which is less than the upper bound $T_s = 336$ seconds given in Theorem 4.4.

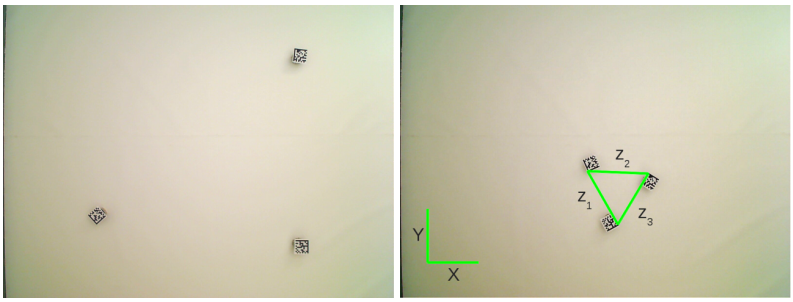

Figure 4.5: *Initial and final positions of the E-pucks after applying the proposed distributed control laws. The final distances $||z_1||, ||z_2||$ and $||z_3||$ between the reference points of the robots are 255, 248 and 249 pixels, respectively.*

The trajectories of the robots are shown in Fig. 4.6. The initial and final positions correspond to the ones shown in Fig. 4.5. The evolutions of the errors e_i for $i = 1, 2, 3$ and the terms of the Lyapunov function (4.17) are shown in Fig. 4.7. As predicted, the three terms of the Lyapunov function are always decreasing over time. The video of the experiment can be checked following the link *https://dl.dropboxusercontent.com/u/2689187/Tcoarse.mp4* .

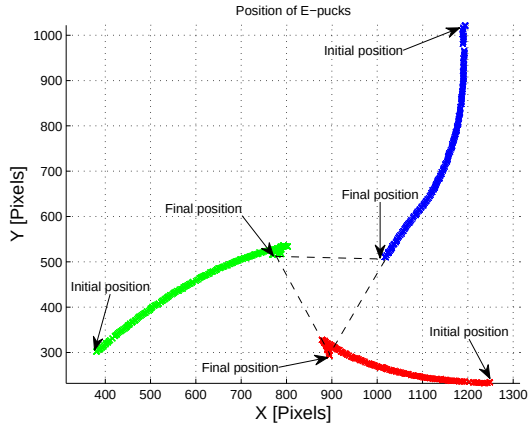

Figure 4.6: *Evolution of the formation converging to the desired equilateral triangle. The red, green and blue colors stand for robots 1, 2 and 3, respectively.*

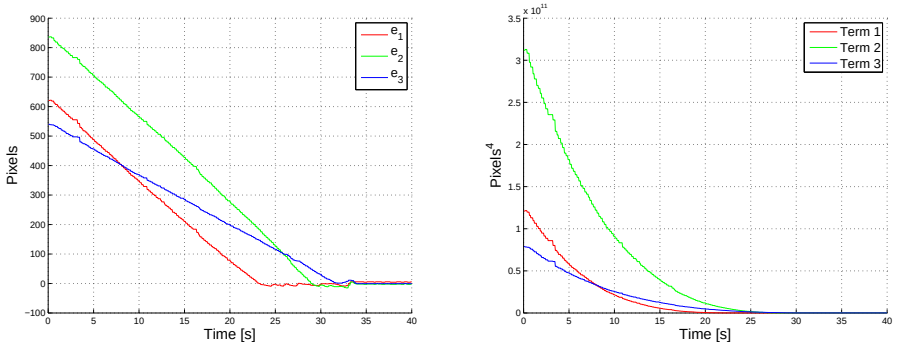

(a) (b)

Figure 4.7: *Evolutions of the errors e_i for $i = 1, 2, 3$ and the terms of the Lyapunov function.*

4.6 Concluding remarks

In this chapter, a gradient-based formation control law using coarse range measurements has been proposed to stabilize three agents moving in a plane to the desired triangular formations. We have proven that under coarse range measurements, the three agents converge to the desired formations as long as they are not initially collinearly positioned. Different from the existing stability results on triangular formations with precise range measurements, it has been shown that the convergence takes place within finite time and that the settling time can be determined by the

geometric information of the initial shape of the formation. The analysis techniques are applicable to larger formations. The challenge will be how to determine the settling time when more agents are involved. We will continue our research in this direction using both theoretical analysis and experimental validations.

Chapter 5

Cooperation in Heterogeneous Agents with Uncertainty

In this chapter, we consider the problem in which N coupled agents described by heterogeneous uncertain linear systems aim at tracking one or more reference signals generated by given exosystems. We consider information constraints that not all the agents can get direct access to the exosystems. To tackle this problem, the reference signals are reconstructed via local interaction among the agents themselves and between agents and the exosystems in accordance with the given communication graph. Then decentralized robust controllers that use the reconstructed reference signals are designed and are shown to result in a closed-loop system whose outputs track the prescribed reference signals. The results presented in this chapter are published in (Liu, De Persis and Cao 2013, De Persis et al. 2012).

5.1 Introduction

In multi-agent coordination problems one of the possible tasks which the agents have to carry out is to track an exogenous signal (Rodriguez-Angeles and Nijmeijer 2004, Arcak 2007, Chung and Slotine 2009, Hokayem et al. 2009, Nuno et al. 2011, Mei, Ren and Ma 2011). Two possible scenarios can be considered. In the first one, all the agents are assumed to know the reference signal and use this information as well as the relative information coming from the neighboring agents to carry out the control task, while the use of the neighbors' information in the control laws may improve the robustness of the overall system. In the second scenario, the reference signal is not available to all the agents, and strategies to overcome this limitation are put in place (Bai et al. 2009, Mei, Ren and Ma 2011, Dong 2011).

A related problem has been considered in (Wieland et al. 2011). Given N heterogeneous linear systems and a communication graph, what are the necessary and sufficient conditions for the systems to achieve output synchronization? Interestingly, the authors have shown that an exosystem (Isidori et al. 2003) which generates the "reference signal" to which all the systems' outputs converge must necessarily exist. As a result, controllers which guarantee output synchronization are those which

solve an output regulation problem associated to that exosystem. In addition, to make sure that the outputs of all the systems converge to a specific reference signal (the same for all the systems) generated by the exosystem, the controllers exchange local information with their neighbors.

Motivated by this result, we turn our attention to the problem in which the systems aim at tracking one or more reference signals generated by exosystems given *in advance* and ask whether there exist controllers which can guarantee the tracking of the reference signals even under the restriction that not all the systems are directly connected to the exosystem. Inspired by (Wieland et al. 2011) we aim at reconstructing the reference signal via local interaction of the systems among themselves and the exosystem in accordance with the given communication graph. Then, controllers which solve the output regulation problem are designed and shown to track the actual reference signal even though they are fed by the local estimate of the signal. Different from (Wieland et al. 2011), we do not assume that the systems' models are perfectly known and robust regulators have to be designed (Isidori et al. 2003). The problem in (Wieland et al. 2011) for the case of uncertain systems has been studied in (Kim et al. 2011) as well but, compared with the latter, the problem formulation in this chapter is different and the approach taken in this chapter seems to lead to simpler analysis.

Similar approaches have been proposed very recently in the literature. In (Wang et al. 2010), the systems which do not have direct access to the exosystem exchange information about the local tracking errors. Compared to our contribution, however, the authors require the communication graph to contain no cycles, with the leader (the exosystem) having a directed path to all the other systems. In this chapter we show that the latter condition is sufficient. Moreover, we assume the uncertainties of the system to range over a(n arbitrarily large) compact set rather than being sufficiently small. The problem of lifting the restrictions on the graph containing no cycles in (Wang et al. 2010) have been also tackled in the subsequent paper (Hong et al. 2011). However, the systems considered in that paper are all assumed to have the same model and no uncertainty is considered.

Other related papers have appeared in the recent literature. To deal with velocity tracking in coordination problems for *passive* systems, (Bai et al. 2011, Chapter 3) proposes an internal model approach in which the reference trajectory is generated by an exosystem which cannot be accessed by the agents except one. Also leader-follower problems using the internal model principle have been studied in (Wieland 2011). In Section III of (Mei, Ren and Ma 2011) an internal model approach to (position and) velocity tracking in networks of Euler-Lagrange systems is pursued, but the exosystem is restricted to the trivial one (constant reference velocity). To deal with non-constant reference velocities the authors rely on a discontinuous

control law and require information about one-hop and two-hop neighbors. Related work is also available in (Dong 2011). Examples on the use of ideas from output regulation theory and multi-agent systems can be found in the work (Gazi 2005), later developed in e.g. (Gazi and Passino 2006), (Gul and Gazi 2010).

We also look at the problem of tracking multiple reference signals in order to realize clustering in multi-agent systems. Clustering has recently been studied as a coordination task (Wu et al. 2009, Xia and Cao 2011, Chen, Lü, Han and Yu 2011), and the main challenge is how to have the agents converge to different asymptotic states under the constraints that all the agents are coupled together throughout the system's evolution. Until now, only few of the existing works have considered the situation when the agents are heterogenous. Building upon our results on tracking a single reference signal, we propose a novel robust decentralized output regulation algorithm to track different reference signals for different subgroups of systems and thus realize clustering.

In Section 5.2 we first formulate the problem of robust decentralized output regulation for uncertain heterogeneous systems along with the standing assumptions, and then state the main results. In Section 5.3, we extend the results in Section 5.2 to study clustering output synchronization. The actual design of the controllers is described in Section 5.4 and then illustrated via two numerical examples in Section 5.5. Conclusions are drawn in Section 5.6.

5.2 Output regulation of uncertain heterogeneous systems

5.2.1 Problem statement and standing assumptions

Consider N heterogeneous uncertain linear dynamical systems

$$\mathcal{S}_i : \quad \begin{array}{rcl} \dot{x}_i & = & A_i(\mu_i)\, x_i + B_i(\mu_i)\, u_i \\ y_i & = & C_i(\mu_i)\, x_i\,, \end{array} \tag{5.1}$$

with state vector $x_i \in \mathbb{R}^{n_i}$, control input $u_i \in \mathbb{R}^{p_i}$, and output vector $y_i \in \mathbb{R}^q$ for $i = 1, \cdots, N$. Each matrix of the system (5.1) depends on a vector μ_i of uncertain parameters which is assumed to range over a given set $\mathcal{P}_i$.
Consider also another system, which we will refer to as the "leader", whose dynamical behavior is described by the following equation:

$$\begin{aligned} \dot{w}_0 &= S w_0 \\ r &= R w_0\,, \end{aligned} \tag{5.2}$$

where $w_0 \in \mathbb{R}^m$, $r \in \mathbb{R}^q$, and matrices $S \in \mathbb{R}^{m\times m}$, $R \in \mathbb{R}^{q\times m}$ are assumed to satisfy the following assumption:

Assumption 5.1 *The real parts of the eigenvalues of S are zero, i.e., $\sigma(S) \subset \mathbb{C}^0$ and (R, S) is detectable.*

The N systems (5.1) exchange information according to the communication topology described by the directed graph $\mathbb{G} = (\mathcal{V}, \mathcal{E})$. Each system is represented by a node in the set $\mathcal{V} = \{1, 2, \ldots, N\}$ and system j sends information to system i if and only if $(j, i) \in \mathcal{E} \subseteq \mathcal{V}\times\mathcal{V}$. Associated to the graph $\mathbb{G}$ is the adjacency matrix $A = [a_{ij}]$. The entry $a_{ij} = 1$ if and only if $(j, i) \in \mathcal{E}$ and 0 otherwise. The entry $a_{ii} = 0$ for each $i = 1, 2, \ldots, N$. The matrix L is the Laplacian matrix associated to the graph $\mathbb{G}$.
In addition to the graph $\mathbb{G}$, we consider the directed graph $\mathbb{G}_0 = (\mathcal{V}_0, \mathcal{E}_0)$, obtained as follows. Let system (5.2) (the leader) be associated with node 0 and set $\mathcal{V}_0 = \mathcal{V} \cup \{0\}$. Moreover, for $i = 1, 2, \ldots, N$, we set $a_{i0} = 1$ if and only if there is an arc from 0 to i and $a_{i0} = 0$ otherwise. Then we set $\mathcal{E}_0 = \mathcal{E} \cup \{(0, i) : a_{i0} = 1\}$. Compared with $\mathbb{G}$, the graph $\mathbb{G}_0$ additionally describes which followers have direct access to the information of the leader.
In what follows we exploit the following lemma (Mei, Ren and Ma 2011), where we refer to the graphs $\mathbb{G}, \mathbb{G}_0$ and the Laplacian L introduced above.

Lemma 5.1 (Mei, Ren and Ma 2011) *If in graph $\mathbb{G}_0$, node 0 has directed paths to all the nodes $i = 1, 2, \ldots, N$, then the matrix $L + \mathrm{diag}(a_{10}, \ldots, a_{N0})$ has all eigenvalues with strictly positive real part.*

The objective of this chapter is to design the control laws u_i which guarantee

$$\lim_{t\to\infty} ||y_i(t) - Rw_0(t)|| = 0, \quad \text{for all } i = 1, \cdots, N,$$

under the following restrictions on the available measurements:
(i) Only the systems $\mathcal{S}_i$ for which $a_{i0} > 0$ can access the leader and therefore the reference signal r. Hence, only these systems $\mathcal{S}_i$ can measure the *tracking error*

$$\epsilon_i = y_i - Rw_0.$$

This restricted access to the leader causes the readability of ϵ_i from y_i to be impossible for some of the systems (Wang et al. 2010) and makes the problem challenging.
(ii) The systems $\mathcal{S}_i$'s exchange only local information on the relative measurements.
(iii) For all $i = 1, \cdots, N$, the system $\mathcal{S}_i$ has access to the relative information with respect to S_j if and only if $\mathcal{S}_j$ is a neighbor of $\mathcal{S}_i$.

Other assumptions are needed in order to state our main result in the next subsection.

Assumption 5.2 *(i) The μ_i-dependent Francis' equations*

$$\begin{aligned} \Pi_i(\mu_i)S &= A_i(\mu_i)\Pi_i(\mu_i) + B_i(\mu_i)\Gamma_i(\mu_i) \\ 0 &= C_i(\mu_i)\Pi_i(\mu_i) - R \end{aligned} \tag{5.3}$$

have a μ_i-dependent solution $\Pi_i(\mu_i)$, $\Gamma_i(\mu_i)$ for each $i = 1, \cdots, N$.

(ii) There exist matrices $\Phi_i, H_i, \Sigma_i(\mu_i)$, with Φ_i, H_i independent of μ_i, such that

$$\begin{aligned} \Sigma_i(\mu_i)S &= \Phi_i\,\Sigma_i(\mu_i) \\ \Gamma_i(\mu_i) &= H_i\Sigma_i(\mu_i) \end{aligned} \tag{5.4}$$

(iii) There exists a matrix G_i independent of μ_i such that the linear system defined by the triplet

$$\begin{pmatrix} A_i(\mu_i) & B_i(\mu_i)H_i \\ 0 & \Phi_i \end{pmatrix} \quad \begin{pmatrix} B_i(\mu_i) \\ G_i \end{pmatrix} \quad \begin{pmatrix} C_i(\mu_i) & 0 \end{pmatrix}$$

is robustly stabilizable by the dynamic output feedback, i.e. there are matrices K_i, L_i, M_i independent of μ_i, such that the matrix

$$\begin{pmatrix} \begin{pmatrix} A_i(\mu_i) & B_i(\mu_i)H_i \\ 0 & \Phi_i \end{pmatrix} & \begin{pmatrix} B_i(\mu_i) \\ G_i \end{pmatrix} M_i \\ K_i \begin{pmatrix} C_i(\mu_i) & 0 \end{pmatrix} & L_i \end{pmatrix} \tag{5.5}$$

is Hurwitz.

A few comments on Assumption 5.2 are as follows.

– Fix $i \in \{1, 2, \ldots, N\}$. Suppose that there exists a controller of the form

$$\begin{aligned} \dot{\xi}_i &= L_i\xi_i + K_i\epsilon_i \\ u_i &= H_i\xi_i + M_i\epsilon_i \end{aligned} \tag{5.6}$$

which robustly stabilizes the system $\mathcal{S}_i$. Then, provided that $\sigma(S) \subset \mathbb{C}^0$ (see Assumption 5.1), equations (5.3), (5.4) are well-known ((Isidori et al. 2003, Proposition 1.4.1)) necessary and sufficient conditions for the controller (5.6) to solve the tracking problem for the system (5.1) for each $\mu_i \in \mathcal{P}_i$. Recall that the controller (5.6) is said to solve the tracking problem for the system (5.1) for each $\mu_i \in \mathcal{P}_i$ if, for each $\mu_i \in \mathcal{P}_i$, (i) the equilibrium $(x_i, \xi_i) = (\mathbf{0}, \mathbf{0})$ of the unforced closed-loop system (5.1), (5.6) is asymptotically stable; (ii) the response of the closed-loop system (5.1), (5.6) is such that $\lim_{t\to\infty} \epsilon_i(t) = \mathbf{0}$.

– If in addition, condition (iii) in Assumption 5.2 holds, then one can prove that the dynamic feedback control law

$$\begin{aligned} \dot{\eta}_i &= \Phi_i\eta_i + G_iM_i\xi_i \\ \dot{\xi}_i &= L_i\xi_i + K_i\epsilon_i \\ u_i &= H_i\eta_i + M_i\xi_i \end{aligned} \tag{5.7}$$

solves the tracking problem. Due to the fact that the tracking error ϵ_i may not be available to the controller of system $\mathcal{S}_i$, the previous controller cannot be implemented. In the next section, we overcome this lack of information on ϵ_i by using the information collected from the neighbors of system $\mathcal{S}_i$.

5.2.2 Tracking a single reference

The control strategy we propose to solve the decentralized output regulation problem formulated in the previous section comprises two steps. Since not all the systems $\mathcal{S}_i$ may have access to the reference signal r, we first design systems which aim at asymptotically reconstructing the reference signal using only locally available relative information. As a second step, we use such an asymptotic estimate of the reference signal to feed the tracking controllers and show that they achieve the prescribed control objective.
Motivated by Lemma 5.1, we introduce the following:

Assumption 5.3 *In graph G_0 the node 0 has directed paths to all the nodes $i = 1, 2, \ldots, N$.*

With the above assumption at hand, we can assume that there exist $1 \leqslant N_1 \leqslant N$ systems which has direct access to the leader. Without loss of generality and for the sake of simplicity, we assume that $N_1 = 1$ and that the system with direct access to the leader is the first one. To reconstruct the reference signal, the systems cooperate to estimate the internal state of the exosystem. For system $\mathcal{S}_1$, the estimation is carried out by

$$\begin{aligned} \dot{\hat{w}}_0 &= S\hat{w}_0 + G_0 R(w_0 - \hat{w}_0) \\ \dot{w}_1 &= Sw_1 + \sum_{j=1}^{N} a_{1j}(w_j - w_1) + a_{10}(\hat{w}_0 - w_1), \end{aligned} \tag{5.8}$$

where the matrix G_0 is properly chosen in such a way that $\sigma(S - G_0\, R) \subset \mathbb{C}^-$ and $\hat{w}_0$ is an asymptotic estimate of the leader's internal state w_0. For system $\mathcal{S}_i, i \in \{2, \ldots, N\}$, the system which carries out the asymptotic estimation is given by

$$\dot{w}_i = Sw_i + \sum_{j=1}^{N} a_{ij}(w_j - w_i). \tag{5.9}$$

For the system

$$\begin{aligned} \dot{w}_0 &= Sw_0 \\ \dot{\hat{w}}_0 &= S\hat{w}_0 + G_0 R(w_0 - \hat{w}_0) \\ \dot{w}_1 &= Sw_1 + \sum_{j=1}^{N} a_{1j}(w_j - w_1) + a_{10}(\hat{w}_0 - w_1) \\ \dot{w}_i &= Sw_i + \sum_{j=1}^{N} a_{ij}(w_j - w_i)\,, \qquad i = 2, \cdots, N, \end{aligned} \tag{5.10}$$

we have the following result for the convergence of w_i:

Lemma 5.2 *Let Assumptions 5.1 and 5.3 hold. Then* $||w_i(t) - w_0(t)|| \to 0$ *exponentially for all* $i = 1, \cdots, N$, *as* $t \to \infty$.

Proof: Let $\tilde{w}_i = w_i - w_0$, for all $i = 1, \cdots, N$. Let $\tilde{w}_0 = \hat{w}_0 - w_0$. Then, we have

$$\dot{\tilde{w}}_1 = \dot{w}_1 - \dot{w}_0 = S\tilde{w}_1 + \sum_{j=1}^{N} a_{1j}(\tilde{w}_j - \tilde{w}_1) + a_{10}(\tilde{w}_0 - \tilde{w}_1)\,,$$

and

$$\dot{\tilde{w}}_i = S\tilde{w}_i + \sum_{j=1}^{N} a_{ij}\,(\tilde{w}_j - \tilde{w}_i)\,.$$

Moreover,

$$\dot{\tilde{w}}_0 = \dot{\hat{w}}_0 - \dot{w}_0 = S(\hat{w}_0 - w_0) + G_0\,R(w_0 - \hat{w}_0) = (S - G_0\,R)\tilde{w}_0\,.$$

Since $\sigma(S - G_0\,R) \subset \mathbb{C}^-$, one obtains that $\tilde{w}_0$ converges to the origin exponentially as $t \to \infty$.
Following (Scardovi and Sepulchre 2009), let $\omega_i = e^{-St}\tilde{w}_i$ for all $i = 0, 1, \cdots, N$. Then we have

$$\begin{aligned}\dot{\omega}_1 &= -Se^{-St}\,\tilde{w}_1 + e^{-St}\,[S\tilde{w}_1 + \sum_{j=1}^{N} a_{1j}(\tilde{w}_j - \tilde{w}_1) + a_{10}(\tilde{w}_0 - \tilde{w}_1)] \\ &= \sum_{j=1}^{N} a_{1j}(\omega_j - \omega_1) + a_{10}(\omega_0 - \omega_1)\,,\end{aligned} \tag{5.11}$$

and

$$\dot{\omega}_i = \sum_{j=1}^{N} a_{ij}\,(\omega_j - \omega_i), \qquad i = 2, \cdots, N\,. \tag{5.12}$$

Let $\omega = (\omega_1^T, \omega_2^T, \cdots, \omega_N^T)^T \in \mathbb{R}^{Nm}$. We write the above two equations into the compact form

$$\begin{aligned}\dot{\omega} &= -(L \otimes I_m)\omega - \left(\begin{array}{c|c} a_{10}I_m & \mathbf{0} \\ \hline \mathbf{0} & \mathbf{0} \end{array}\right)\begin{pmatrix}\omega_1 \\ \mathbf{0}\end{pmatrix} + \left(\begin{array}{c|c} a_{10}I_m & \mathbf{0} \\ \hline \mathbf{0} & \mathbf{0} \end{array}\right)\begin{pmatrix}\omega_0 \\ \mathbf{0}\end{pmatrix} \\ &= -(\tilde{L} \otimes I_m)\omega + \left(\begin{array}{c|c} a_{10}I_m & \mathbf{0} \\ \hline \mathbf{0} & \mathbf{0} \end{array}\right)\begin{pmatrix}\omega_0 \\ \mathbf{0}\end{pmatrix},\end{aligned}$$

where $-\tilde{L} = -L - \mathrm{diag}(a_{10}, 0, \cdots, 0)$ and $\otimes$ denotes the Kronecker product. According to Lemma 5.1, $-\tilde{L}$ is Hurwitz. Thus, $-\tilde{L} \otimes I_m$ is Hurwitz. Moreover, it has been proved that $\tilde{w}_0$ converges to the origin exponentially as $t \to \infty$. Thus, $\omega_0 = e^{-St}\,\tilde{w}_0$ converges to zero exponentially as $t \to \infty$, since $\sigma(S) \subset \mathbb{C}^0$. Therefore, ω converges to the origin exponentially as $t \to \infty$. Since $\tilde{w}_i = e^{St}\omega_i$ for $i = 1, \cdots, N$ and $\sigma(S) \subset \mathbb{C}^0$, one has that $\tilde{w}_i \to \mathbf{0}$ exponentially as $t \to \infty$. Thus, we arrive at the result $||w_i(t) - w_0(t)|| \to 0$ exponentially for all $i = 1, \cdots, N$, as $t \to \infty$. ▫

Remark 5.1 *Clearly the signals $Rw_i(t)$, $i = 1, 2, \ldots, N$, converge exponentially to $r(t)$.*

Next, we introduce the controllers for systems (5.1) as follows. As system $\mathcal{S}_1$ has access to w_0, we design u_1 as

$$\begin{aligned}
\dot{\hat{w}}_0 &= S\hat{w}_0 + G_0R(w_0 - \hat{w}_0)\\
\dot{w}_1 &= Sw_1 + \textstyle\sum_{j=1}^{N} a_{1j}(w_j - w_1) + a_{10}(\hat{w}_0 - w_1)\\
\dot{\eta}_1 &= \Phi_1\,\eta_1 + G_1M_1\xi_1\\
\dot{\xi}_1 &= L_1\xi_1 + K_1(y_1 - Rw_1)\\
u_1 &= H_1\eta_1 + M_1\xi_1
\end{aligned} \tag{5.13}$$

For agent $i = 2, \cdots, N$, we design u_i as

$$\begin{aligned}
\dot{w}_i &= Sw_i + \textstyle\sum_{j=1}^{N} a_{ij}(w_j - w_i)\\
\dot{\eta}_i &= \Phi_i\,\eta_i + G_i\,M_i\xi_i\\
\dot{\xi}_i &= L_i\xi_i + K_i(y_i - Rw_i)\\
u_i &= H_i\eta_i + M_i\xi_i
\end{aligned} \tag{5.14}$$

The matrices $\Phi_i, G_i, M_i, L_i, K_i, H_i$ are those found in Assumption 5.2. The design of η_i, ξ_i, u_i in the above controllers is inspired by the output regulation method for a single system in (Isidori et al. 2003).

Theorem 5.1 *Consider N heterogeneous linear systems (5.1) coupled via the dynamic couplings (5.13) and (5.14). Suppose Assumptions 5.1–5.3 hold. Then, $||y_i(t) - Rw_0(t)||$ exponentially converges to 0 as $t \to \infty$ for all $i = 1, \cdots, N$.*

*P*roof: Let $\tilde{x}_i = x_i - \Pi_i(\mu_i)w_i$, $\tilde{\eta}_i = \eta_i - \Sigma_i(\mu_i)w_i$. Recall that $a_{i0} > 0$ if and only if $i = 1$ and 0 otherwise. Then, according to equations (5.1), (5.8) and (5.9), we have

$$\dot{\tilde{x}}_i = A_i(\mu_i)\tilde{x}_i + B_i(\mu_i)H_i\tilde{\eta}_i + B_i(\mu_i)M_i\xi_i - \Pi_i(\mu_i)\left(\sum_{j=1}^{N} a_{ij}(w_j - w_i) + a_{i0}(\hat{w}_0 - w_i)\right),$$

where we have exploited the first equation of (5.3) and the second equation of (5.4) in Assumption 5.2. Furthermore, standard manipulations and the first equation of (5.4) in Assumption 5.2 lead to the equation

$$\dot{\tilde{\eta}}_i = \Phi_i\tilde{\eta}_i + G_iM_i\xi_i - \Sigma_i(\mu_i)\cdot\left(\sum_{j=1}^{N} a_{ij}(w_j - w_i) + a_{i0}(\hat{w}_0 - w_i)\right).$$

One can also observe that

$$\begin{aligned} y_i - Rw_i &= C_i(\mu_i)x_i - Rw_i \\ &= C_i(\mu_i)\tilde{x}_i + \Big(C_i(\mu_i)\Pi_i(\mu_i) - R\Big)w_i \\ &= C_i(\mu_i)\tilde{x}_i\,, \end{aligned}$$

where we have used the second equation of (5.3) in Assumption 5.2. Hence,

$$\begin{aligned} \dot{\xi}_i &= L_i\xi_i + K_i(y_i - Rw_i) \\ &= L_i\xi_i + K_i \begin{pmatrix} C_i(\mu_i) & \mathbf{0} \end{pmatrix} \begin{pmatrix} \tilde{x}_i \\ \tilde{\eta}_i \end{pmatrix}. \end{aligned} \tag{5.15}$$

Using the new coordinates $\tilde{x}_i, \tilde{\eta}_i$ and ξ_i, we write the dynamics in the compact form

$$\begin{aligned} \begin{pmatrix} \dot{\tilde{x}}_i \\ \dot{\tilde{\eta}}_i \end{pmatrix} &= \begin{pmatrix} A_i(\mu_i) & B_i(\mu_i)H_i \\ \mathbf{0} & \Phi_i \end{pmatrix} \begin{pmatrix} \tilde{x}_i \\ \tilde{\eta}_i \end{pmatrix} + \begin{pmatrix} B_i(\mu_i) \\ G_i \end{pmatrix} M_i\xi_i \\ &\quad - \begin{pmatrix} \Pi_i(\mu_i) \\ \Sigma_i(\mu_i) \end{pmatrix} \Big(\sum_{j=1}^{N} a_{ij}(w_j - w_i) + a_{i0}(\hat{w}_0 - w_i) \Big) \\ \dot{\xi}_i &= L_i\xi_i + K_i \begin{pmatrix} C_i(\mu_i) & \mathbf{0} \end{pmatrix} \begin{pmatrix} \tilde{x}_i \\ \tilde{\eta}_i \end{pmatrix}. \end{aligned} \tag{5.16}$$

The third condition of Assumption 5.2 shows that the dynamic matrix of the closed loop system (5.16) is Hurwitz. Since $\sum_{j=1}^{N} a_{ij}(w_j - w_i) + a_{i0}(\hat{w}_0 - w_i)$ converges exponentially to zero, then $\tilde{x}_i \to \mathbf{0}\,, \tilde{\eta}_i \to \mathbf{0}$ exponentially. Furthermore, $y_i - Rw_i = C_i(\mu_i)\tilde{x}_i \to \mathbf{0}$ exponentially. As $w_i - w_0 \to \mathbf{0}$ for all i exponentially, then the latter implies that $y_i(t) \to Rw_0(t)$ for all i exponentially. □

Remark 5.2 *Theorem 5.1 solves the robust decentralized output regulation problem, in which the actual reference signal is tracked relying on local estimates of the signal. The papers (Wieland et al. 2011, Kim et al. 2011, Su and Huang 2012a, Su and Huang 2012b) have addressed similar problems, with some differences that we are going to discuss below. Differently from (Wieland et al. 2011), we do not assume that the systems' models are perfectly known and robust regulators have to be designed. The problem in (Wieland et al. 2011) has been studied in (Kim et al. 2011) in the case of uncertain systems. Compared with (Kim et al. 2011), the systems' models in this chapter can have large uncertainties. In addition, it is worth mentioning that the problem formulation in this chapter is different from that in (Wieland et al. 2011, Kim et al. 2011). The work in (Wieland et al. 2011, Kim et al. 2011) deals with synchronization problem without any leader and thus they cannot enforce the desired asymptotic regime of individual systems. In contrast, our problem requires that the*

outputs of individual systems track the prescribed reference signal. More recently, (Su and Huang 2012a, Su and Huang 2012b) have studied the leader-follower output synchronization problem of heterogeneous linear multi-agent systems. However, the systems considered in the two papers are perfectly known and assumed to have no uncertainty.

The design of robust regulators that fulfill the conditions in Assumption 5.2 will be discussed in Section 5.4. For such a design, we will need Corollary 5.1 below which deals with the case in which the dynamics of each system (5.1) is affected by the signals w_i, namely

$$\mathcal{S}_i^w : \quad \begin{array}{rcl} \dot{x}_i & = & A_i(\mu_i)\, x_i + B_i(\mu_i)\, u_i + P_i(\mu_i)\, w \\ y_i & = & C_i(\mu_i)\, x_i\,, \end{array} \tag{5.17}$$

where $w = (w_1^T \dots w_N^T)^T$ is the vector of signals generated by (5.8), (5.9) and

$$P_i(\mu_i) = (P_{i1}(\mu_i) \dots P_{iN}(\mu_i)).$$

The previous theorem can be easily extended provided that Assumption 5.2 is modified as follows:

Assumption 5.4 *(i) the μ_i-dependent Francis' equations*

$$\begin{array}{rcl} \Pi_i(\mu_i)S = A_i(\mu_i)\Pi_i(\mu_i) + B_i(\mu_i)\Gamma_i(\mu_i) + \sum_{j=1}^{N} P_{ij}(\mu_i) \\ 0 = C_i(\mu_i)\Pi_i(\mu_i) - R \end{array} \tag{5.18}$$

have a μ_i-dependent solution $\Pi_i(\mu_i)$, $\Gamma_i(\mu_i)$ for each $i = 1, \cdots, N$.
(ii) and (iii) are as in Assumption 5.2.

The result below is used in Section 5.4 to design the output regulators.

Corollary 5.1 *Consider N heterogeneous linear systems (5.17). Suppose the systems are coupled via the dynamic couplings (5.13) and (5.14). Suppose Assumptions 5.1, 5.3 and 5.4 hold. Then, $||y_i(t) - Rw_0(t)||$ exponentially converges to 0 as $t \to \infty$ for all $i = 1, \cdots, N$.*

Proof: The result descends from the proof of Theorem 5.1 after making necessary modifications. In view of (5.18), the variable $\tilde{x}_i$ of the closed-loop system (5.17), (5.13) and (5.14) satisfies the equation

$$\begin{array}{rcl} \dot{\tilde{x}}_i & = & A_i(\mu_i)\tilde{x}_i + B_i(\mu_i)H_i\tilde{\eta}_i + B_i(\mu_i)M_i\xi_i + \\ & & \sum_{j=1}^{N} P_{ij}(\mu_i)(w_j - w_i) - \Pi_i(\mu_i) \cdot \left(\sum_{j=1}^{N} a_{ij}(w_j - w_i) + a_{i0}(\hat{w}_0 - w_1) \right). \end{array}$$

Repeating the same arguments of Theorem 5.1, one arrives at the following system:

$$\begin{aligned}\begin{pmatrix}\dot{\tilde{x}}_i\\ \dot{\tilde{\eta}}_i\end{pmatrix} &= \begin{pmatrix}A_i(\mu_i) & B_i(\mu_i)H_i\\ \mathbf{0} & \Phi_i\end{pmatrix}\begin{pmatrix}\tilde{x}_i\\ \tilde{\eta}_i\end{pmatrix} + \begin{pmatrix}B_i(\mu_i)\\ G_i\end{pmatrix} M_i\xi_i\\ &+ \begin{pmatrix}\sum_{j=1}^{N} P_{ij}(\mu_i)(w_j - w_i)\\ \mathbf{0}\end{pmatrix} - \begin{pmatrix}\Pi_i(\mu_i)\\ \Sigma_i(\mu_i)\end{pmatrix}\left(\sum_{j=1}^{N} a_{ij}(w_j - w_i) + a_{i0}(\hat{w}_0 - w_1)\right)\\ \dot{\xi}_i &= L_i\xi_i + K_i\begin{pmatrix}C_i(\mu_i) & \mathbf{0}\end{pmatrix}\begin{pmatrix}\tilde{x}_i\\ \tilde{\eta}_i\end{pmatrix}\end{aligned}$$

As before, the system above is Hurwitz and driven by signals which converge exponentially to zero. The states converge exponentially to zero and the thesis follows. □

In the next section, we further expand the results to the case where multiple reference signals have to be tracked.

5.3 Clustering through output regulation

5.3.1 Problem statement

We again consider N heterogeneous uncertain linear dynamical systems $\mathcal{S}_i$, $1 \leqslant i \leqslant N$, given by (5.1). In addition, we consider another n systems $\mathcal{L}_j$, $1 \leqslant j \leqslant n$, called "leaders", with state variables $w_{01}, w_{02}, \ldots, w_{0n}$. Their dynamics are of the same form described by

$$\begin{aligned}\dot{w}_{0j} &= Sw_{0j}\\ r_j &= Rw_{0j}\,, \forall j = 1, \ldots, n\end{aligned} \tag{5.19}$$

but with different initial conditions, i.e., $w_{01}(0), w_{02}(0), \ldots, w_{0n}(0)$ are different from each other. This problem formulation is inspired by cooperation in a group of multi-agents in which the agents achieve different phase states. For example, it requires to generate the anti-phase sinusoidal body-wave for robotic fish in the imitation of fish schooling (Wang et al. 2011). We will explore topological connections and design decentralized controllers such that, for a given partition of the N heterogeneous systems $\mathcal{S}_i$ with n subsets, the output of each system in the same subset asymptotically converges to the same reference signal Rw_{0j} for $j \in \{1, \ldots, n\}$ and the outputs of the systems in different subsets converge to different reference signals. The desired behavior is formalized as follows.

Definition 5.1 *Let $\{\mathbb{N}_1, \mathbb{N}_2, \ldots, \mathbb{N}_n\}$ be a partition of the set $\{1, 2, \ldots, N\}$ into n nonempty subsets, which satisfy $\mathbb{N}_i \cap \mathbb{N}_j = \varnothing$ where $i \neq j$ and $\bigcup_{i=1}^{n} \mathbb{N}_i = \{1, 2, \ldots, N\}$. Suppose*

that $\mathbb{N}_1 = \{1, \ldots, h_1\}, \mathbb{N}_2 = \{h_1 + 1, \ldots, h_1 + h_2\}, \ldots, \mathbb{N}_n = \{h_1 + \ldots + h_{n-1} + 1, \ldots, h_1 + \ldots + h_{n-1} + h_n\}$*, where* $1 < n < N$*,* $1 \leqslant h_i < N$*, and* $\sum_{i=1}^{n} h_i = N$*. A network of* N *heterogeneous linear systems* $\mathcal{S}_i$*, partitioned according to* $\{\mathbb{N}_1, \mathbb{N}_2, \ldots, \mathbb{N}_n\}$ *is said to realize an* n*-cluster output synchronization, if the outputs* y_i *of the heterogeneous systems (5.1) satisfy* $\lim_{t\to+\infty} \sum_{j=1}^{n} \sum_{i\in\mathbb{N}_j} ||y_i(t) - Rw_{0j}(t)|| = 0$*.*

The N systems $\mathcal{S}_i$ exchange information according to the topology described by the directed graph $\mathbb{G}$. Associated to the graph $\mathbb{G}$ is the adjacency matrix $A = [a_{ij}] \in \mathbb{R}^{N\times N}$. The entry a_{ij} equals 1 or -1 for $1 \leqslant i, j \leqslant N, i \neq j$, if and only if there is a coupling from $\mathcal{S}_j$ to the system $\mathcal{S}_i$; otherwise $a_{ij} = 0$. In this section, we allow couplings among the agents that belong to different subsets to be negative, and as a result $a_{ij} \in \{1, 0, -1\}$. We set $a_{ii} = 0$ for each $i = 1, \ldots, N$. Moreover, the partition $\{\mathbb{N}_1, \mathbb{N}_2, \ldots, \mathbb{N}_n\}$ induces the following block-matrix structure of the matrix A:

$$A = \begin{pmatrix} A_{11} & A_{12} & \ldots & A_{1n} \\ A_{21} & A_{22} & \ldots & A_{2n} \\ \ldots & \ldots & \ldots & \ldots \\ A_{n1} & A_{n2} & \ldots & A_{nn} \end{pmatrix}.$$

The Laplacian matrix $L = [l_{ij}] \in \mathbb{R}^{N\times N}$ associated with the graph $\mathbb{G}$ is the matrix $L = D - A$, with $D = \mathrm{diag}(d_1, \ldots, d_N)$ where $d_i = \sum_{j=1, j\neq i}^{N} a_{ij}$. Similar to A, the matrix L can be written as

$$L = \begin{pmatrix} L_{11} & L_{12} & \ldots & L_{1n} \\ L_{21} & L_{22} & \ldots & L_{2n} \\ \ldots & \ldots & \ldots & \ldots \\ L_{n1} & L_{n2} & \ldots & L_{nn} \end{pmatrix},$$

with $L_{ij} \in \mathbb{R}^{h_i\times h_j}$ for $i, j = 1, \ldots, n$.

The matrix L is assumed to satisfy the following:

Assumption 5.5 *Suppose that the block-matrices* $L_{ij} \in \mathbb{R}^{h_i\times h_j}$*,* $i, j = 1, \ldots, n$*, have zero row sums, namely* $\sum_{\ell=1}^{h_j} l_{k_i+m,k_j+\ell} = 0$ *for all* $m = 1, \ldots, h_i$*,* $k_i = h_1 + \ldots h_{i-1}$ *and* $k_j = h_1 + \ldots h_{j-1}$*. Furthermore, the off-diagonal elements of* $L_{ii} \in \mathbb{R}^{h_i\times h_i}$ *are non-positive.*

A few explanations on Assumption 5.5 are in order. The assumption that all L_{ij} have zero row sums is natural and necessary. It means that the sum of the couplings from the systems in the jth subset to each system in the ith ($i \neq j$) subset is zero. Thus the effect from the systems in the jth subset to each system in the ith subset will vanish when synchronization in each subset of systems is achieved. This guarantees that clustering synchronization can be realized.

Next we explain the existence of negative elements in the adjacency matrix A in the framework of clustering synchronization. If $a_{ij} > 0$, a cooperative coupling is enforced, while if $a_{ij} < 0$ the coupling is competitive or repulsive. Intuitively, competition or repulsion can affect the synchronization behavior and may result in diverse behaviors in a coupled network. Hence, it is natural to allow negative couplings among different subsets of systems, and to have positive couplings among the systems in the same subset.
In what follows we will also need the following connectivity assumption:

Assumption 5.6 *For each $j = 1, \dots, n$, there exists at least one system $\mathcal{S}_i, i \in \mathbb{N}_j$ which is connected to the leader $\mathcal{L}_j$.*

Moreover, we assume that there is a unique leader for each subset of systems. That is to say, we exclude the possibility that a system $\mathcal{S}_i, i \in \mathbb{N}_j$, is connected to a leader $\mathcal{L}_k$ where $k \neq j$. We use $a_{10}, a_{20}, \dots, a_{N0}$ to describe the existence of a directed edge from the leader to a system. Namely, for each $j = 1, 2, \dots, n$, if there is a coupling from the leader $\mathcal{L}_j$ to the system $\mathcal{S}_i, i \in \mathbb{N}_j$, then $a_{i0} = 1$; otherwise $a_{i0} = 0$.

The matrix A only describes the underlying communication topological structure. It does not provide any information about how strong the couplings or connections are. We use the notion of "coupling strength" to describe the strength of the coupling for an edge. Intuitively, enhancing the couplings among agents inside the same subset will help the whole network to realize clustering synchronization. Hence, we set the coupling strengths among the systems that are inside the set $\mathbb{N}_j$ to be equal to the positive constant $c_j \geqslant 1$. And we set the coupling strengths of the directed edges from the leader $\mathcal{L}_j$ to the systems $\mathcal{S}_i$ where $i \in \mathbb{N}_j$ to be equal to the constant c_j as well. We call the parameters c_j, for $j = 1, \dots, n$ as the inner coupling strengths.

5.3.2 Tracking multiple references

The control strategy, which we propose to solve the clustering output synchronization problem formulated in Definition 5.1, comprises two steps. Since not all the systems $\mathcal{S}_i$ may have access to the leaders, we first design systems which aim at asymptotically reconstructing the reference signals using only locally available relative information. As a second step, we use such an asymptotic estimate of the reference signal to feed the tracking controllers and show that they achieve the prescribed control objective.

To reconstruct the reference signal, the systems cooperate to estimate the internal state of the exosystems. Using the above setting for the communication graph $\mathbb{G}_0$,

for system $\mathcal{S}_i, i \in \mathbb{N}_j, j = 1, \ldots, n$, the estimation is carried out by

$$\begin{aligned}
\dot{\hat{w}}_{0j} &= S\hat{w}_{0j} + G_0\, R(w_{0j} - \hat{w}_{0j})\,, \\
\dot{w}_i &= Sw_i + \sum_{k\in\mathbb{N}_j} c_j\, a_{ik}(w_k - w_i) + \sum_{k=1,k\notin\mathbb{N}_j}^{N} a_{ik}(w_k - w_i) + c_j\, a_{i0}(\hat{w}_{0j} - w_i)\,,
\end{aligned} \tag{5.20}$$

where the matrix G_0 is properly chosen in such a way that $\sigma(S - G_0\, R) \subset \mathbb{C}^-$ and $\hat{w}_{0j}$ is an asymptotic estimate of the leader's internal state w_{0j}. Let matrix $\Xi_j \in \mathbb{R}^{h_j \times h_j}$ denote the diagonal matrix

$$\mathrm{diag}(a_{k_j+1,0}, \ldots, a_{k_j+h_j,0}).$$

In compact form, let $\bar{w}_{h_1} = (w_1^T, \ldots, w_{h_1}^T)^T, \ldots, \bar{w}_{h_n} = (w_{h_1+\cdots+h_{n-1}+1}^T, \ldots, w_{h_1+\cdots+h_n}^T)^T$. We now write the dynamics of the estimations as follows:

$$\begin{aligned}
\begin{pmatrix} \dot{\bar{w}}_{h_1} \\ \dot{\bar{w}}_{h_2} \\ \vdots \\ \dot{\bar{w}}_{h_n} \end{pmatrix} &= (I_N \otimes S) \begin{pmatrix} \bar{w}_{h_1} \\ \bar{w}_{h_2} \\ \vdots \\ \bar{w}_{h_n} \end{pmatrix} - \begin{pmatrix} c_1\, L_{11} & L_{12} & \ldots & L_{1n} \\ L_{21} & c_2\, L_{22} & \ldots & L_{2n} \\ \ldots & \ldots & \ldots & \ldots \\ L_{n1} & L_{n2} & \ldots & c_n\, L_{nn} \end{pmatrix} \otimes I_m \cdot \begin{pmatrix} \bar{w}_{h_1} \\ \bar{w}_{h_2} \\ \vdots \\ \bar{w}_{h_n} \end{pmatrix} \\
&\quad + \mathrm{diag}\,\{c_1\,\Xi_1, c_2\,\Xi_2, \ldots, c_n\,\Xi_n\} \otimes I_m \cdot \begin{pmatrix} \mathbf{1}_{h_1} \otimes \hat{w}_{01} - \bar{w}_{h_1} \\ \mathbf{1}_{h_2} \otimes \hat{w}_{02} - \bar{w}_{h_2} \\ \vdots \\ \mathbf{1}_{h_n} \otimes \hat{w}_{0n} - \bar{w}_{h_n} \end{pmatrix},
\end{aligned} \tag{5.21}$$

where $\mathbf{1}_{h_j} \in \mathbb{R}^{h_j}$ are vectors of all ones, for $j = 1, \ldots, n$.

To show the convergence of w_i, we first introduce some notations of block matrices. Let the matrices

$$L_\Xi \triangleq \begin{pmatrix} c_1\, L_{11} + c_1\,\Xi_1 & L_{12} & \ldots & L_{1n} \\ L_{21} & c_2\, L_{22} + c_2\,\Xi_2 & \ldots & L_{2n} \\ \ldots & \ldots & \ldots & \ldots \\ L_{n1} & L_{n2} & \ldots & c_n\, L_{nn} + c_n\,\Xi_n \end{pmatrix}, \tag{5.22}$$

$L_\Xi^{(1)} \triangleq \mathrm{diag}\{c_1\, L_{11} + c_1\,\Xi_1, c_2\, L_{22} + c_2\,\Xi_2, \ldots, c_n\, L_{nn} + c_n\,\Xi_n\}$, $L_\Xi^{(2)} \triangleq L_\Xi - L_\Xi^{(1)}$, and $D_\Xi \triangleq \mathrm{diag}\,\{c_1\,\Xi_1, c_2\,\Xi_2, \ldots, c_n\,\Xi_n\}$. We have the following result for the convergence of w_i:

Lemma 5.3 *Suppose that Assumptions 5.5 and 5.6 hold. If the matrix L_Ξ is positive definite, then $w_i, i \in \mathbb{N}_j$ for all $j = 1, \ldots, n$ will asymptotically track the references w_{0j}, i.e., it holds that* $\lim_{t\to+\infty} \sum_{j=1}^{n} \sum_{i\in\mathbb{N}_j} ||w_i(t) - w_{0j}(t)|| = 0$.

Proof: Let $\tilde{w}_{h_j} = \bar{w}_{h_j} - \mathbf{1}_{h_j} \otimes w_{0j}$ and $\tilde{w}_{0j} = \hat{w}_{0j} - w_{0j}$ for $j = 1, \dots, n$. From (5.21), one has

$$\begin{aligned}\begin{pmatrix} \dot{\tilde{w}}_{h_1} \\ \dot{\tilde{w}}_{h_2} \\ \vdots \\ \dot{\tilde{w}}_{h_n} \end{pmatrix} &= (I_N \otimes S) \begin{pmatrix} \tilde{w}_{h_1} \\ \tilde{w}_{h_2} \\ \vdots \\ \tilde{w}_{h_n} \end{pmatrix} - \begin{pmatrix} c_1 L_{11} & L_{12} & \dots & L_{1n} \\ L_{21} & c_2 L_{22} & \dots & L_{2n} \\ \dots & \dots & \dots & \dots \\ L_{n1} & L_{n2} & \dots & c_n L_{nn} \end{pmatrix} \otimes I_m \cdot \begin{pmatrix} \bar{w}_{h_1} \\ \bar{w}_{h_2} \\ \vdots \\ \bar{w}_{h_n} \end{pmatrix} \\ &\quad - (D_\Xi \otimes I_m) \cdot \begin{pmatrix} \tilde{w}_{h_1} \\ \tilde{w}_{h_2} \\ \vdots \\ \tilde{w}_{h_n} \end{pmatrix} + (D_\Xi \otimes I_m) \cdot \begin{pmatrix} \mathbf{1}_{h_1} \otimes \tilde{w}_{01} \\ \mathbf{1}_{h_2} \otimes \tilde{w}_{02} \\ \vdots \\ \mathbf{1}_{h_n} \otimes \tilde{w}_{0n} \end{pmatrix}\end{aligned} \tag{5.23}$$

Note that L_{ij} are zero-row-sum matrices. It follows that

$$\begin{pmatrix} c_1 L_{11} & L_{12} & \dots & L_{1n} \\ L_{21} & c_2 L_{22} & \dots & L_{2n} \\ \dots & \dots & \dots & \dots \\ L_{n1} & L_{n2} & \dots & c_n L_{nn} \end{pmatrix} \otimes I_m \cdot \begin{pmatrix} \mathbf{1}_{h_1} \otimes w_{01} \\ \mathbf{1}_{h_2} \otimes w_{02} \\ \vdots \\ \mathbf{1}_{h_n} \otimes w_{0n} \end{pmatrix} = \mathbf{0}\,.$$

Using the above equation and the notation L_Ξ, we can rewrite (5.23) as

$$\begin{pmatrix} \dot{\tilde{w}}_{h_1} \\ \dot{\tilde{w}}_{h_2} \\ \vdots \\ \dot{\tilde{w}}_{h_n} \end{pmatrix} = (I_N \otimes S) \begin{pmatrix} \tilde{w}_{h_1} \\ \tilde{w}_{h_2} \\ \vdots \\ \tilde{w}_{h_n} \end{pmatrix} - (L_\Xi \otimes I_m) \begin{pmatrix} \tilde{w}_{h_1} \\ \tilde{w}_{h_2} \\ \vdots \\ \tilde{w}_{h_n} \end{pmatrix} + (D_\Xi \otimes I_m) \cdot \begin{pmatrix} \mathbf{1}_{h_1} \otimes \tilde{w}_{01} \\ \mathbf{1}_{h_2} \otimes \tilde{w}_{02} \\ \vdots \\ \mathbf{1}_{h_n} \otimes \tilde{w}_{0n} \end{pmatrix} \tag{5.24}$$

Let $\tilde{w} \triangleq (\tilde{w}_{h_1}^T, \tilde{w}_{h_2}^T, \dots, \tilde{w}_{h_n}^T)^T$, $\tilde{w}_0^* \triangleq \big((\mathbf{1}_{h_1} \otimes \tilde{w}_{01})^T, (\mathbf{1}_{h_2} \otimes \tilde{w}_{02})^T, \dots, (\mathbf{1}_{h_n} \otimes \tilde{w}_{0n})^T\big)^T$. Then (5.24) can be written into the compact form

$$\dot{\tilde{w}} = (I_N \otimes S)\tilde{w} - (L_\Xi \otimes I_m)\tilde{w} + (D_\Xi \otimes I_m)\,\tilde{w}_0^*. \tag{5.25}$$

Let $\varpi = (I_N \otimes e^{-St})\tilde{w}$ and $\varphi = (I_N \otimes e^{-St})\tilde{w}_0^*$. Then one has

$$\begin{aligned}\dot{\varpi} &= -(I_N \otimes e^{-St}S)\tilde{w} + (I_N \otimes e^{-St})\dot{\tilde{w}} \\ &= -(I_N \otimes e^{-St})(L_\Xi \otimes I_m)\tilde{w} + (I_N \otimes e^{-St})(D_\Xi \otimes I_m)\tilde{w}_0^* \\ &= -(L_\Xi \otimes I_m)\varpi + (D_\Xi \otimes I_m)\varphi\,.\end{aligned} \tag{5.26}$$

According to the condition in Lemma 5.3, the matrix $-(L_\Xi \otimes I_m)$ is Hurwitz. Moreover, from $\dot{\tilde{w}}_{0j} = \dot{\hat{w}}_{0j} - \dot{w}_{0j} = (S - G_0\,R)\tilde{w}_{0j}$ and $\sigma(S - G_0\,R) \subset \mathbb{C}^-$, one has

that $\tilde{w}_0^*$ converges to zero exponentially as $t \to \infty$. It further implies $\varphi = (I_N \otimes e^{-St})\tilde{w}_0^*$ converges to zero exponentially. Therefore, one has that ϖ converges to the origin exponentially as $t \to \infty$. Furthermore, because $\tilde{w} = (I_N \otimes e^{St})\varpi$ and $\sigma(S) \subset \mathbb{C}^0$, one has that $\tilde{w} \to \mathbf{0}$ exponentially as $t \to \infty$. Thus, one obtains that $\lim_{t\to+\infty} \sum_{j=1}^{n} \sum_{i\in\mathbb{N}_j} ||w_i(t) - w_{0j}(t)|| = 0$. ▫

Remark 5.3 *Assumption 5.5 is a trivial condition when clustering synchronization is discussed in multi-agent systems with diffusively coupled dynamic oscillators. For example, Assumption 5.5 on the Laplacian matrix L is the same as the one in Definition 4 in (Wu et al. 2009), and similar to that in Proposition 2 in (Xia and Cao 2011). However, in this subsection we study different system dynamics and thus a different problem. We have proposed the stability criterion for system (5.20) in Lemma 5.3 under suitable assumptions on the communication topologies.*

The condition on the matrix L_Ξ is an algebraic condition, which is difficult to check in applications. Now we specify the connectivity strengths such that the matrix L_Ξ is negative definitive. The way to construct the connectivity strengths is motivated by some results in (Wu et al. 2009, Xia and Cao 2011). Since the results in (Wu et al. 2009, Xia and Cao 2011) cannot be applied to our problem directly, we carry out the construction as follows:

Lemma 5.4 (Horn and Johnson 1985) *Let A and B be $N \times N$ Hermitian matrices, and let the eigenvalues $\lambda_i(A)$, $\lambda_i(B)$, $\lambda_i(A+B)$ be arranged in increasing order as $\lambda_1(\cdot) \leqslant \lambda_2(\cdot) \leqslant \ldots \leqslant \lambda_N(\cdot)$. For each $k = 1, 2, \ldots, N$, we have*

$$\lambda_k(A) + \lambda_1(B) \leqslant \lambda_k(A+B) \leqslant \lambda_k(A) + \lambda_N(B)\,.$$

Lemma 5.5 *Suppose that Assumptions 5.5 and 5.6 hold. And suppose that the matrix L is symmetric and the matrices L_{jj} for $j = 1, \ldots, n$ are irreducible. If*

$$c_j > \max\left\{-\frac{\lambda_{\min}(L_\Xi^{(2)})}{\lambda_{\min}(L_{jj} + \Xi_j)}\,, 0\right\}$$

for all $j = 1, \ldots, n$, then the matrix L_Ξ is positive definitive.

Proof: We will prove that the matrix L_Ξ is positive definite if the constants c_j for $j = 1, \ldots, n$ are sufficiently large. From Lemma 5.4, one has

$$\begin{aligned}
\lambda_{\min}(L_\Xi) &\geqslant \lambda_{\min}(L_\Xi^{(1)}) + \lambda_{\min}(L_\Xi^{(2)}) \\
&= \min_{1\leqslant j\leqslant n}\{\lambda_{\min}(c_j\, L_{jj} + c_j\, \Xi_j)\} + \lambda_{\min}(L_\Xi^{(2)}) \\
&= \min_{1\leqslant j\leqslant n}\{c_j\, \lambda_{\min}(L_{jj} + \Xi_j)\} + \lambda_{\min}(L_\Xi^{(2)})\,.
\end{aligned}$$

Note that L_{jj} for $j = \{1, \ldots, n\}$ are Laplacian matrices satisfying zero row sums and non-positive off-diagonal elements. Thus L_{jj} are positive semi-definite. In addition, L_{jj} are irreducible. According to Lemma 1, the matrices $L_{jj} + \Xi_j$ for $j = 1, \ldots, n$ are positive definite. Thus, if $c_j > -\frac{\lambda_{\min}(L_\Xi^{(2)})}{\lambda_{\min}(L_{jj}+\Xi_j)}$ for $j = 1, \ldots, n$, then $\lambda_{\min}(L_\Xi) > 0$. We have arrived at the conclusion that the matrix L_Ξ is positive definite if $c_j > \max\left\{-\frac{\lambda_{\min}(L_\Xi^{(2)})}{\lambda_{\min}(L_{jj}+\Xi_j)}, 0\right\}$ for $j = 1, \ldots, n$. □

Now we give some comments on the condition of the inner coupling strengths c_j in Lemma 5.5.

Remark 5.4 *There might exist other connection patterns such that L_Ξ is positive definite. Lemma 5.5 provides one way to construct communication topologies for this purpose. It requires lower bounds for c_j to guarantee the positive-definiteness of L_Ξ which implies that large inner couplings are good for clustering synchronization in a network. This also can be understood in real-world situations, as clustering is likely to happen in a network if inner connections inside clusters are strong while connections among different clusters are weak. In addition, if more systems in the subset $\mathbb{N}_j$ are connected to their leader $\mathcal{L}_j$, it results in a larger positive value of $\lambda_{\min}(L_{jj} + \Xi_j)$. According to the lower bound for c_j in Lemma 5.5, a smaller positive c_j may be obtained consequently. This also makes sense in practice.*

We have discussed clustering synchronization of the reference trajectories in Lemma 5.3. The estimations w_i can be treated as a group of reference signals, and used to tackle the decentralized n-cluster output synchronization problem for heterogeneous systems. This is pursued below.

We introduce the controllers for systems (5.1) as follows. For agent $i \in \mathbb{N}_j, j = 1, \ldots, n$, we design u_i as

$$\begin{aligned}
\dot{\hat{w}}_{0j} &= S\hat{w}_{0j} + G_0\, R(w_{0j} - \hat{w}_{0j}) \\
\dot{w}_i &= Sw_i + \sum_{k\in\mathbb{N}_j} c_j\, a_{ik}(w_k - w_i) + \sum_{k=1,k\notin\mathbb{N}_j}^{N} a_{ik}(w_k - w_i) + c_j\, a_{i0}(\hat{w}_{0j} - w_i) \\
\dot{\eta}_i &= \Phi_i\, \eta_i + G_i\, M_i \xi_i \\
\dot{\xi}_i &= L_i\xi_i + K_i(y_i - Rw_i) \\
u_i &= H_i\eta_i + M_i\xi_i
\end{aligned} \tag{5.27}$$

The matrices $\Phi_i, G_i, M_i, L_i, K_i, H_i$ are those found in Assumption 5.2. The design of η_i, ξ_i, u_i is inspired by the output regulation method for a single system in (Isidori et al. 2003).

Theorem 5.2 *Consider N heterogeneous linear systems (5.1) coupled via the dynamic couplings (5.27). Suppose that Assumptions 5.1 and 5.2 hold, and the assumptions in Lemma 5.3 hold. Then,* $\lim_{t\to+\infty} \sum_{j=1}^{n} \sum_{i\in\mathbb{N}_j} ||y_i(t) - Rw_{0j}(t)|| = 0$.

*P*roof: Let $\tilde{x}_i = x_i - \Pi_i(\mu_i)w_i$, $\tilde{\eta}_i = \eta_i - \Sigma_i(\mu_i)w_i$. Similar manipulations as those in the proof of Theorem 5.1 lead to

$$\dot{\tilde{x}}_i = A_i(\mu_i)\tilde{x}_i + B_i(\mu_i)H_i\tilde{\eta}_i + B_i(\mu_i)M_i\xi_i - \Pi_i(\mu_i)\left(\sum_{k\in\mathbb{N}_j} c_j\, a_{ik}(w_k - w_i) + \sum_{k=1,k\notin\mathbb{N}_j}^{N} a_{ik}(w_k - w_i) + c_j\, a_{i0}(\hat{w}_{0j} - w_i)\right),$$

and

$$\dot{\tilde{\eta}}_i = \Phi_i\tilde{\eta}_i + G_iM_i\xi_i - \Sigma_i(\mu_i)\cdot \cdot\left(\sum_{k\in\mathbb{N}_j} c_j\, a_{ik}(w_k - w_i) + \sum_{k=1,k\notin\mathbb{N}_j}^{N} a_{ik}(w_k - w_i) + c_j\, a_{i0}(\hat{w}_{0j} - w_i)\right).$$

Furthermore $y_i - Rw_i = C_i(\mu_i)\tilde{x}_i$. Hence,

$$\begin{aligned}\dot{\xi}_i &= L_i\xi_i + K_i(y_i - Rw_i)\\ &= L_i\xi_i + K_i\begin{pmatrix} C_i(\mu_i) & \mathbf{0}\end{pmatrix}\begin{pmatrix}\tilde{x}_i\\ \tilde{\eta}_i\end{pmatrix}.\end{aligned} \tag{5.28}$$

In the new coordinates $\tilde{x}_i, \tilde{\eta}_i$ and ξ_i, the system can be written as

$$\begin{aligned}\begin{pmatrix}\dot{\tilde{x}}_i\\ \dot{\tilde{\eta}}_i\end{pmatrix} &= \begin{pmatrix}A_i(\mu_i) & B_i(\mu_i)H_i\\ \mathbf{0} & \Phi_i\end{pmatrix}\begin{pmatrix}\tilde{x}_i\\ \tilde{\eta}_i\end{pmatrix} + \begin{pmatrix}B_i(\mu_i)\\ G_i\end{pmatrix}M_i\xi_i\\ &\quad - \begin{pmatrix}\Pi_i(\mu_i)\\ \Sigma_i(\mu_i)\end{pmatrix}\left(\sum_{k\in\mathbb{N}_j} c_j\, a_{ik}(w_k - w_i) + \sum_{k=1,k\notin\mathbb{N}_j}^{N} a_{ik}(w_k - w_i) + c_j\, a_{i0}(\hat{w}_{0j} - w_i)\right)\\ \dot{\xi}_i &= L_i\xi_i + K_i\begin{pmatrix}C_i(\mu_i) & \mathbf{0}\end{pmatrix}\begin{pmatrix}\tilde{x}_i\\ \tilde{\eta}_i\end{pmatrix}.\end{aligned} \tag{5.29}$$

By Assumption 5.2, the dynamic matrix of the closed loop system (5.29) is Hurwitz. Moreover, all the forcing inputs decay exponentially to zero. As a result $\lim_{t\to+\infty} \sum_{j=1}^{n} \sum_{i\in\mathbb{N}_j} ||y_i(t) - Rw_{0j}(t)|| = 0$. □

5.4 Design of the controllers

The actual design of the controllers in the previous sections 5.2 and 5.3 depends on the fulfillment of the conditions in Assumption 5.2 or 5.4. In this section we discuss

how this can be achieved. The arguments follow the treatment in (Isidori et al. 2003, Section 1.5). For the sake of simplicity, we only focus on the design of controllers discussed in Section 5.2. The controllers discussed in Section 5.3 can be designed similarly.

We start with condition (ii), namely with the fulfillment of the internal model principle. Let Φ, H and $\Sigma_i(\mu_i)$ be the matrices

$$\Phi = \begin{pmatrix} 0 & 1 & 0 & \dots & 0 \\ 0 & 0 & 1 & \dots & 0 \\ \vdots & \vdots & \vdots & \ddots & \vdots \\ 0 & 0 & 0 & \dots & 1 \\ -a_0 & -a_1 & -a_2 & \dots & -a_d \end{pmatrix}, H = \begin{pmatrix} 1 \\ 0 \\ 0 \\ \dots \\ 0 \end{pmatrix}^T$$

$$\Sigma_i(\mu_i) = \begin{pmatrix} \Gamma_i(\mu_i) \\ \Gamma_i(\mu_i)S \\ \vdots \\ \Gamma_i(\mu_i)S^{d-2} \\ \Gamma_i(\mu_i)S^{d-1} \end{pmatrix}$$

where $\lambda^d + a_{d-1}\lambda^{d-1} + a_1 d + a_0$ is the minimal polynomial of S and $\Gamma_i(\mu_i)$ is the matrix which appears in the regulator equations (5.3). It is straightforward to check that these matrices satisfy the internal model condition (5.4).

To the purpose of fulfilling also the robust stability condition (iii), it is convenient to introduce other matrices F_i, G_i, Ψ_i, T_i which also fulfill the internal model principle. These matrices are detailed in the following lemma:

Lemma 5.6 (Isidori et al. 2003, Lemma 1.5.6) *Let F_i be any Hurwitz $s \times s$ matrix and let G_i be any $s \times 1$ vector such that the pair (F_i, G_i) is controllable. Let Φ be any $s \times s$ matrix whose eigenvalues are all in $\overline{\mathbb{C}^+}$ and let H be any $1 \times s$ vector such that the pair (H, Φ) is observable.*

Then there exist a $1 \times s$ vector Ψ_i and a nonsingular $s \times s$ matrix T_i such that

$$\begin{aligned} (F_i + G_i\Psi_i)T_i &= T_i\Phi \\ \Psi_i T_i &= H. \end{aligned} \tag{5.30}$$

It is immediate to see that the matrix $\tilde{\Sigma}_i(\mu_i) = T_i\Sigma_i(\mu_i)$ satisfies

$$\begin{aligned} \tilde{\Sigma}_i(\mu_i)S &= (F_i + G_i\Psi_i)\tilde{\Sigma}_i(\mu_i) \\ \Gamma_i(\mu_i) &= \Psi_i\tilde{\Sigma}_i(\mu_i)\ . \end{aligned}$$

Hence, the internal model principle property (5.4) is fulfilled by the matrices $F_i + G_i\Psi_i$, Ψ_i, $\tilde{\Sigma}_i(\mu_i)$.

The controllers introduced in Section 5.2.2 can be rewritten as:

$$\begin{aligned}
\dot{\hat{w}}_0 &= S\hat{w}_0 + G_0 R(w_0 - \hat{w}_0) \\
\dot{w}_1 &= Sw_1 + \sum_{j=1}^{N} a_{1j}(w_j - w_1) + a_{10}(\hat{w}_0 - w_1) \\
\dot{\eta}_1 &= (F_1 + G_1\Psi_1)\,\eta_1 + G_1 M_1 \xi_1 \\
\dot{\xi}_1 &= L_1\xi_1 + K_1(y_1 - Rw_1) \\
u_1 &= \Psi_1\eta_1 + M_1\xi_1
\end{aligned} \tag{5.31}$$

and, for agent $i = 2, \cdots, N$,

$$\begin{aligned}
\dot{w}_i &= Sw_i + \sum_{j=1}^{N} a_{ij}(w_j - w_i) \\
\dot{\eta}_i &= (F_i + G_i\Psi_i)\,\eta_i + G_i\, M_i\xi_i \\
\dot{\xi}_i &= L_i\xi_i + K_i(y_i - Rw_i) \\
u_i &= \Psi_i\eta_i + M_i\xi_i
\end{aligned} \tag{5.32}$$

For the purpose of stabilizing the overall closed-loop system (requirement (iii) in Assumption 5.2), it is more convenient to work with these controllers (5.31),(5.32) rather than with those in (5.13), (5.14). In the rest of the section, we turn now to the problem of determining the stabilizing matrices L_i, K_i, M_i, $i = 1, 2, \ldots, N$.
For each i, consider the system (5.1) with output $\varepsilon_i = y_i - Rw_i$, namely

$$\begin{aligned}
\dot{x}_i &= A_i(\mu_i)\, x_i + B_i(\mu_i)\, u_i \\
\varepsilon_i &= C_i(\mu_i)\, x_i - Rw_i\,.
\end{aligned} \tag{5.33}$$

As in (Isidori et al. 2003), to reduce the notational burden, we focus on the case in which the inputs u_i and the outputs y_i are scalar, i.e. $p_i = 1$ for $i = 1, 2, \ldots, N$ and $q = 1$. Further assume that $\mathcal{P}_i$ is a compact set and that for each $\mu_i \in \mathcal{P}_i$, the system (5.33) has the same relative degree r_i from u_i to ε_i. Namely, there exists an integer $r_i \geqslant 1$ such that for each $\mu_i \in \mathcal{P}_i$

$$\begin{aligned}
C_i(\mu_i)A_i^j(\mu_i)B_i(\mu_i) = 0\ ,\ j = 0, 1, \ldots, r_i - 2 \\
C_i(\mu_i)A_i^{r_i-1}(\mu_i)B_i(\mu_i) \neq 0\ .
\end{aligned}$$

Then there exists a μ_i-dependent change of coordinates

$$\begin{pmatrix} z_i \\ e_i \end{pmatrix} = \begin{pmatrix} \dfrac{Z_i(\mu_i)}{C_i(\mu_i)} \\ C_i(\mu_i)A_i(\mu_i) \\ \vdots \\ C_i(\mu_i)A_i(\mu_i)^{r_i-1} \end{pmatrix} x_i =: \tilde{Z}_i(\mu_i)x_i, \tag{5.34}$$

where $Z_i(\mu_i)$ is a suitable matrix such that $\tilde{Z}_i(\mu_i)$ is nonsingular, such that the system (5.33) in the new coordinates becomes

$$\begin{array}{rcl} \dot{z}_i & = & A_i^{(11)}(\mu_i)z_i + A_i^{(12)}(\mu_i)e_i \\ \dot{e}_{i1} & = & e_{i2} \\ & \vdots & \\ \dot{e}_{i,r_i-1} & = & e_{ir_i} \\ \dot{e}_{i,r_i} & = & A_i^{(21)}(\mu_i)z_i + A_i^{(22)}(\mu_i)e_i + b_i(\mu_i)u_i \\ \varepsilon_i & = & e_{i1} - Rw_i = \overline{C}e_i - Rw_i, \end{array} \tag{5.35}$$

where in particular $b_i(\mu_i) = C_i(\mu_i)A_i^{r_i-1}(\mu_i)B_i(\mu_i) \neq 0$.
We further change the coordinates in the following way:

$$\tilde{e}_i = e_i + Q_i w$$

where $Q_i = (Q_{i1}^T \dots Q_{ir}^T)^T$, $w = (w_1^T \dots w_N^T)^T$,

$$\begin{array}{rcl} Q_{i1} & = & (\mathbf{0}_{1\times m} \dots \mathbf{0}_{1\times m} \ -R\, \mathbf{0}_{1\times m} \dots \mathbf{0}_{1\times m}) \ , \\ Q_{i,j+1} & = & Q_{i,j}\tilde{S}, \quad j = 1, 2, \dots r_i - 1 \end{array}$$

and $\tilde{S} = (I_N \otimes S - L \otimes I_m)$. Then we obtain

$$\begin{array}{rcl} \dot{z}_i & = & A_i^{(11)}(\mu_i)z_i + A_i^{(12)}(\mu_i)\tilde{e}_i + \overline{Q}_i(\mu_i)w \\ \dot{\tilde{e}}_{i1} & = & \tilde{e}_{i2} \\ & \vdots & \\ \dot{\tilde{e}}_{i,r_i-1} & = & \tilde{e}_{ir_i} \\ \dot{\tilde{e}}_{i,r_i} & = & A_i^{(21)}(\mu_i)z_i + A_i^{(22)}(\mu_i)\tilde{e}_i + \tilde{Q}_i(\mu_i)w + b_i(\mu_i)u_i \\ \varepsilon_i & = & \tilde{e}_{i1}, \end{array} \tag{5.36}$$

with

$$\overline{Q}_i(\mu_i) = -A_i^{(12)}(\mu_i)Q_i, \tilde{Q}_i(\mu_i) = -A_i^{(22)}(\mu_i)Q_i.$$

Below we use the following partition for the two matrices:

$$\begin{array}{rcl} \overline{Q}_i(\mu_i) & = & (\overline{Q}_{i1}(\mu_i) \dots \overline{Q}_{iN}(\mu_i)) \\ \tilde{Q}_i(\mu_i) & = & (\tilde{Q}_{i1}(\mu_i) \dots \tilde{Q}_{iN}(\mu_i)). \end{array}$$

Observe that due to the latter change of coordinates the signal w affects the dynamics of the systems. Hence, (5.36) falls in the class of systems considered in (5.17) and Corollary 5.1 applies. Before doing this, we need an additional assumption. Let the system (5.33) be minimum-phase, namely

Assumption 5.7 *For each $\mu_i \in \mathcal{P}_i$, all the eigenvalues of $A_i^{(11)}(\mu_i)$ have strictly negative real parts.*

As a consequence of this assumption it is promptly verified (see (Isidori et al. 2003), page 27) that the matrices

$$\begin{aligned} \Pi_i(\mu_i) &= \begin{pmatrix} \Pi_{i1}(\mu_i)^T & 0 & \dots & 0 \end{pmatrix}^T \\ \Gamma_i(\mu_i) &= -\frac{1}{b_i(\mu_i)} \left[A_i^{(21)}(\mu_i)\Pi_{i1}(\mu_i) - \sum_{j=1}^{N} \tilde{Q}_{ij}(\mu_i) \right], \end{aligned} \tag{5.37}$$

where $\Pi_{i1}(\mu_i)$ is the unique $r_i \times r_i$ matrix which solves the Sylvester equation

$$\Pi_{i1}(\mu_i)S = A_i^{(11)}(\mu_i)\Pi_{i1}(\mu_i) + \sum_{j=1}^{N} \overline{Q}_{ij}(\mu_i), \tag{5.38}$$

satisfy condition (i) in Assumption 5.4 with

$$P_i(\mu_i) = \begin{pmatrix} \overline{Q}_i(\mu_i) \\ 0 \\ \vdots \\ 0 \\ \tilde{Q}_i(\mu_i) \end{pmatrix}.$$

Before carrying out the next step of our robust controllers design, we explain the differences of our design method explored in the above, compared with the basic robust regulator design method in (Isidori et al. 2003).

Remark 5.5 *The arguments on the actual design of the decentralized robust controllers follow closely the treatment in (Isidori et al. 2003), but they are not the same. The robust controller design method in (Isidori et al. 2003) only deals with output regulation of a single system. In our case, we design decentralized robust controllers for the cooperative multi-agent systems (5.1). Consequently, we have to deal with the dynamical coupling terms existing in the controllers (5.31) and (5.32). To be specific, in our case only system $\mathcal{S}_1$ has direct access to the exosystem, the other systems $\mathcal{S}_2, \dots, \mathcal{S}_N$ are fed by the local estimates of the reference signal. As a result, the systems' controllers are coupled with each other through the estimates, and the controllers cannot be designed separately for each system $\mathcal{S}_i$ to track the corresponding reconstructed reference signal w_i. To deal with the difficulties caused by the dynamical couplings and the cooperation framework discussed in this chapter, in the calculations to obtain (5.36) we treat the reconstructed references $w_1, \dots, w_N$ as a whole, that is generated by an exosystem $\dot{w} = \tilde{S}\, w$. Finally, we have adopted different coordinate changes for $\tilde{e}_i$, compared with those in (Isidori et al. 2003, Section 1.5).*

The design of the matrices K_i, L_i, M_i such that condition (iii) is satisfied can be carried out in two steps. Consider the system (5.36) and write it in the compact form

$$\begin{aligned}\dot{z}_i &= A_i^{(11)}(\mu_i)z_i + A_i^{(12)}(\mu_i)\tilde{e}_i + \overline{Q}_i(\mu_i)w \\ \dot{\tilde{e}}_i &= \overline{A}\tilde{e}_i + \overline{B}\left[A_i^{(21)}(\mu_i)z_i + A_i^{(22)}(\mu_i)\tilde{e}_i + \tilde{Q}_i(\mu_i)w + b_i(\mu_i)u_i\right] \\ \varepsilon_i &= \overline{C}\tilde{e}_i,\end{aligned} \tag{5.39}$$

where $\overline{A}, \overline{B}, \overline{C}$ are understood from the context. Also consider a controller of the form

$$\begin{aligned}\dot{\eta}_i &= F_i\eta_i + G_iu_i \\ u_i &= \Psi_i\eta_i + v_i\end{aligned} \tag{5.40}$$

where v_i is an additional control input and obtain the closed-loop system

$$\begin{aligned}\dot{\eta}_i &= (F_i + G_i\Psi_i)\eta_i + G_iv_i \\ \dot{z}_i &= A_i^{(11)}(\mu_i)z_i + A_i^{(12)}(\mu_i)\tilde{e}_i + \overline{Q}_i(\mu_i)w \\ \dot{\tilde{e}}_i &= \overline{A}\tilde{e}_i + \overline{B}\Big[A_i^{(21)}(\mu_i)z_i + A_i^{(22)}(\mu_i)\tilde{e}_i + \\ &\qquad \tilde{Q}_i(\mu_i)w + b_i(\mu_i)(\Psi_i\eta_i + v_i)\Big] \\ \varepsilon_i &= \overline{C}\tilde{e}_i.\end{aligned} \tag{5.41}$$

The change of coordinates

$$\chi_i = \eta_i - \frac{1}{b_i(\mu_i)}G_i\overline{C}\,\overline{A}^{r_i-1}\tilde{e}_i$$

yields the closed-loop system

$$\begin{aligned}\begin{pmatrix}\dot{\chi}_i \\ \dot{z}_i\end{pmatrix} &= \begin{pmatrix}F_i(\mu_i) & -\frac{1}{b_i(\mu_i)}G_iA_i^{(21)}(\mu_i) \\ 0 & A_i^{(11)}(\mu_i)\end{pmatrix}\begin{pmatrix}\chi_i \\ z_i\end{pmatrix} + \\ &\quad \begin{pmatrix}\frac{1}{b_i(\mu_i)}\left[F_iG_i\overline{C}\,\overline{A}^{r_i-1} - G_iA_i^{(22)}(\mu_i)\right] \\ A_i^{(12)}(\mu_i)\end{pmatrix}\tilde{e}_i + \begin{pmatrix}-\frac{1}{b_i(\mu_i)}G_i\tilde{Q}_i(\mu_i) \\ \overline{Q}_i(\mu_i)\end{pmatrix}w \\ \dot{\tilde{e}}_i &= \overline{A}\tilde{e}_i + \overline{B}\Big[b_i(\mu_i)\Psi_i\chi_i + A_i^{(21)}(\mu_i)z_i + \\ &\qquad (A_i^{(22)}(\mu_i) + \Psi_iG_i\overline{CA}^{r_i-1})\tilde{e}_i + b_i(\mu_i)v_i + \tilde{Q}_i(\mu_i)w\Big] \\ \varepsilon_i &= \overline{C}\tilde{e}_i.\end{aligned} \tag{5.42}$$

The zero dynamics of the system is

$$\begin{pmatrix}\dot{\chi}_i \\ \dot{z}_i\end{pmatrix} = \begin{pmatrix}F_i & -\frac{1}{b_i(\mu_i)}G_iA_i^{(21)}(\mu_i) \\ 0 & A_i^{(11)}(\mu_i)\end{pmatrix}\begin{pmatrix}\chi_i \\ z_i\end{pmatrix}.$$

This is asymptotically stable for each $\mu_i \in \mathcal{P}_i$ since F_i is Hurwitz by construction and $A_i^{(11)}(\mu_i)$ is Hurwitz by Assumption 5.7. In view of this property, it is proven in (Isidori et al. 2003, Lemma 1.5.4) that under the assumption that $b_i(\mu_i) \geqslant \bar{b}_i > 0$ for all $\mu_i \in \mathcal{P}_i$, there exists a positive gain k_i^*, a $1 \times r_i$ vector $\overline{M}_i$ such that for all $k_i \geqslant k_i^*$, the feedback

$$v_i = -k_i \overline{M}_i \tilde{e}_i =: M_i \tilde{e}_i \tag{5.43}$$

stabilizes the system (5.42) for all $\mu_i \in \mathcal{P}_i$. Moreover, the matrix $\overline{M}_i$ is of the form

$$\overline{M}_i = (d_{i0}\ d_{i1}\ \ldots\ d_{i,r_i-2}\ 1)$$

where $\lambda^{r_i-1} + d_{i,r_i-2}\lambda^{r_1-2} + \ldots + d_{i0}$ is any polynomial having all the roots with strictly negative real parts.
The feedback (5.43) cannot be implemented since it requires the knowledge of $\tilde{e}_i$ which is not available. The second step of the construction consists in the design of a controller which uses an estimate of $\tilde{e}_i$. This design can be carried out following (Isidori et al. 2003, Lemma 1.5.5). Consider the dynamic feedback controller

$$\begin{array}{rcl} \dot{\xi}_i & = & L_i \xi_i + K_i \varepsilon_i \\ v_i & = & M_i \xi_i, \end{array} \tag{5.44}$$

where

$$L_i = \begin{pmatrix} -g_i c_{i,r_i-1} & 1 & \ldots & 0 \\ -g_i^2 c_{i,r_i-2} & 0 & \ldots & 0 \\ \vdots & \vdots & \ddots & \vdots \\ -g_i^{r_i-1} c_{i,1} & 0 & \ldots & 1 \\ -g_i^{r_i} c_{i,0} & 0 & \ldots & 0 \end{pmatrix}, K_i = \begin{pmatrix} g_i c_{i,r_i-1} \\ g_i^2 c_{i,r_i-2} \\ \vdots \\ g_i^{r_i-1} c_{i,1} \\ g_i^{r_i} c_{i,0} \end{pmatrix} \tag{5.45}$$

the polynomial $\lambda^{r_i} + c_{i,r_i-1}\lambda^{r_i-1} + \ldots + c_{i,1}\lambda^1 + c_{i,0}$ is any polynomial having all the roots with negative real part, $g_i > 0$ is a design parameter and M_i is as in (5.43). Under Assumption 5.7, if $b_i(\mu_i) \geqslant \bar{b}_i > 0$ for all $\mu_i \in \mathcal{P}_i$, it can be shown that there exists a positive gain $g_i^* > 0$ such that, for all $g_i \geqslant g_i^*$, the controller (5.44) asymptotically stabilize the system (5.42) for all $\mu_i \in \mathcal{P}_i$.
The latter statement allows us to summarize as follows:

Proposition 5.1 *Consider the system (5.39). Let Assumption 5.7 hold and assume that $b_i(\mu_i) \geqslant \bar{b}_i > 0$ for all $\mu_i \in \mathcal{P}_i$, with $\mathcal{P}_i$ a compact set. Then there exists a positive gain $g_i^* > 0$ such that, for all $g_i \geqslant g_i^*$, the matrices L_i, K_i, M_i defined in (5.45) and (5.43) are such that the dynamic feedback controller (5.44) globally asymptotically stabilizes (5.42) for all $\mu_i \in \mathcal{P}_i$.*

Remark 5.6 *The overall controller is given by the interconnection of the internal model (5.40) and the stabilizer (5.44). We observe that the design of the two controllers requires local information only. As a matter of fact, the matrices F_i, G_i, Ψ_i of the internal model can be obtained via Lemma 5.6. On the other hand, the controller (5.44) is designed to robustly stabilize the system (5.39). Since the only terms in the system (5.39) that depend on the Laplacian matrix L are the "disturbance" vectors $\overline{Q}_i(\mu_i), \tilde{Q}_i(\mu_i)$ which play no role in the stability property of the closed-loop system, one infers that the design of L_i, K_i, M_i is independent of the knowledge of the graph topology.*

Remark 5.7 *We do not assume explicit bounds for the uncertainties μ_i, but implicit in Assumption 5.7.*

5.5 Numerical examples

5.5.1 Tracking a single reference

In this section we illustrate the design of the robust controllers for decentralized output regulation via a numerical example. The example we consider corresponds to a network of double integrators with different actuator dynamics, namely we consider the case in which the systems (5.1) are modeled as

$$\begin{aligned} \dot{x}_i &= \underbrace{\begin{pmatrix} 0 & 1 & 0 \\ 0 & 0 & c_i \\ 0 & -d_i & -a_i \end{pmatrix}}_{A_i(\mu_i)} x_i + \underbrace{\begin{pmatrix} 0 \\ 0 \\ b_i \end{pmatrix}}_{B_i(\mu_i)} u_i \\ y_i &= \underbrace{\begin{pmatrix} 1 & 0 & 0 \end{pmatrix}}_{C_i(\mu_i)} x_i, \quad i = 1, 2, \ldots, N, \end{aligned} \tag{5.46}$$

where $\mu_i = (a_i\, b_i\, c_i\, d_i)^T$ is the vector of uncertain parameters. The example was proposed in (Wieland et al. 2011) where it was assumed that the parameters appearing in the equations are known and used to design the controllers. Here we consider the case when these parameters are uncertain. Hence the controllers have to be designed differently. We assume that μ_i is not precisely known and ranges over a compact set $\mathcal{P}_i$ which is contained in $\mathbb{R}^3_{>0} \times \mathbb{R}_{\geqslant 0}$. Observe that the uncertain parameters a_i, b_i, c_i are bounded away from zero. We consider the problem in which the matrices which define the leader's equation (5.2) are given by

$$S = \begin{pmatrix} 0 & 1 \\ 0 & 0 \end{pmatrix}, \quad R = \begin{pmatrix} 1 & 0 \end{pmatrix}. \tag{5.47}$$

In other words, the position of the systems (5.46) has to asymptotically evolve as the ramp reference signal set by the leader.
Following the previous section, we first compute the relative degree r_i of each system. It is easily verified that

$$\begin{aligned} C_i(\mu_i)B_i(\mu_i) = C_i(\mu_i)A_i(\mu_i)B_i(\mu_i) = 0 \\ C_i(\mu_i)A_i^2(\mu_i)B_i(\mu_i) = b_i c_i \ . \end{aligned}$$

Since $b_i c_i \neq 0$ for each $\mu_i \in \mathcal{P}_i$, the previous equalities show that each system has a relative degree $r_i = 3$. As the relative degree equals the dimension of the systems, the matrix $\tilde{Z}_i(\mu_i)$ in the change of coordinates (5.34) can be written as

$$\tilde{Z}_i(\mu_i) = \begin{pmatrix} C_i(\mu_i) \\ C_i(\mu_i)A_i(\mu_i) \\ C_i(\mu_i)A_i(\mu_i)^2 \end{pmatrix} = \begin{pmatrix} 1 & 0 & 0 \\ 0 & 1 & 0 \\ 0 & 0 & c_i \end{pmatrix}$$

and in the new coordinates the system (5.35) can be written as

$$\begin{aligned} \dot{e}_{i1} &= e_{i2} \\ \dot{e}_{i2} &= e_{i3} \\ \dot{e}_{i3} &= -c_i d_i e_{i2} - a_i e_{i3} + b_i c_i u_i. \end{aligned} \tag{5.48}$$

When compared with (5.35), we observe that the system has no zero dynamics and checking Assumption 5.7 becomes superfluous. Moreover,

$$A_i^{(21)}(\mu_i) = 0, A_i^{(22)}(\mu_i) = -\begin{pmatrix} 0 & c_i d_i & a_i \end{pmatrix}, b_i(\mu_i) = b_i c_i,$$

from which we conclude that $b_i(\mu_i) \geqslant \bar{b}_i > 0$, for all $\mu_i \in \mathcal{P}_i$, for some $\bar{b}_i$.
Having verified that all the assumptions of Proposition 5.1 hold, we can determine the controllers. First of all, we determine the matrices F_i, G_i, Ψ_i in (5.40). This computation is carried out as in the proof of (Isidori et al. 2003, Lemma 1.5.6). Since the minimal polynomial of S is λ^2, we have

$$\Phi = \begin{pmatrix} 0 & 1 \\ 0 & 0 \end{pmatrix} \quad H = \begin{pmatrix} 1 & 0 \end{pmatrix}$$

and let (see Lemma 5.6 above)

$$F_i = \begin{pmatrix} 0 & 1 \\ -1 & -2 \end{pmatrix}, \quad G_i = \begin{pmatrix} 0 \\ 1 \end{pmatrix}$$

be a pair of matrices with F_i Hurwitz and (F_i, G_i) controllable. Here, for the sake of simplicity, we take F_i, G_i to be the same for each $i = 1, 2, \ldots, N$. Following the

proof of (Isidori et al. 2003, Lemma 1.5.6), one can construct the vector Ψ_i and the nonsingular matrix T_i which satisfy (5.30) and obtain

$$\Psi_i = \begin{pmatrix} 1 & 2 \end{pmatrix}, \quad T_i = \begin{pmatrix} 1 & -2 \\ 0 & 1 \end{pmatrix}.$$

This concludes the computation of the matrices F_i, G_i, Ψ_i which appear in (5.40).
We turn now to the design of the matrices L_i, K_i, M_i which appear in (5.7). Since $r_i = 3$, and letting $\lambda^2+d_{i1}\lambda+d_{i0} = \lambda^2+2\lambda+1$, $\lambda^3+c_{i2}\lambda^2+c_{i1}\lambda+c_{i0} = \lambda^3+3\lambda^2+3\lambda+1$ two polynomials with all the roots having strictly negative real parts, the matrices L_i, K_i, M_i are given by

$$L_i = \begin{pmatrix} -3g_i & 1 & 0 \\ -3g_i^2 & 0 & 1 \\ -g_i^3 & 0 & 0 \end{pmatrix}, \quad K_i = \begin{pmatrix} 3g_i \\ 3g_i^2 \\ g_i^3 \end{pmatrix},$$
$$M_i = -k_i \begin{pmatrix} 1 & 2 & 1 \end{pmatrix}$$

where k_i, g_i are gains to be chosen sufficiently large. Finally, we let $G_0 = (2\ 1)^T$ be such that $S - G_0 R$ is Hurwitz.
We conclude that the controllers (5.31), (5.32) with the matrices $F_i, G_i, \Psi_i, L_i, K_i, M_i$, G_0 computed above, solve the decentralized output regulation problem for the systems (5.46), (5.47).
We have run a simulation for $N = 4$ systems with parameters $\{a_i, b_i, c_i, d_i\}$ chosen to be $\{1+\mu_1, 1+\mu_2, 1+\mu_3, \mu_4\}$, $\{2.5+\mu_1, 2+\mu_2, 1+\mu_3, \mu_4\}$, $\{2+\mu_1, 1+\mu_2, 1+\mu_3, 0.5+\mu_4\}$, $\{2+\mu_1, 1+\mu_2, 1+\mu_3, 1+\mu_4\}$ respectively, where $\mu_1, \mu_2, \mu_3, \mu_4$ are $0.3, 0.4, 0.5, 0.7$ respectively. We set the gains $k = 1.1$, $g = 14$. As for the communication graph, we have chosen one with a direct link between the exosystem and the system $\mathcal{S}_1$, i.e. there is a directed link $(0, 1)$. The communication graph among the systems $\mathcal{S}_i$, $i = 1, 2, 3, 4$ is set to be the undirected and static graph with edges $\{(1, 2), (2, 3), (3, 4), (4, 1)\}$. The initial value for the exosystem w_0 is taken to be $(2\ 1)^T$ while all the other initial values are randomly chosen in the interval $[0, 10]$.
Fig. 5.1 shows that the outputs y_i, $i = 1, 2, 3, 4$ of the systems successfully track the exosystem output Rw_0. The simulation result supports the conclusions of Theorem 1 and the controller design method.

5.5.2 Tracking multiple references

In this subsection we illustrate the design of the robust controllers for decentralized clustering output synchronization through a numerical example. The example we

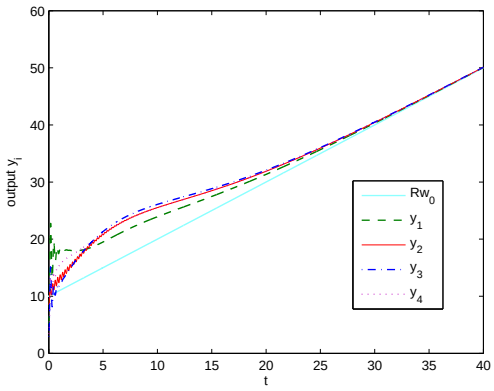

Figure 5.1: *The outputs of the systems track the signal* Rw_0.

consider corresponds to a network of double integrators with different actuator dynamics, namely we consider the case in which systems (5.1) are modeled by (5.46) as well. We consider the problem in which the matrices which define the leader's dynamics (5.19) are given by

$$S = \begin{pmatrix} 0 & 1 \\ -1 & 0 \end{pmatrix}, \quad R = \begin{pmatrix} 1 & 0 \end{pmatrix}. \tag{5.49}$$

In other words, the trajectory of systems (5.46) has to converge asymptotically to the sinusoidal reference signals of the leaders.
For systems (5.46), we have verified that all the assumptions of Proposition 5.1 hold in the previous subsection. Thus, we can determine the controllers, using the approach given in Section 5.4.
First of all, we remark that the matrices F_i, G_i in (5.40) are the same as in the previous subsection. Following again the proof of (Isidori et al. 2003, Lemma 1.5.6), we arrive at the vector Ψ_i and at the nonsingular matrix T_i

$$\Psi_i = \begin{pmatrix} 0 & 2 \end{pmatrix}, \quad T_i = \begin{pmatrix} 0 & -\frac{1}{2} \\ \frac{1}{2} & 0 \end{pmatrix}$$

such that (5.30) is satisfied. The matrices L_i, K_i, M_i in (5.7) can be chosen as in the previous subsection.

Therefore, the controllers

$$\begin{aligned}
\dot{\hat{w}}_{0j} &= S\hat{w}_{0j} + G_0\, R(w_{0j} - \hat{w}_{0j}) \\
\dot{w}_i &= Sw_i + \sum_{k\in\mathbb{N}_j} c_j\, a_{ik}(w_k - w_i) + \sum_{k=1,k\notin\mathbb{N}_j}^{N} a_{ik}(w_k - w_i) + c_j\, a_{i0}(\hat{w}_{0j} - w_i) \\
\dot{\eta}_i &= (F_i + G_i\Psi_i)\,\eta_i + G_i\, M_i\xi_i \\
\dot{\xi}_i &= L_i\xi_i + K_i(y_i - Rw_i) \\
u_i &= \Psi_i\eta_i + M_i\xi_i
\end{aligned} \tag{5.50}$$

for $i \in \mathbb{N}_j, j = 1,\dots,n$, with $G_0 = (2\ 1)^T$ and the matrices F_i, G_i, Ψ_i, L_i, K_i, M_i computed above, solve the decentralized output regulation problem for systems (5.46), (5.49).

We consider $N = 6$ heterogeneous systems with parameters $\{a_i, b_i, c_i, d_i\}$ for $i = 1,\dots,6$ chosen to be $\{1+\mu_1, 1+\mu_2, 1+\mu_3, \mu_4\}$, $\{2.5+\mu_1, 2+\mu_2, 1+\mu_3, \mu_4\}$, $\{2+\mu_1, 1+\mu_2, 1+\mu_3, 0.5+\mu_4\}$, $\{2+\mu_1, 1+\mu_2, 1+\mu_3, 1+\mu_4\}$, $\{2.5+\mu_1, 1.5+\mu_2, 1+\mu_3, 0.5+\mu_4\}$, $\{1+\mu_1, 2+\mu_2, 1+\mu_3, 1+\mu_4\}$ respectively, where the uncertainties $\mu_1, \mu_2, \mu_3, \mu_4$ are $0.3, 0.4, 0.5, 0.7$ respectively. Those systems communicate according to graph $\mathbb{G}$ shown in Figure 5.2. There are two different leaders $\mathcal{L}_1, \mathcal{L}_2$ as shown in Figure 5.2. We pick systems 1 and 5 to be connected to the two leaders $\mathcal{L}_1, \mathcal{L}_2$ respectively, such that the systems in the network realize a 2-cluster synchronization and track the two different trajectories of the leaders $\mathcal{L}_1, \mathcal{L}_2$. To be specific, there is a directed edge from leader $\mathcal{L}_1$ to system 1, and a directed edge from leader $\mathcal{L}_2$ to system 5. Leader $\mathcal{L}_1$ has directed paths to all the nodes in $\mathbb{N}_1 = \{1,2,3,4\}$, although $\{1,2\}$ and $\{3,4\}$ are connected indirectly through the nodes $\{5,6\}$. We set the inner coupling strengths $c_1 = c_2 = 2$. Then the matrix L_Ξ in (5.22) can be described as $L_\Xi = \left(\begin{array}{c|c} c_1\, L_{11} & L_{12} \\ \hline L_{21} & c_2\, L_{22} \end{array}\right) + \mathrm{diag}\{2,0,0,0,2,0\}$, where

$$\left(\begin{array}{c|c} c_1\, L_{11} & L_{12} \\ \hline L_{21} & c_2\, L_{22} \end{array}\right) = \left(\begin{array}{cccc|cc} 2 & -2 & 0 & 0 & 1 & -1 \\ -2 & 2 & 0 & 0 & 0 & 0 \\ 0 & 0 & 2 & -2 & -1 & 1 \\ 0 & 0 & -2 & 2 & 0 & 0 \\ \hline 0 & -1 & 0 & 1 & 2 & -2 \\ 0 & 1 & 0 & -1 & -2 & 2 \end{array}\right). \tag{5.51}$$

One can check that the matrix L_Ξ is positive definite.

We consider the leader $\mathcal{L}_1$ satisfying $\dot{w}_{01} = Sw_{01}$ with $w_{01}(0) = (-2,0)^T$, and the leader $\mathcal{L}_2$ satisfying $\dot{w}_{02} = Sw_{02}$ with $w_{02}(0) = (2,0)^T$, where S has been given in

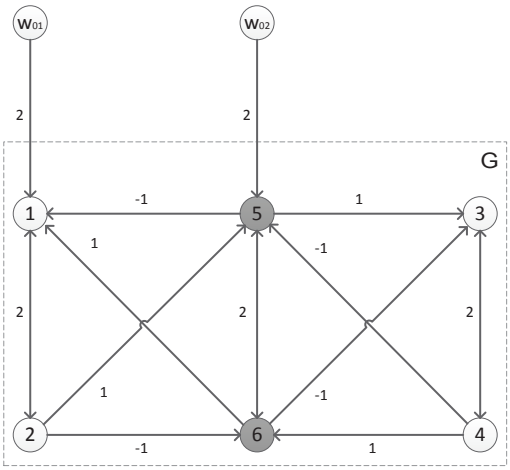

Figure 5.2: *Communication graph.*

(5.49). The initial values of w_i for $i = 1, \ldots, 6$ are randomly selected from the interval $[0, 5]$. We ran the simulation for systems (5.46) and controllers (5.50) in which the gains k, g are set to be 0.8 and 12 respectively. Figure 5.3 shows that the outputs y_i, $i = 1, 2, 3, 4$ of the systems asymptotically track the exosystem output Rw_{01}, and the outputs y_i, $i = 5, 6$ asymptotically track the exosystem output Rw_{02}. The simulation result illustrates the conclusions of Theorem 5.2 and the controller design method.

5.6 Concluding remarks

We have tackled the problem of designing decentralized controllers able to track prescribed reference signals generated by exosystems under the restriction that not all the systems can access the information available at the exosystem. Under the assumption that each leader (exosystem) has a directed path to its follower systems, we have shown that there exist decentralized controllers which achieve the desired regulation task in the presence of arbitrarily large but bounded uncertainties in the systems' models.

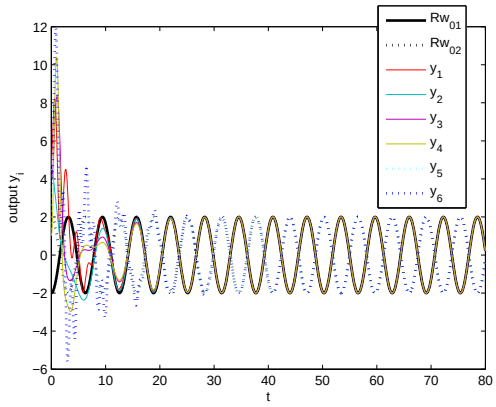

Figure 5.3: *The outputs of the systems are synchronized in clusters and track the exosystem outputs* Rw_{01}, Rw_{02}.

Chapter 6

Synchronization and Network Topologies

The study of synchronization in complex networks has many diverse applications, such as flocking behavior in birds and social insects, social dynamics in populations, and coordination strategies in mobile autonomous robots. This research area has been a hot issue in the past decades. In this chapter, using spectral graph theory and especially its graph comparison techniques, we propose new methodologies to allocate coupling strengths to guarantee global complete synchronization in complex networks. The key step is that all the eigenvalues of the Laplacian matrix associated with a given network can be estimated by flexibly utilizing topological features of the network. The proposed methodologies enable the construction of different coupling-strength combinations in response to different knowledge about sub-networks. Adaptive allocation strategies can be carried out as well using only local network topological information. For large directed networks that can be decomposed into a set of smaller strongly connected components, we apply the methodology at the local level to improve computational efficiency. Besides formal analysis, we use simulation examples to demonstrate how to apply the methodologies to typical complex networks. The results presented in Section 6.3 of this chapter are published in (Liu, Cao and Wu 2013a, Liu, Cao and Wu 2013b), and the result presented in Section 6.4 includes the publication (Liu, Cao and Wu 2013c).

6.1 Introduction

Synchronization phenomena in various complex networks have attracted great attention in the past decades (Pecora and Carroll 1998, Wu and Chua 1995, Strogatz 2003, Wu 2007, Newman 2010, Mei, Zhang and Cao 2011, Xia and Cao 2011, Liu et al. 2009). The master stability function method has been established as a powerful tool in (Pecora and Carroll 1998) to study the local synchronization problem for linearly coupled chaotic systems. In (Wu 2007), a general systematic framework was presented for the study of synchronization of nonlinear dynamical systems with

diffusive couplings. When deriving various synchronization conditions, one focus is how to assign coupling strengths to the interconnections between systems, and intuitively it is natural to assume that the synchronized behavior of any two systems is always possible to take place provided that the coupling strength between them is sufficiently large (Wu 2007). In order to provide a lower bound on the coupling strengths for interconnected systems, for a network with diffusive and symmetric couplings, one can further investigate the synchronizability of the network by examining the magnitude of the second smallest eigenvalue of the Laplacian matrix, called algebraic connectivity, of the network (Wu 2003). A range of related research problems, such as robustness issues, have been studied following this approach (Lü, Yu and Chen 2004, Lü, Yu, Chen and Cheng 2004, Wang and Chen 2002). In parallel, a different line of research has also been developed to study the global synchronization of complex networks, which uses extensively the topological information of the graph that describes the couplings between the systems in a network (Belykh et al. 2004). The main idea is to construct a bound on the total length of all the paths passing through a chosen edge in the graph. This bound can then be exploited to allocate coupling strengths to all the edges in order to achieve global synchronization in the network. One aim of this chapter is to bridge the main results developed separately with these two different approaches and propose new coupling strength allocation methods to guarantee global complete synchronization in complex networks. Newly obtained results from spectral graph theory will be utilized towards this end.

Graph comparison techniques have been developed in the past to bound the second smallest eigenvalues of Laplacian matrices of *undirected* graphs (Guattery et al. 1999, Guattery and Miller 2000, Kahale 1998), where the bounds are obtained by embedding complete graphs into the graph under study. More general ideas for graph comparison have been reported in (Spielman 2004, Spielman 2012), where the comparison of combinatorial features can be carried out between two arbitrary graphs with the same vertex set for the purpose of bounding any eigenvalues of Laplacian matrices of the graphs. In this chapter, we follow the approach delineated in (Spielman 2004, Spielman 2012) to study conditions based on graph comparison for synchronization in complex networks. By doing so, we prove that the synchronization condition given in (Belykh et al. 2004) for allocating coupling strengths can be explained by comparing the network graph with the corresponding complete graph. We then propose different coupling strength allocation strategies by comparing the network graphs with other typical network structures. Since adaptive allocations can be carried out using only local network topological information, our method

is especially useful in large, time-varying, complex networks. So the main contribution of this chapter lies in a set of new methodologies using graph comparison to allocate coupling strengths to guarantee complete synchronization in complex networks.

We further develop our methodologies for general networks associated with *directed* graphs. We prove that the synchronization conditions given in (Belykh et al. 2006a) and (Belykh et al. 2006b) for allocating coupling strengths can be explained by comparing the network graphs with the corresponding complete graphs. We construct an algorithm that incorporates graph comparison procedures to find candidate sets of coupling strengths for synchronization. To keep the computation tractable, for a large network that can be decomposed into smaller strongly connected subnetworks, we run the algorithm locally for each subnetwork. The proposed algorithm is novel in that no graph comparison results for directed networks have been reported before in the literature. In addition, the topological conditions proposed are typically much easier to check.

The rest of this chapter is organized as follows. In Section 6.2, we review a classical complex dynamical network model and some relevant results in the literature on synchronization. Then we give several synchronization criteria using tools from spectral graph theory and propose methods to allocate coupling strengths. In particular, we deal with undirected networks and directed networks in Sections 6.3 and 6.4 respectively. Finally, concluding remarks are given in Section 6.5.

6.2 Problem formulation

We consider a network of $n > 1$ coupled identical oscillators whose dynamics are described by

$$\dot{x}_i = f(x_i) + \sum_{j=1}^{n} \varepsilon_{ij}(t)\, P\, x_j, \qquad i = 1, \ldots, n\,, \tag{6.1}$$

where $x_i \in \mathbb{R}^d$ is the state of the ith oscillator, $f(\cdot) : \mathbb{R}^d \to \mathbb{R}^d$ denotes the identical self-dynamics of each oscillator, $\varepsilon_{ij}(t) \geqslant 0$ $(i \neq j)$ describes the strength of the coupling from oscillator j to i, $\varepsilon_{ii}(t) = -\sum_{j=1, j\neq i}^{n} \varepsilon_{ij}(t)$, and the diagonal $(0,1)$-matrix $P \in \mathbb{R}^{d\times d}$ determines through which components of the states that the oscillators are coupled together. The couplings between the oscillators can be conveniently described by a weighted graph $\mathbb{G} = (\mathcal{V}, \mathcal{E}, \varepsilon(t))$ with the vertex set $\mathcal{V} = \{1, \ldots, n\}$, the edge set $\mathcal{E}$, and the weight function $\varepsilon : \mathcal{E} \to \mathbb{R}$. There is an edge from vertex j to i if

and only if $\varepsilon_{ij}(t) > 0$. Let $L_{\mathbb{G}(t)} \in \mathbb{R}^{n\times n}$ be the Laplacian matrix of the graph $\mathbb{G}(t)$. Then the ijth entry of $L_{\mathbb{G}(t)}$ is $-\varepsilon_{ij}(t)$ for $1 \leqslant i, j \leqslant n$.

System (6.1) has been used widely to study under what conditions the coupled oscillators can achieve asymptotically global and complete synchronization, where for any initial condition, $||x_i(t) - x_j(t)|| \to 0$ as $t \to \infty$ for all i, j (Wu 2007). In this chapter, we explore such synchronization conditions using spectral graph theory. Towards this end, we make one standard technical assumption about system (6.1).

Assumption 6.1 *For a sufficiently large positive constant a, it holds that*

$$(x_j - x_i)^T \left[(f(x_j) - f(x_i)) - aP(x_j - x_i)\right] \leqslant -c||x_j - x_i||^2 ,$$

for some $c > 0$ and for any $x_i, x_j \in \mathbb{R}^d$.

Here the constant a is determined by both the function f and the inner coupling matrix P. Assumption 6.1 implies that any two coupled oscillators are always able to get synchronized when their coupling is sufficiently strong. An equivalent assumption has been made in (Belykh et al. 2004, Belykh et al. 2006a, Belykh et al. 2006b), which guarantee that the whole network of oscillators can get synchronized when the coupling strengths between oscillators are sufficiently large. Such networks that satisfy Assumption 6.1 include most of the coupled limit-cycle or chaotic oscillators. For those networks that do not satisfy this assumption, it is likely that increasing the coupling strengths between some pairs of oscillators may destroy the network's locally stable synchronous states (Pecora and Carroll 1998). We refer the interested reader to (Pecora and Carroll 1998) and a more recent paper (Tang et al. 2012) for a systematic classification of different network synchronization behavior.

In the following, we introduce a general synchronization criterion for networks with time-varying dynamics. We use $\mathcal{W}_s$ to denote the set of irreducible, symmetric matrices that have zero row sums and non-positive off-diagonal elements.

Lemma 6.1 *(Minor rephrasing of Theorem 2 from* (Wu 2003) *and a result in Chapter 4 from* (Wu 2007)*) Let $Y(t)$ be a $d \times d$ time-varying matrix and V a $d \times d$ symmetric, positive definite matrix such that $(y - z)^T V(f(y, t) + Y(t)y - f(z, t) - Y(t)z) \leqslant -c||y - z||^2$ for some $c > 0$ and all y, z, t. Then system (6.1) synchronizes globally if there exists an $n \times n$ matrix $U \in \mathcal{W}_s$ such that*

$$(U \otimes V)(L_{\mathbb{G}(t)} \otimes (-P) - I_n \otimes Y(t)) \preceq 0 \tag{6.2}$$

for all t.

Now we present a synchronization criterion using properties of graphs. Here, graph $\mathbb{G}(t)$ can be undirected or directed.

Theorem 6.1 *Under Assumption 6.1, the synchronization manifold of system (6.1) is globally asymptotically stable if there exists a connected undirected graph $\mathbb{G}_0$ with the same vertex set of $\mathbb{G}(t)$ such that*

$$L_{\mathbb{G}_0} L_{\mathbb{G}(t)} - a L_{\mathbb{G}_0} \succ 0\,, \quad \textit{for all } t. \tag{6.3}$$

Proof: Assumption 6.1 on the self-dynamics $f(\cdot)$ is equivalent to the condition that $(y-z)^T V(f(y,t)+Y(t)y - f(z,t) - Y(t)z) \leqslant -c||y-z||^2$ when we set $Y(t) = -aP$, $V = I_d$. To apply Lemma 6.1, we choose $Y(t) = -aP$, $V = I_d$, and $U = L_{\mathbb{G}_0}$. Then from (6.2) we have $(L_{\mathbb{G}_0} \otimes I_d)(L_{\mathbb{G}(t)} \otimes (-P) - I_n \otimes (-aP)) \preceq 0$, i.e., $L_{\mathbb{G}_0} L_{\mathbb{G}(t)} \otimes (-P) - aL_{\mathbb{G}_0} \otimes (-P) \preceq 0$. Since $-P \preceq 0$, this is satisfied if $L_{\mathbb{G}_0} L_{\mathbb{G}(t)} - aL_{\mathbb{G}_0} \succeq 0$. Therefore, the complete synchronization of system (6.1) is guaranteed if $L_{\mathbb{G}_0} L_{\mathbb{G}(t)} \succ a L_{\mathbb{G}_0}$ for all t. □

6.3 Graphical synchronization criteria for undirected complex networks

In this section, we look at graphical synchronization criteria for undirected complex networks. Towards this end, we introduce some notations and discuss some algebraic properties of graphs. We say $A \succ B$ if $A - B \succ 0$. Similarly, we say $A \succeq B$ if $A - B \succeq 0$. We extend this notation for graphs as follows.

Definition 6.1 *For two undirected graphs $\mathbb{G}$ and $\mathbb{H}$ with the same vertex set $\mathcal{V} = \{1, \ldots, n\}$, we say*

$$\mathbb{G} \succeq \mathbb{H}$$

if their Laplacian matrices satisfy $L_{\mathbb{G}} \succeq L_{\mathbb{H}}$.

For an undirected graph $\mathbb{G}$ with vertex set $\mathcal{V}$, we use λ_k, $1 \leqslant k \leqslant n$, to denote the kth smallest eigenvalue of $L_{\mathbb{G}}$. For graphs $\mathbb{G}$ and $\mathbb{H}$ with the same vertex set, we consider some multiple $c\,\mathbb{G}$ of graph $\mathbb{G}$. Using Courant-Fischer Theorem (Spielman 2012), one can easily prove the following result.

Lemma 6.2 (Spielman 2012) *If $\mathbb{G}$ and $\mathbb{H}$ are the graphs with the same vertex set $\mathcal{V}$ satisfying $c\mathbb{G} \succeq \mathbb{H}$, then*

$$c\lambda_k(\mathbb{G}) \geqslant \lambda_k(\mathbb{H})$$

for all $1 \leqslant k \leqslant n$.

6.3.1 Comparison with complete graphs

Theorem 6.1 gives a synchronization condition based on graph comparison. One natural idea is to compare the system graph $\mathbb{G}(t)$ with the complete graph. Let $\mathbb{K}_n$ denote the unweighted, undirected complete graph with n vertices. We have the following theorem.

Theorem 6.2 *Suppose that graph $\mathbb{G}(t)$ is undirected and connected. Under Assumption 6.1, the synchronization manifold of system (6.1) is globally asymptotically stable if*

$$\mathbb{G}(t) \succ \frac{a}{n}\,\mathbb{K}_n\,, \quad \textit{for all } t. \tag{6.4}$$

Proof: The result in Theorem 6.2 can be obtained from Theorem 6.1. If we take the graph $\mathbb{G}_0$ in Theorem 6.1 to be $\mathbb{K}_n$, then one has that the synchronization manifold of system (6.1) is globally asymptotically stable if $L_{\mathbb{K}_n}\, L_{\mathbb{G}(t)} \succ a\, L_{\mathbb{K}_n}$ for all t. Note that $L_{\mathbb{K}_n} = n\, I_n - J$ where J is the $n \times n$ all-one matrix. We know then $L_{\mathbb{K}_n}\, L_{\mathbb{G}(t)} = (nI_n - J)L_{\mathbb{G}(t)} = n\, L_{\mathbb{G}(t)} \succ aL_{\mathbb{K}_n}$. Thus, the synchronization manifold of system (6.1) is globally asymptotically stable if $L_{\mathbb{G}(t)} \succ \frac{a}{n}\, L_{\mathbb{K}_n}$. □

The implication of Theorem 6.2 is profound. For any coupled oscillators whose couplings are described by a weighted undirected graph $\mathbb{G}(t)$, one can always examine whether $\mathbb{G}(t) \succ \frac{a}{n}\,\mathbb{K}_n$ holds by comparing $\mathbb{G}(t)$ to the complete graph with identical edge weight $\frac{a}{n}$. Now we show that the inequality in Theorem 6.2 can be stated differently.

Theorem 6.3 *For an undirected graph $\mathbb{G}(t)$, it holds that*

$$\mathbb{G}(t) \succ \frac{a}{n}\,\mathbb{K}_n \Leftrightarrow \lambda_2(\mathbb{G}(t)) > a\,.$$

Proof: "⇒": From $\mathbb{G}(t) \succ \frac{a}{n}\,\mathbb{K}_n$ for each t and Lemma 6.2, we know $\lambda_2(\mathbb{G}(t)) > \frac{a}{n}\,\lambda_2(\mathbb{K}_n)$ for each t. Since $\lambda_2(\mathbb{K}_n) = n$, it then must be true that $\lambda_2(\mathbb{G}(t)) > a$ for each t.
"⇐": Since the all-one vector $\mathbf{1} = [1, \ldots, 1]^T$ is in the kernel of $L_{\mathbb{G}(t)}$ and $L_{\mathbb{K}_n}$, to prove $\mathbb{G}(t) \succ \frac{a}{n}\,\mathbb{K}_n$, it suffices to prove that $x^T(L_{\mathbb{G}(t)} - \frac{a}{n}\,L_{\mathbb{K}_n})x > 0$ for any $x \in \mathbb{R}^n$ that is not in the kernel of $L_{\mathbb{G}(t)}$ and $L_{\mathbb{K}_n}$. Furthermore, one can easily see that it suffices to prove that $x^T(L_{\mathbb{G}(t)} - \frac{a}{n}\,L_{\mathbb{K}_n})x > 0$ for all the vector $x \in \mathbb{R}^n$ orthogonal to $\mathbf{1}$.
For any vector x orthogonal to $\mathbf{1}$, from Courant-Fischer theorem (Spielman 2012), one has

$$\lambda_2(\mathbb{G}(t)) \leqslant \min_{x \perp \mathbf{1}} \frac{x^T L_{\mathbb{G}(t)} x}{x^T x}, \quad \text{for each } t.$$

Thus one has

$$\lambda_2(\mathbb{G}(t))x^T x \leqslant x^T L_{\mathbb{G}(t)} x\,, \quad \forall x \perp \mathbf{1}\,.$$

Since $\lambda_2(\mathbb{G}(t)) > a$, we know $x^T L_{\mathbb{G}(t)} x > a x^T x$ for all $x \perp \mathbf{1}$. Using the fact that $L_{\mathbb{K}_n} = nI_n - J$, we have

$$\begin{aligned} x^T \left(nL_{\mathbb{G}(t)} - aL_{\mathbb{K}_n}\right)x &= x^T \left(nL_{\mathbb{G}(t)} - a(nI_n - J)\right)x \\ &= nx^T L_{\mathbb{G}(t)} x - nax^T x + ax^T Jx \\ &\geqslant n(x^T L_{\mathbb{G}(t)} x - ax^T x) > 0, \end{aligned}$$

which implies that $n\mathbb{G}(t) - a\mathbb{K}_n > 0$ for all $x \perp \mathbf{1}$, namely $\mathbb{G}(t) > \frac{a}{n}\,\mathbb{K}_n$. □

Remark 6.1 *In Theorem 3 in (Wu 2003), a lower bound for $\lambda_2(\mathbb{G}(t))$ has been given to guarantee the synchronization of coupled dynamical oscillators under certain assumptions. In Theorem 6.3, we have shown the equivalence between graph comparisons and bounding from below the second smallest eigenvalues of the Laplacian matrices of graphs.*

To apply more tools from spectral graph theory, we need to introduce another equivalent definition of the Laplacian matrix of graphs. Following (Spielman 2004), we define the elementary Laplacian $L_{(u,v)}$ to be the Laplacian of the graph with the vertex set $\mathcal{V}$ and only one edge between vertices u and v. Then for an undirected graph $\mathbb{G}(t) = (\mathcal{V}, \mathcal{E}, \varepsilon(t))$ consisting of the vertex set $\mathcal{V}$, the edge set $\mathcal{E}$, and the weight function $\varepsilon : \mathcal{E} \to \mathbb{R}$, its Laplacian matrix has the form

$$L(\mathbb{G}(t)) \triangleq \sum_{(u,v)\in\mathcal{E}} \varepsilon_{(u,v)}(t) \cdot L_{(u,v)}. \tag{6.5}$$

Moreover, we say graph $\mathbb{G}$ is unweighted if the weights $\varepsilon_{(u,v)} = 1$ for all $u \neq v$.

Now we introduce two graphical inequalities, which have been proved in (Spielman 2004).

Lemma 6.3 (Spielman 2004) *Let $c_1, \ldots, c_{n-1} > 0$. Then for graph $\mathbb{G}$ with vertex set $\mathcal{E}$, one has*

$$c\left(\sum_{i=1}^{n-1} c_i\, L_{(i,i+1)}\right) \geq L_{(1,n)},$$

where $c = \sum_i \frac{1}{c_i}$.

If we take $c_1 = c_2 = \ldots = c_{n-1} = 1$, then Lemma 6.3 becomes the following result.

Lemma 6.4 (Spielman 2004) *For graph $\mathbb{G}$ with vertex set $\mathcal{E}$, it holds that*

$$(n-1)\left(\sum_{i=1}^{n-1} L_{(i,i+1)}\right) \succeq L_{(1,n)}.$$

With these graphical tools at hand, Theorem 6.2 can be further used to give graphical conditions for the synchronization of system (6.1). In the following, we present some sufficient conditions for synchronization using features of graph $\mathbb{G}(t)$. Consider a set of paths $\mathcal{P} = \{\mathcal{P}_{ij} | i, j = 1, \ldots, n, j > i\}$, one for each pair of distinct vertices i and j. We denote the length of the path $\mathcal{P}_{ij}$ by $|\mathcal{P}_{ij}|$, which is the number of edges in $\mathcal{P}_{ij}$. We assume that there are altogether m edges in the edge set $\mathcal{E}$ of graph $\mathbb{G}(t)$. If we label the edges of $\mathbb{G}(t)$ by $1, \ldots, m$, then the lower bounds on the coupling strengths of all the edges can be constructed to guarantee that the inequality in Theorem 6.2 holds. We state it more formally as follows.

Theorem 6.4 *Suppose that graph $\mathbb{G}(t)$ is undirected and connected. Under Assumption 6.1, the synchronization manifold of system (6.1) is globally asymptotically stable if*

$$\varepsilon_k(t) > \frac{b_k}{n}\, a, \qquad \textit{for } k = 1, \ldots, m,$$

where $b_k = \sum_{j>i; k\in\mathcal{P}_{ij}} |\mathcal{P}_{ij}|$ is the sum of the lengths of all those paths $\mathcal{P}_{ij}$ in $\mathcal{P}$ that contain edge k.

Proof: From the definition introduced by (6.5), it holds that

$$\frac{a}{n} L_{\mathbb{K}_n} = \frac{a}{n} \sum_{i=1}^{n-1} \sum_{j>i} L_{(i,j)}\,.$$

For each pair of (i, j) where $j > i$, we choose one path in the topological graph $\mathbb{G}$ with two associated vertices i and j. Then one can apply Lemma 6.4 by comparing the sum of all the Laplacian matrices L_k, $k \in \mathcal{P}_{ij}$, of all the edges along this chosen path and the Laplacian matrix $L_{(i,j)}$ of the single edge (i, j), which leads to

$$|\mathcal{P}_{ij}| \sum_{k\in\mathcal{P}_{ij}} L_k \succeq L_{(i,j)}. \tag{6.6}$$

Choosing such paths in graph $\mathbb{G}$ for all the pairs of i, j where $j > i$, one obtains that

$$\begin{aligned}
\frac{a}{n} L_{\mathbb{K}_n} &\preceq \frac{a}{n} \sum_{j>i} \left(|\mathcal{P}_{ij}| \sum_{\substack{k \in \mathcal{P}_{ij} \\ k \in \mathcal{E}(\mathbb{G})}} L_k \right) \\
&= \frac{a}{n} \sum_{k=1}^{m} \left(\sum_{\substack{j>i \\ k \in \mathcal{P}_{ij}}} |\mathcal{P}_{ij}| \right) L_k \\
&= \frac{a}{n} \sum_{k=1}^{m} b_k \, L_k \\
&< \sum_{k=1}^{m} \varepsilon_k(t) \, L_k = L_{\mathbb{G}} \, ,
\end{aligned}$$

where $b_k = \sum_{\substack{j>i \\ k \in \mathcal{P}_{ij}}} |\mathcal{P}_{ij}|$. And the last inequality holds trivially when $\varepsilon_k(t) > \frac{a}{n} \, b_k$ for each edge k. Therefore, the constructed coupling strengths ε_k for $k = 1, \ldots, m$ guarantee that $\mathbb{G}(t) > \frac{a}{n} \, \mathbb{K}_n$ holds. Thus we arrive at the conclusion. ▫

Remark 6.2 *Theorem 6.4 presents a synchronization condition for allocating coupling strengths for $\mathbb{G}(t)$. The same result has been achieved in (Belykh et al. 2004). Here we give a different interpretation of the result by using graph comparison. In contrast with (Belykh et al. 2004), we prove the result by using combinatorial features of the topological graph $\mathbb{G}$, which leads to the construction of efficient algorithms determining the coupling strengths as we show later.*

Up to now, we have only compared graph $\mathbb{G}(t)$ with the complete graph $\mathbb{K}_n$. It is natural to ask what different synchronization criteria can be obtained if we compare $\mathbb{G}(t)$ with other graphs. We explore in this direction in the next subsection.

6.3.2 Comparison with other special graphs

Coupling strength allocation

In Theorem 6.2, the synchronization criteria are given based on the comparison between the given graph $\mathbb{G}$ with the complete graph. In addition, Theorem 6.4 gives lower bounds of coupling strengths in order to achieve complete synchronization.

In what follows, we show how to allocate coupling strengths systematically by comparing $\mathbb{G}$ with some special graphs. We list below some results about the eigenvalues of some special classes of graphs.

Lemma 6.5 (Spielman 2004) *(a) The Laplacian matrix of the complete graph $\mathbb{K}_n$ has eigenvalue 0 with multiplicity 1 and n with multiplicity $n-1$.*
(b) The Laplacian matrix of the ring graph $\mathbb{R}_n$ has eigenvalues $2-2\cos(2\pi k/n)$ for $0 \leqslant k \leqslant n/2$.
(c) The Laplacian matrix of the path graph $\mathbb{P}_n$ has eigenvalues $2-2\cos(\pi\, k/n)$ for $0 \leqslant k \leqslant n-1$.
(d) The Laplacian matrix of the star graph $\mathbb{S}_n$ has 1 as its second smallest eigenvalue.

In fact, one can compare any two undirected and connected graphs, and obtain a graphical inequality as a result. One can find more details in (Spielman 2004, Spielman 2012). Thus, for a graph, such as $\mathbb{R}_n, \mathbb{P}_n, \mathbb{S}_n$, whose second smallest eigenvalue is known, we can always compare it with $\mathbb{G}(t)$ and obtain a set of coupling strengths to guarantee complete synchronization of the dynamical network (6.1), as we see later in this section. To show how to implement this idea, we give an example now on comparing graph $\mathbb{G}(t)$ with a star graph. Similar results can be achieved when $\mathbb{G}(t)$ is compared with other typical graphs, such as ring graphs, path graphs, and any graphs with known second smallest eigenvalues.

Now consider an n-vertex star graph $\mathbb{S}_n$, in which without loss of generality we assume vertex 1 has $n-1$ neighbors. Then $L_{\mathbb{S}_n} = \sum_{i=2}^{n} L_{(1,i)}$. We consider two cases for all the edges $(1,i)$, $2 \leqslant i \leqslant n$, in $\mathbb{S}_n$:
1. Edge $(1,i)$ is not in the edge set $\mathcal{E}$ of $\mathbb{G}$. Since $\mathbb{G}$ is connected, there must exist some paths in $\mathbb{G}$ connecting vertices 1 and i. We choose arbitrarily one of those paths, which is denoted by $\mathcal{P}_{1,i}$. Then we have

$$L_{(1,i)} \preceq |\mathcal{P}_{1,i}| \sum_{\substack{k\in\mathcal{P}_{1,i}\\ k\in\mathcal{E}(\mathbb{G})}} L_k. \tag{6.7}$$

2. Edge $(1,i)$ is in $\mathcal{E}$. There are two options: one is to use $(1,i)$ directly and the other is to choose arbitrarily another path between vertices 1 and i, if such a path exists. We set the probability of the first option to be $1-\alpha_i$, and that for the second α_i where $0 \leqslant \alpha_i < 1$. If there are no paths between 1 and i other than the edge $(1,i)$, we always set $\alpha_i = 0$. Thus we have

$$L_{(1,i)} \preceq (1-\alpha_i)L_{(1,i)} + \alpha_i\, |\mathcal{P}_{1,i}| \sum_{\substack{k\in\mathcal{P}_{1,i}\\ k\in\mathcal{E}(\mathbb{G})}} L_k\,. \tag{6.8}$$

Note that (6.7) is the special case of (6.8) when α_i is taken to be 1. Hence, we can use the inequality (6.8) with a proper choice of $\alpha_i \in [0,1]$ for each $i \in \{2,\dots,n\}$, and so

$$\begin{aligned}
L_{\mathbb{S}_n} &= \sum_{i=2}^{n} L_{(1,i)} \\
&\preceq \sum_{i=2}^{n} \left[(1-\alpha_i) L_{(1,i)} + \alpha_i \left|\mathcal{P}_{1,i}\right| \sum_{\substack{k\in\mathcal{P}_{1,i} \\ k\in\mathcal{E}(\mathbb{G})}} L_k \right] \\
&= \sum_{i=2}^{n} (1-\alpha_i) L_{(1,i)} + \sum_{i=2}^{n} \left[\alpha_i \left|\mathcal{P}_{1,i}\right| \sum_{\substack{k\in\mathcal{P}_{1,i} \\ k\in\mathcal{E}(\mathbb{G})}} L_k \right] \\
&= \sum_{k=1}^{m} \left[\sum_{\substack{i=2 \\ k\in\mathcal{P}_{1,i}}}^{n} \alpha_i \left|\mathcal{P}_{1,i}\right| \right] L_k + \sum_{i=2}^{n} (1-\alpha_i) L_{(1,i)} \\
&= \sum_{k=1}^{m} \left[\sum_{\substack{i=2 \\ k\in\mathcal{P}_{1,i}}}^{n} \alpha_i \left|\mathcal{P}_{1,i}\right| + \varphi(1-\alpha_i) \right] L_k \,,
\end{aligned}$$

where the real valued function $\varphi(1-\alpha_i)$ satisfies

$$\varphi(1-\alpha_i) = \begin{cases} 1-\alpha_i \neq 0 & \text{if } (1,i) \text{ is the edge } k\,, \\ 0 & \text{otherwise}\,. \end{cases}$$

Let

$$b_k^{'} = \sum_{\substack{i=2 \\ k\in\mathcal{P}_{1,i}}}^{n} \alpha_i \left|\mathcal{P}_{1,i}\right| + \varphi(1-\alpha_i). \tag{6.9}$$

Then we have $\mathbb{G}(t) > a\mathbb{S}_n$ if the weight of the edge k satisfies $\varepsilon_k(t) > a\, b_k^{'}$ for $k = 1,\dots,m$. From Lemma 6.2 one has $\lambda_2(\mathbb{G}(t)) > \lambda_2(a\mathbb{S}_n) = a\lambda_2(\mathbb{S}_n) = a$ if $\varepsilon_k(t) > a\, b_k^{'}$ for all k. From Theorem 6.3, the synchronization manifold of the dynamical system (6.1) is globally asymptotically stable, if $\varepsilon_k(t) > a\, b_k^{'}$ for $k = 1,\dots,m$. Thus we have proved the following theorem.

Theorem 6.5 *Suppose that graph $\mathbb{G}(t)$ is undirected and connected. Under Assumption 6.1, the synchronization manifold of system (6.1) is globally asymptotically stable if the coupling strength of edge k satisfies $\varepsilon_k(t) > a\, b_k^{'}$ for all $k = 1, \ldots, m$, where $b_k^{'}$ is given by (6.9).*

Remark 6.3 *In the above two cases for the edge $(1, i)$, one can choose arbitrarily the path in $\mathbb{G}$ that connects vertices 1 and i. However, we choose the shortest path(s). To specify the choice of these shortest paths, we set the rule as follows: for any two different vertices i and j in $\mathbb{G}$, we consider the set of all the shortest paths connecting i and j, which is denoted by $\{\mathcal{P}_{ij}^{(1)}, \mathcal{P}_{ij}^{(2)}, \ldots, \mathcal{P}_{ij}^{(n_{ij})}\}$ with $n_{ij} \geqslant 1$. We choose a path in the set with equal probability $\frac{1}{n_{ij}}$. This rule is reasonable since the shortest paths are one of the most critical characterizations of connectivity between vertices in graphs and all the shortest paths between the same pair of vertices are usually equally important.*

Remark 6.4 *Compared with the graphical condition in Theorem 6.4, the method in Theorem 6.5 greatly reduces the computational complexity. There are only $n-1$ paths that need to be considered in our algorithm, while one needs to check $n(n-1)/2$ paths to apply Theorem 6.4.*

Remark 6.5 *The coupling strength allocation strategy in Theorem 6.4 (resp. Theorem 6.5) is obtained based on the comparison between the given graph $\mathbb{G}$ and the complete graph $\mathbb{K}_n$ (resp. the star graph $\mathbb{S}_n$). Similar coupling strength allocation strategies can be obtained when $\mathbb{G}$ is compared with other graphs, such as rings and paths. A proper choice of the graphs in comparison is helpful to obtain less conservative lower bounds for coupling strengths and reduce the computational complexity of the comparison at the same time.*

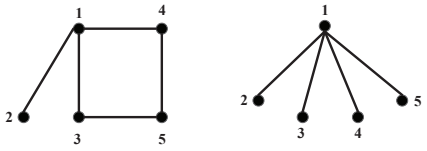

Figure 6.1: *Comparing $\mathbb{G}_5$ with the star $\mathbb{S}_5$.*

Now we use one simple example to demonstrate the differences between the synchronization conditions in Theorems 6.5 and 6.4. Consider an undirected graph $\mathbb{G}_5$, consisting of five vertices $\{v_1, v_2, v_3, v_4, v_5\}$ and five edges $\{(1,2), (1,3), (1,4), (3,5), (4,5)\}$, which is shown on the left of Fig. 6.1. Suppose that $\mathbb{G}_5$ is compared

with the star graph $\mathbb{S}_5$ on the right of Fig. 6.1. Comparing the two graphs, we use the edge $(1,2)$ in $\mathbb{G}_5$ to represent the path connecting vertices v_1, v_2, $(1,3)$ for v_1, v_3, $(1,4)$ for v_1, v_4, and candidate paths $(1,3,5)$ and $(1,4,5)$ for vertices v_1, v_5. Then we have

$$\begin{aligned}
L_{\mathbb{S}_5} &= L_{(1,2)} + L_{(1,3)} + L_{(1,4)} + L_{(1,5)} \\
&\preceq L_{(1,2)} + L_{(1,3)} + L_{(1,4)} \\
&\quad + \left[\frac{1}{2}(2L_{(1,3)} + 2L_{(3,5)}) + \frac{1}{2}(2L_{(1,4)} + 2L_{(4,5)})\right] \\
&= L_{(1,2)} + 2L_{(1,3)} + 2L_{(1,4)} + L_{(3,5)} + L_{(4,5)}.
\end{aligned}$$

Thus we have $b'_{(1,2)} = 1$, $b'_{(1,3)} = 2$, $b'_{(1,4)} = 2$, $b'_{(3,5)} = 1$, and $b'_{(4,5)} = 1$. From Theorem 6.5, we obtain the bounds for the edges in $\mathbb{G}_5$: $\varepsilon_{(1,2)} \geqslant a$, $\varepsilon_{(1,3)} \geqslant 2a$, $\varepsilon_{(1,4)} \geqslant 2a$, $\varepsilon_{(3,5)} \geqslant a$, $\varepsilon_{(4,5)} \geqslant a$.

In comparison, now we compare the two graphs $\mathbb{G}_5$ and $\mathbb{K}_5$. We use edge $(1,2)$ in $\mathbb{G}_5$ to represent the path connecting vertices v_1, v_2, edge $(1,3)$ for vertices v_1, v_3, edge $(1,4)$ for vertices v_1, v_4, edge $(3,5)$ for vertices v_3, v_5, edge $(4,5)$ for vertices v_4, v_5, and candidate paths $(1,3,5)$ and $(1,4,5)$ for vertices v_1, v_5, path $(2,1,3)$ for vertices v_2, v_3, path $(2,1,4)$ for vertices v_2, v_4, paths $(2,1,4,5)$ and $(2,1,3,5)$ for vertices v_2, v_5, paths $(3,1,4)$ and $(3,5,4)$ for vertices v_3, v_4. Then we have

$$\begin{aligned}
L_{\mathbb{K}_5} &= L_{(1,2)} + L_{(1,3)} + L_{(1,4)} + L_{(1,5)} \\
&\quad + L_{(2,3)} + L_{(2,4)} + L_{(2,5)} + L_{(3,4)} + L_{(3,5)} + L_{(4,5)} \\
&\preceq L_{(1,2)} + L_{(1,3)} + L_{(1,4)} \\
&\quad + \left[\frac{1}{2}(2L_{(1,4)} + 2L_{(4,5)}) + \frac{1}{2}(2L_{(1,3)} + 2L_{(3,5)})\right] \\
&\quad + (2L_{(1,2)} + 2L_{(1,3)}) + (2L_{(1,2)} + 2L_{(1,4)}) \\
&\quad + \left[\frac{1}{2}(3L_{(1,2)} + 3L_{(1,3)} + 3L_{(3,5)}) + \frac{1}{2}(3L_{(1,2)} + 3L_{(1,4)} + 3L_{(4,5)})\right] \\
&\quad + \left[\frac{1}{2}(2L_{(3,5)} + 2L_{(4,5)}) + \frac{1}{2}(2L_{(1,3)} + 2L_{(1,4)})\right] + L_{(3,5)} + L_{(4,5)} \\
&= 8L_{(1,2)} + \frac{13}{2}L_{(1,3)} + \frac{13}{2}L_{(1,4)} + \frac{9}{2}L_{(3,5)} + \frac{9}{2}L_{(4,5)}.
\end{aligned}$$

Thus we have $b_{(1,2)} = 8$, $b_{(1,3)} = 6.5$, $b_{(1,4)} = 6.5$, $b_{(3,5)} = 4.5$, and $b_{(4,5)} = 4.5$. From Theorem 6.4, one of the possible sets of bounds is as follows: $\varepsilon_{(1,2)} \geqslant \frac{8a}{5} = 1.6a$, $\varepsilon_{(1,3)} \geqslant \frac{6.5a}{5} = 1.3a$, $\varepsilon_{(1,4)} \geqslant \frac{6.5a}{5} = 1.3a$, $\varepsilon_{(3,5)} \geqslant \frac{4.5a}{5} = 0.9a$, and $\varepsilon_{(4,5)} \geqslant \frac{4.5a}{5} = 0.9a$.

From the above calculations, one can see that there are only 4 paths taken into consideration in $\mathbb{G}_5$ according to the proposed method in Theorem 6.5, while there are $\frac{5\times4}{2} = 10$ paths considered according to the method in Theorem 6.4. This example demonstrates less computational complexity of Theorem 6.5. In addition, we have obtained another set of bounds for the coupling strengths, in which $\varepsilon_{(1,2)}$ is smaller. Using Theorem 6.5, the obtained bounds for the coupling strengths of an arbitrary network may be looser or tighter, which depends on the specific application.

Benefits from comparing with stars

Now we give an example to demonstrate the advantages of using the synchronization condition in Theorem 6.5. To simplify our calculation, we consider a fractal tree with ten vertices, shown on the left of Fig. 6.2. First, let the fractal graph $\mathbb{G}_{10}$ be compared with the star graph $\mathbb{S}_{10}$. Because of the fractal structure of graph $\mathbb{G}_{10}$, we only need to focus on the calculations of bounds for the edges $(1,2),(2,5),(2,6)$. And we have the comparison:

$$\begin{aligned} L_{\mathbb{S}_{10}} &= L_{(1,2)} + L_{(1,5)} + L_{(1,6)} + \dots \\ &\leq L_{(1,2)} + 2(L_{(1,2)} + L_{(2,5)}) + 2(L_{(1,2)} + L_{(2,6)}) + \dots \\ &= 5L_{(1,2)} + 2L_{(2,5)} + 2L_{(2,6)} + \dots . \end{aligned}$$

Thus we have $b^{'}_{(1,2)} = 5$, $b^{'}_{(1,3)} = 2$, and $b^{'}_{(2,6)} = 2$. From Theorem 6.5, we obtain the bounds for the edges $(1,2)$, $(2,5)$, $(2,6)$ in graph $\mathbb{G}_{10}$:

$$\varepsilon_{(1,2)} \geqslant 5a, \quad \varepsilon_{(2,5)} \geqslant 2a, \quad \varepsilon_{(2,6)} \geqslant 2a. \tag{6.10}$$

Second, we give another set of bounds for the edges in $\mathbb{G}_{10}$ using the method in Theorem 6.4. We implement graph comparison between graph $\mathbb{G}_{10}$ and the complete graph $\mathbb{K}_{10}$. Thus we need to consider the paths in $\mathbb{G}_{10}$ for every pair of vertices. The choice of the path in $\mathbb{G}_{10}$ for each pair of vertices is unique, because there is no cycle in $\mathbb{G}_{10}$. We only need to calculate the bounds for the edges $(1,2)$, $(2,5)$, $(2,6)$. To do so, we first list all the possible paths that pass through at lease one of these edges, which are shown in Fig. 6.3. Then, from $b_k = \sum_{j>i;k\in\mathcal{P}_{ij}} |\mathcal{P}_{ij}|$ in Theorem 6.4, we have

$$\begin{aligned} b_{(1,2)} &= |\mathcal{P}_{1,2}| + |\mathcal{P}_{1,5}| + |\mathcal{P}_{1,6}| + |\mathcal{P}_{2,3}| + |\mathcal{P}_{2,4}| \\ &\quad + |\mathcal{P}_{2,7}| + |\mathcal{P}_{2,8}| + |\mathcal{P}_{2,9}| + |\mathcal{P}_{2,10}| + |\mathcal{P}_{3,5}| + |\mathcal{P}_{3,6}| + |\mathcal{P}_{4,5}| + |\mathcal{P}_{4,6}| \\ &\quad + |\mathcal{P}_{5,7}| + |\mathcal{P}_{5,8}| + |\mathcal{P}_{5,9}| + |\mathcal{P}_{5,10}| + |\mathcal{P}_{6,7}| + |\mathcal{P}_{6,8}| + |\mathcal{P}_{6,9}| + |\mathcal{P}_{6,10}| \\ &= 1 + 2\times4 + 3\times8 + 4\times8 = 65\,. \end{aligned}$$

Following the same reasoning, we have

$$\begin{aligned} b_{(2,5)} &= |\mathcal{P}_{1,5}| + |\mathcal{P}_{2,5}| + |\mathcal{P}_{3,5}| + |\mathcal{P}_{4,5}| + |\mathcal{P}_{5,6}| \\ &\quad + |\mathcal{P}_{5,7}| + |\mathcal{P}_{5,8}| + |\mathcal{P}_{5,9}| + |\mathcal{P}_{5,10}| \\ &= 2 + 1 + 3 + 3 + 2 + 4 \times 4 = 27\,. \end{aligned}$$

and $b_{(2,6)} = 27$ can be calculated similarly.
According to $\varepsilon_k > \frac{b_k}{n}\, a$ in Theorem 6.4, we obtain the bounds for the coupling strengths of the edges $(1,2)$, $(2,5)$, and $(2,6)$ as

$$\begin{aligned} &\varepsilon_{(1,2)} \geqslant \frac{b_{(1,2)}}{10}\, a = 6.5a, \\ &\varepsilon_{(2,5)} \geqslant \frac{b_{(2,5)}}{10}\, a = 2.7a, \quad \varepsilon_{(2,6)} \geqslant \frac{b_{(2,6)}}{10}\, a = 2.7a\,. \end{aligned} \tag{6.11}$$

The above calculations show that the computational complexity of graph comparisons is greatly reduced by using the method in Theorem 6.5, comparing with what obtained using Theorem 6.4. In addition, we have obtained another set of bounds for coupling strengths of $\mathbb{G}_{10}$, in which each bound is much smaller. The proposed method is especially effective when networks are large and sparse, since these networks are more similar to the star graphs (or rings, path graphs) than to the complete graphs.

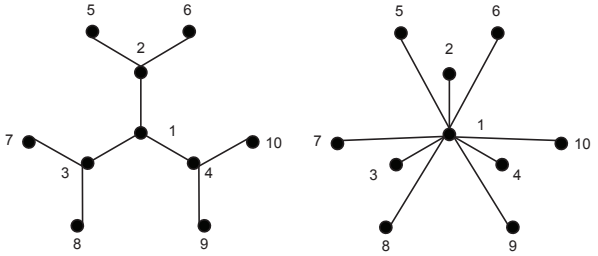

Figure 6.2: *Comparing a fractal tree with the star* $\mathbb{S}_{10}$.

Furthermore, the method we proposed can be applied to adaptively adjust the allocation of coupling strengths in order to ensure the synchronization of a dynamical network when its topology changes with time. We explore in this direction next.

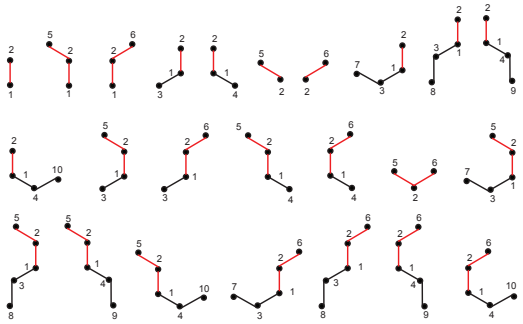

Figure 6.3: *The paths in* $\mathbb{G}_{10}$ *that pass through one of these edges* $(1,2)$, $(2,5)$, $(2,6)$.

Applications in networks with continuing growth

Now we apply Theorem 6.5 to allocate coupling strengths in a network with continuing growth. A growing graph considered in this subsection is the graph in which the number of the vertices increases. It is much easier to compare a growing graph with a growing star, with the same vertex set, than with a growing complete graph. If one more vertex is added to the star graph $\mathbb{S}_n$, only one more edge needs to be added. However, if one more vertex is added to the complete graph $\mathbb{K}_n$, n new edges need to get involved in calculation. Moreover, the second smallest eigenvalue of star graphs is the constant 1. These motivate us to apply Theorem 6.5 on dynamic networks with continuing growth.

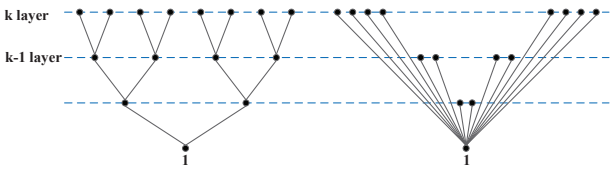

Figure 6.4: *Compare the growing complete binary tree with the growing star.*

In the following, we use complete binary trees to illustrate the application. The complete binary tree $\mathbb{T}_n$ with $n = 2^d - 1$ vertices is the graph with the edges of the form $(u, 2u)$ and $(u, 2u+1)$ for integer $u < n/2$ (Spielman 2004). The complete binary tree $\mathbb{T}_n$ is shown on the left of Figure 6.4. In this subsection we use $b^{'}(k-1,k,d)$ to denote the value of $b^{'}$ for the edges between the $(k-1)$th layer and the kth layer in the binary tree $\mathbb{T}_n$ with $n = 2^d - 1$, and $\varepsilon(k-1,k,d)$ to denote the couplings between

the $(k-1)$th layer and the kth layer in $\mathbb{T}_n$. The synchronization condition for the complete binary tree $\mathbb{T}_n$ is given in the proposition below.

Proposition 6.1 *Under Assumption 6.1, for the complete binary tree $\mathbb{T}_n$ with $n = 2^d - 1$ vertices, the global synchronization of system (6.1) is guaranteed if the couplings between the $(k-1)$th layer and the kth layer satisfy*

$$\varepsilon(k-1,k,d) \geqslant \sum_{j=k}^{d} (j-1) \times 2^{j-k}\, a, \qquad 2 \leqslant k \leqslant d.$$

Proof: We start with the complete binary tree with two layers $d = 2$. Comparing it with the star $\mathbb{S}_3$, we have

$$L_{\mathbb{S}_3} = L_{(1,2)} + L_{(1,3)}\,.$$

From Theorem 6.5, it is easy to obtain the bounds for the edges in $\mathbb{T}_3$: $\varepsilon_{(1,2)} \geqslant a$, and $\varepsilon_{(1,3)} \geqslant a$.
Compare the complete binary tree with $d = 3$ with $\mathbb{S}_7$:

$$\begin{aligned} L_{\mathbb{S}_7} &= L_{(1,2)} + L_{(1,3)} + L_{(1,4)} + L_{(1,5)} + L_{(1,6)} + L_{(1,7)} \\ &\preceq L_{(1,2)} + L_{(1,3)} + 2[L_{(1,2)} + L_{(2,4)}] + 2[L_{(1,2)} + L_{(2,5)}] \\ &\qquad + 2[L_{(1,3)} + L_{(3,6)}] + 2[L_{1,3} + L_{(3,7)}] \\ &= (1 + 2 \times 2)L_{(1,2)} + (1 + 2 \times 2)L_{(1,3)} + 2L_{(2,4)} + 2L_{(2,5)} + 2L_{(3,6)} + 2L_{(3,7)} \end{aligned}$$

and for the complete binary tree with $d = 4$:

$$\begin{aligned} L_{\mathbb{S}_{15}} &= L_{(1,2)} + L_{(1,3)} + L_{(1,4)} + \cdots + L_{(1,15)} \\ &\preceq (1 + 2 \times 2 + 3 \times 2^2)L_{(1,2)} + (1 + 2 \times 2 + 3 \times 2^2)L_{(1,3)} \\ &\quad + (2 + 3 \times 2)L_{(2,4)} + (2 + 3 \times 2)L_{(2,5)} + (2 + 3 \times 2)L_{(3,6)} + (2 + 3 \times 2)L_{(3,7)} \\ &\quad + 3L_{(4,8)} + 3L_{(4,9)} + 3L_{(5,10)} + 3L_{(5,11)} \\ &\quad + 3L_{(6,12)} + 3L_{(6,13)} + 3L_{(7,14)} + 3L_{(7,15)}\,. \end{aligned}$$

We obtain the weights for the edges in the complete binary tree $\mathbb{T}_n$ with $n = 2^d - 1$ by induction, and we postulate

$$b^{'}(k-1,k,d) = \sum_{j=k}^{d} (j-1) \times 2^{j-k} \tag{6.12}$$

for the edges of the form $(u, 2u)$ and $(u, 2u+1)$ with $u = 2^{k-2}, \ldots, 2^{k-1} - 1$ where $2 \leqslant k \leqslant d$ (the edges from the $(k-1)$th layer to the kth layer).

Now we use induction to prove our conjecture. Suppose that (6.12) holds for the complete binary tree $\mathbb{T}_n$ with $n = 2^d - 1$. Then we calculate $b^{'}(k-1, k, d+1)$ for the binary tree with $n^{'} = 2^{d+1} - 1$. The depth of $\mathbb{T}_{n^{'}}$ is $d+1$. The binary tree $\mathbb{T}_{n^{'}}$ has one more layer, and has 2^d more vertices which are labeled by $v_{2^d}, v_{2^d+1}, \ldots, v_{2^{d+1}-1}$. In order to assign couplings in $\mathbb{T}_{n^{'}}$, we compare $\mathbb{T}_{n^{'}}$ with the star graph $\mathbb{S}_{2^{d+1}-1}$, and calculate for the edges of the form $(u, 2u)$ and $(u, 2u+1)$ with $u = 2^{k-2}, \ldots, 2^{k-1} - 1$ and $2 \leqslant k \leqslant d+1$ (the edges from the $(k-1)$th layer to the kth layer):

$$\begin{aligned} b^{'}(k-1, k, d+1) &= b^{'}(k-1, k, d) + d \times 2^{d-k+1} \\ &= \sum_{j=k}^{d} (j-1) \times 2^{j-k} + d \times 2^{d-k+1} \\ &= \sum_{j=k}^{d+1} (j-1) \times 2^{j-k}. \end{aligned}$$

This shows that (6.12) still holds for the binary tree $\mathbb{T}_{n^{'}}$ with $d+1$ layers, and hence by induction we have proved that (6.12) is correct. Thus, for the binary tree $\mathbb{T}_n$ with $n = 2^d - 1$, the weights for the edges of the form $(u, 2u)$ and $(u, 2u+1)$ for $u = 2^{k-2}, \ldots, 2^{k-1} - 1$ where $2 \leqslant k \leqslant d$ (the edges from the $(k-1)$th layer to the k-th layer) should satisfy $\varepsilon(k-1, k, d) \geqslant \sum_{j=k}^{d} (j-1) \times 2^{j-k}\, a$. This completes the proof. □

6.3.3 Application to synchronizability

In this subsection, we look at how to construct a lower bound for $\lambda_2(L_{\mathbb{G}})$ when the weights of $\mathbb{G}$ is fixed and given beforehand. In this case, $\lambda_2(L_{\mathbb{G}})$ is referred to as the algebraic connectivity (Godsil and Royle 2001) of $\mathbb{G}$ and describes how well $\mathbb{G}$ is connected; it has also been used to measure the synchronizability of a coupled dynamical network (Wu 2003). However, it is usually not so easy to calculate $\lambda_2(\mathbb{G})$ using local information of graph $\mathbb{G}$. In the following, we propose a way to construct a lower bound for $\lambda_2(\mathbb{G})$ using the pairwise path information of $\mathbb{G}$, which is inspired by the graph comparisons done in Theorems 6.3, 6.4 and 6.5.

Measure synchronizability of unweighted graphs

We first assume that $\mathbb{G}$ is unweighted and time-invariant, and construct a lower bound for $\lambda_2(\mathbb{G})$ using b_k defined in Theorem 6.4.

Theorem 6.6 *a) Let* $b_{\max}$ *denote* $\max_{1\leqslant k\leqslant m} b_k$*, where* $b_k = \sum_{j>i;k\in\mathcal{P}_{ij}} |\mathcal{P}_{ij}|$*. It holds that*

$$\lambda_2(L_{\mathbb{G}}) \geqslant \frac{n}{b_{\max}};$$

b) Let $b_{\max}^{'}$ *denote* $\max_{1\leqslant k\leqslant m} b_k^{'}$*, where* $b_k^{'}$ *is defined by (6.9). It holds that*

$$\lambda_2(L_{\mathbb{G}}) \geqslant \frac{1}{b_{\max}^{'}}.$$

Proof: a) We compare the complete graph $\mathbb{K}_n$ with the union of all the possible paths in $\mathbb{G}$. In the proof of Theorem 6.4, we have proven that

$$L_{\mathbb{K}_n} \preceq \sum_{k=1}^{m} b_k L_k, \quad \text{where } b_k = \sum_{j>i;k\in\mathcal{P}_{ij}} |\mathcal{P}_{ij}|.$$

Since $b_{\max} = \max_{1\leqslant k\leqslant m} b_k$, one has

$$L_{\mathbb{K}_n} \preceq b_{\max} \sum_{k=1}^{m} L_k = b_{\max} L_{\mathbb{G}}.$$

From Theorem 6.3, $b_{\max}\,\mathbb{G} \succeq \mathbb{K}_n$ is equivalent to $\lambda_2(L_{\mathbb{G}}) \geqslant \frac{\lambda_2(L_{\mathbb{K}_n})}{b_{\max}} = \frac{n}{b_{\max}}$.
b) We compare the star $\mathbb{S}_n$ with the union of the paths $(1, j), j = 2, \ldots, n$ in $\mathbb{G}$. In the proof of Theorem 6.5, we have shown that

$$L_{\mathbb{S}_n} \preceq \sum_{k=1}^{m} b_k^{'} L_k,$$

where $b_k^{'}$ is defined by (6.9). Since $b_{\max}^{'} = \max_{1\leqslant k\leqslant m} b_k^{'}$, one has

$$L_{\mathbb{S}_n} \preceq b_{\max}^{'} \sum_{k=1}^{m} L_k = b_{\max}^{'} L_{\mathbb{G}}.$$

From Theorem 6.3, one has $\lambda_2(L_{\mathbb{G}}) \geqslant \frac{\lambda_2(L_{\mathbb{S}_n})}{b_{\max}^{'}} = \frac{1}{b_{\max}^{'}}$. □

Remark 6.6 *The constructions of a lower bound of* $\lambda_2(L_{\mathbb{G}})$ *in papers (Rad et al. 2011, Guattery et al. 1999) are similar to our estimation given by Theorem 6.6 a). However, we have taken a different approach, following a simpler derivation.*

Remark 6.7 *Theorem 6.6 b) is obtained through comparing graph* $\mathbb{G}$ *with the star* $\mathbb{S}_n$*. Other lower bounds can be obtained similarly if graph* $\mathbb{G}$ *is compared with graphs whose second*

smallest eigenvalues are known beforehand. A proper choice of the compared graphs is helpful to obtain tighter lower bounds for $\lambda_2(\mathbb{G})$ and reduce the computational complexity of comparison. In general, Theorem 6.6 b) is more efficient than a) especially when $\mathbb{G}$ is sparse and large.

Now we give an example to show the effectiveness of the estimations in Theorem 6.6. We consider the unweighted fractal graph whose topology is shown on the left of Fig. 6.2. From the calculations in (6.11) and (6.10), we have $b_{\max}/n = \max\{65, 27\}/10 = 6.5$ and $b'_{\max} = \max\{5, 2\} = 5$. Then the calculated lower bounds for λ_2 are 0.1538 and 0.2 according to Theorem 6.6 a) and Theorem 6.6 b) respectively. The actual value of λ_2 of this graph is 0.2679. In comparison, one can obtain the lower bound $\frac{4}{10\times 4} = 0.1$ using Mohar's lower bound (Mohar 1991) $\lambda_2 \geqslant \frac{4}{n\, D_{\max}}$ where $D_{\max}$ is the diameter of the graph.

Measure synchronizability of weighted graphs

There have been different methods (de Abreu 2007) to estimate the second smallest eigenvalues of the Laplacian matrices of unweighted graphs, but there is few result for weighted graphs. In this subsection, we measure the synchronizability of a weighted network by expanding the result in the previous subsection.

Theorem 6.7 *Let the weights of the m edges of $\mathbb{G}$ be $c_1, c_2, \ldots, c_m$. Let*

$$b_k^* \triangleq \sum_{j>i, k\in\mathcal{P}_{ij}} \Big(\sum_{h\in\mathcal{P}_{ij}} \frac{1}{c_h}\Big), \quad \text{for } 1 \leqslant k \leqslant m\,. \tag{6.13}$$

It holds that $\lambda_2(L_{\mathbb{G}}) \geqslant \frac{n}{b^*_{\max}}$, where $b^*_{\max}$ is the maximum of all b_k^*.

Proof: For each pair of (i, j) where $j > i$, we choose one path in the weighted graph $\mathbb{G}$ with two associated vertices i, j. Then from Lemma 6.3, we have

$$L_{(i,j)} \preceq \Big(\sum_{k\in\mathcal{P}_{ij}} \frac{1}{c_k}\Big) \sum_{k\in\mathcal{P}_{ij}} c_k\, L_k\,.$$

We compare the complete graph $\mathbb{K}_n$ with the union of all possible paths in the weighted graph $\mathbb{G}$. Thus we have

$$\begin{aligned} L_{\mathbb{K}_n} &= \sum_{j>i} L_{(i,j)} \\ &\preceq \sum_{j>i} \left(\Big(\sum_{k\in\mathcal{P}_{ij}} \frac{1}{c_k}\Big) \sum_{k\in\mathcal{P}_{ij}} c_k\, L_k \right) \end{aligned}$$

$$
\begin{aligned}
&= \sum_{k=1}^{m} \left(\sum_{j>i, k\in\mathcal{P}_{ij}} \Big(\sum_{h\in\mathcal{P}_{ij}} \frac{1}{c_h} \Big) \right) c_k\, L_k \\
&= \sum_{k=1}^{m} b_k^*\, c_k\, L_k \\
&\preceq b_{\max}^* \sum_{k=1}^{m} c_k\, L_k = b_{\max}^*\, L_{\mathbb{G}}\,.
\end{aligned}
$$

From Theorem 6.3, $b_{\max}^*\,\mathbb{G} \succeq \mathbb{K}_n$ is equivalent to

$$\lambda_2(L_{\mathbb{G}}) \geqslant \frac{\lambda_2(L_{\mathbb{K}_n})}{b_{\max}^*} = \frac{n}{b_{\max}^*}.$$

Thus we have arrived at the conclusion. □

Remark 6.8 *Theorem 6.6 a) is a special case of Theorem 6.7, which can be verified by setting* $c_1 = c_2 = \cdots = c_m = 1$ *in (6.13). In this case one obtains* $b_k^* = \sum_{j>i, k\in\mathcal{P}_{ij}} |\mathcal{P}_{ij}|$ *from (6.13). In addition, Theorem 6.7 is obtained through comparing the weighted graph* $\mathbb{G}$ *with the complete graph with the same vertex set. Other lower bounds can be obtained similarly if* $\mathbb{G}$ *is compared with other fundamental graphs whose second smallest eigenvalues are known beforehand.*

Now we give an example to show how to use graph comparison to estimate lower bounds for synchronizability of weighted graphs. We again consider the fractal graph $\mathbb{G}_{10}$ whose topology is shown on the left of Fig. 6.2, however all the edges in the graph are weighted in this example. Suppose the weights of the edges $(1,2),(1,3),(1,4)$ are c_1, and the weights of the other edges are c_2. To simplify the calculations in graph comparison, we choose to compare the fractal graph $\mathbb{G}_{10}$ with the star $\mathbb{S}_{10}$, rather than with the complete graph $\mathbb{K}_{10}$. In view of Lemma 6.3, we can compare edge $(1,5)$ in $\mathbb{S}_{10}$ with the weighted edges $(1,2),(2,5)$ in $\mathbb{G}_{10}$, and obtain that $L_{(1,5)} \preceq (\frac{1}{c_1}+\frac{1}{c_2})\,(c_1\,L_{(1,2)} + c_2\,L_{(2,5)})$. Similarly, we have $L_{(1,6)} \preceq (\frac{1}{c_1}+\frac{1}{c_2})\,(c_1\,L_{(1,2)} + c_2\,L_{(2,6)})$.
Because of the fractal structure of $\mathbb{G}_{10}$, we only need to focus on the calculations for the edges $(1,2),(2,5),(2,6)$ and thus obtain

$$
\begin{aligned}
L_{\mathbb{S}_{10}} &= L_{(1,2)} + L_{(1,5)} + L_{(1,6)} + \dots \\
&\preceq L_{(1,2)} + \Big(\frac{1}{c_1}+\frac{1}{c_2}\Big)\,(c_1\,L_{(1,2)} + c_2\,L_{(2,5)}) \\
&\quad + \Big(\frac{1}{c_1}+\frac{1}{c_2}\Big)\,(c_1\,L_{(1,2)} + c_2\,L_{(2,6)}) + \dots
\end{aligned}
$$

$$= (\frac{3}{c_1} + \frac{2}{c_2})\, c_1\, L_{(1,2)} + (\frac{1}{c_1} + \frac{1}{c_2})\, c_2\, L_{(2,5)} + (\frac{1}{c_1} + \frac{1}{c_2})\, c_2\, L_{(2,6)} + \dots .$$

So we have $b^{'}_{\max} = \max\{\frac{3}{c_1} + \frac{2}{c_2}, \frac{1}{c_1} + \frac{1}{c_2}\} = \frac{3}{c_1} + \frac{2}{c_2}$. Note that the Laplacian matrix of $\mathbb{G}_{10}$ can be written as $L_{\mathbb{G}_{10}} = c_1\,[L_{(1,2)} + L_{(1,3)} + L_{(1,4)}] + c_2\,[L_{(2,5)} + L_{(2,6)} + L_{(3,7)} + L_{(3,8)} + L_{(4,9)} + L_{(4,10)}]$. Then one has $L_{\mathbb{S}_{10}} \preceq b^{'}_{\max}\, L_{\mathbb{G}_{10}}$. Therefore $\lambda_2(L_{\mathbb{G}_{10}}) \geqslant \frac{\lambda_2(\mathbb{S}_{10})}{b^{'}_{\max}} = \frac{c_1 c_2}{2c_1+3c_2}$.

6.3.4 Numerical simulations

In this subsection, we provide a numerical example to illustrate Theorem 6.5. Given the self-dynamics $f(\cdot)$ and the inner coupling matrix P, we first need to figure out the value a in Assumption 6.1. This has been extensively studied in the literature on control and synchronization of chaotic dynamical systems (Wu and Chua 1994, Kurths et al. 2003). For instance, two mutually coupled Chua's circuits can synchronize by choosing $P = \mathrm{diag}\{1, 0, 0\}$ for a large enough scalar $a > \frac{\max(-G_a, -G_b)}{C_1}$ (Wu and Chua 1994, Corollary 10), where G_a, G_b, C_1 are parameters of Chua's circuits. As another example, two Lorenz systems mutually coupled through the first component of their states can synchronize when a is greater than a computable threshold (Belykh et al. 2004, Appendix A). In this simulation, we consider the network (6.1) consisting of n Lorenz systems coupled through the first components of their states. To be specific, the dynamics of the network are given by

$$\begin{cases} \dot{x}_i = \sigma\,(y_i - x_i) + \sum_{j=1}^{n} \varepsilon_{ij}(t)\, x_j \\ \dot{y}_i = r x_i - y_i - x_i\, z_i \\ \dot{z}_i = -b\, z_i + x_i\, y_i \end{cases} \tag{6.14}$$

and the inner coupling matrix is $P = \mathrm{diag}\{1, 0, 0\}$. According to (Belykh et al. 2004, Appendix A), the quantity $a > a^* = \frac{b(b+1)(r+\sigma)^2}{16(b-1)} - \sigma$. We choose the fractal graph with $n = 10$ vertices on the left of Fig. 6.2 to be the network topology used in the simulation. The bounds for coupling strengths have been calculated and given by (6.10), and so we set the coupling strengths $\varepsilon_{(1,2)} = \varepsilon_{(1,3)} = \varepsilon_{(1,4)} = 5a$, and the coupling strengths for the other edges $2a$. The parameters in (6.14) are set to be $\sigma = 10, r = 25, b = 8/3$. The initial states are randomly chosen from $[0, 30]$. The three subfigures in Fig. 6.5 show the state of the coupled network (6.14) in its

$x, y, z-$dimension respectively. From Fig. 6.5, one can see that the coupled Lorenz oscillators asymptotically synchronize by adopting the coupling strength allocation (6.10) obtained according to Theorem 6.5. The simulation results illustrate the correctness of Theorem 6.5.

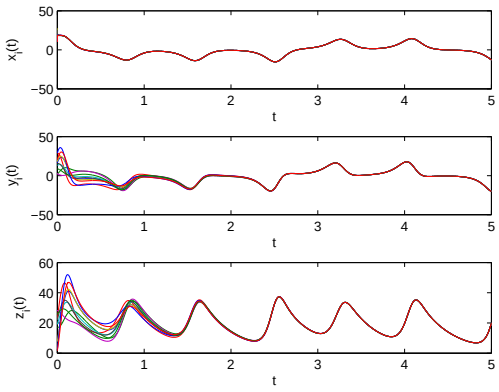

Figure 6.5: *The states of the coupled Lorenz oscillators (6.14).*

Up to now, we have presented new ways to allocate coupling strengths using spectral graph theory in order to achieve synchronization in complex networks. The main idea is to bound the second-smallest eigenvalues of Laplacian matrices associated with the given networks by comparing the corresponding network graphs to complete or other special graphs with the same vertex sets. In the next section, we will look into applying the proposed methodologies to networks with directed topologies. The main challenge is then how to deal with the fact that the Laplacian matrices associated with directed graphs are not guaranteed to be positive semi-definite anymore.

6.4 Graphical synchronization criteria for directed complex networks

6.4.1 Spectral graph theoretic conditions

First, we investigate the graph theoretic condition for synchronization in directed complex dynamical networks. In Theorem 6.1, we take graph $\mathbb{G}_0$ to be the complete

graph $\mathbb{K}_n$. Therefore the complete synchronization of system (6.1) is guaranteed if

$$L_{\mathbb{K}_n} L_{\mathbb{G}} \succ a\, L_{\mathbb{K}_n}\,. \tag{6.15}$$

Note that $L_{\mathbb{K}_n} = nI_n - J$ where J is the $n \times n$ all-one matrix. From (6.15), one has

$$nL_{\mathbb{G}} - JL_{\mathbb{G}} \succ aL_{\mathbb{K}_n}. \tag{6.16}$$

In the case where $\mathbb{G}$ is undirected, (6.16) can be further reduced to $\mathbb{G} \succ \frac{a}{n}\mathbb{K}_n$. However, in this section we are looking at the more challenging scenario where the networks are directed. We will use the following property of directed graphs.

Lemma 6.6 *For a directed graph $\mathbb{G}$, the condition $nL_{\mathbb{G}} - JL_{\mathbb{G}} \succ aL_{\mathbb{K}_n}$ is equivalent to $\frac{n}{2}(L_{\mathbb{G}} + L_{\mathbb{G}}^T) - \frac{1}{2}(JL_{\mathbb{G}} + L_{\mathbb{G}}^T J) \succ aL_{\mathbb{K}_n}$.*

Proof: i) "⇒" From $nL_{\mathbb{G}} - JL_{\mathbb{G}} \succ aL_{\mathbb{K}_n}$, it follows that $nL_{\mathbb{G}}^T - (JL_{\mathbb{G}})^T \succ aL_{\mathbb{K}_n}$. From these two inequalities, we have $\frac{n}{2}(L_{\mathbb{G}} + L_{\mathbb{G}}^T) - \frac{1}{2}(JL_{\mathbb{G}} + L_{\mathbb{G}}^T J) \succ aL_{\mathbb{K}_n}$.
ii) "⇐" From $\frac{n}{2}(L_{\mathbb{G}} + L_{\mathbb{G}}^T) - \frac{1}{2}(JL_{\mathbb{G}} + L_{\mathbb{G}}^T J) \succ aL_{\mathbb{K}_n}$, we have

$$\begin{aligned}
&x^T \left(\frac{n}{2}(L_{\mathbb{G}} + L_{\mathbb{G}}^T) - \frac{1}{2}(JL_{\mathbb{G}} + L_{\mathbb{G}}^T J) - aL_{\mathbb{K}_n}\right) x \\
&= x^T \left(\frac{n}{2}L_{\mathbb{G}} - \frac{1}{2}\,JL_{\mathbb{G}} - \frac{a}{2}L_{\mathbb{K}_n}\right) x + x^T \left(\frac{n}{2}L_{\mathbb{G}}^T - \frac{1}{2}\,L_{\mathbb{G}}^T J - \frac{a}{2}L_{\mathbb{K}_n}\right) x \\
&= x^T(nL_{\mathbb{G}} - \,JL_{\mathbb{G}} - aL_{\mathbb{K}_n})x > 0
\end{aligned}$$

for all $x \in \mathbb{R}^n$. It implies then that $nL_{\mathbb{G}} - JL_{\mathbb{G}} \succ aL_{\mathbb{K}_n}$. □

Now we present a general graph theoretic synchronization criterion.

Theorem 6.8 *Suppose that Assumption 6.1 holds, and that graph $\mathbb{G}$ contains a spanning directed tree. The synchronization manifold of system (6.1) is globally asymptotically stable if*

$$\frac{n}{2}(L_{\mathbb{G}} + L_{\mathbb{G}}^T) - \frac{1}{2}(JL_{\mathbb{G}} + L_{\mathbb{G}}^T J) \succ aL_{\mathbb{K}_n}\,. \tag{6.17}$$

Proof: From Lemma 6.6, the inequality (6.17) is equivalent to $nL_{\mathbb{G}} - JL_{\mathbb{G}} \succ aL_{\mathbb{K}_n}$. The latter is equivalent to $L_{\mathbb{K}_n} L_{\mathbb{G}} \succ a\, L_{\mathbb{K}_n}$, noting that $L_{\mathbb{K}_n} = nI_n - J$. Let $\mathbb{G}_0$ in Theorem 6.1 to be $\mathbb{K}_n$. Thus there exist the connected undirected graph $\mathbb{G}_0$, which equals $\mathbb{K}_n$, such that the inequality (6.3) holds. This guarantees that the synchronization manifold of system (6.1) is globally asymptotically stable. □

In the following, we will show how to interpret (6.17) from the perspective of graph comparisons. Let D_i^c denote the vertex unbalance (Belykh et al. 2006a) of vertex i, namely $D_i^c = \sum_{k=1}^n \varepsilon_{ki} = \sum_{k\neq i} \varepsilon_{ki} + \varepsilon_{ii} = \sum_{k\neq i} \varepsilon_{ki} - \sum_{k\neq i} \varepsilon_{ik}$, which is the difference between the out-degree and in-degree of vertex i. It holds that

$$\begin{aligned} J\,L_{\mathbb{G}} &= \mathbf{1} \otimes \begin{bmatrix} -\sum_{k=1}^n \varepsilon_{k1} & -\sum_{k=1}^n \varepsilon_{k2} & \dots & -\sum_{k=1}^n \varepsilon_{kn} \end{bmatrix} \\ &= -\mathbf{1} \otimes \begin{bmatrix} D_1^c & D_2^c & \dots & D_n^c \end{bmatrix} \end{aligned}$$

And one has

$$L_{\mathbb{G}}^T\, J = -\mathbf{1}^T \otimes \begin{bmatrix} D_1^c & D_2^c & \dots & D_n^c \end{bmatrix}^T .$$

It follows that the matrix $-(J\,L_{\mathbb{G}} + L_{\mathbb{G}}^T\, J)$ is

$$\begin{bmatrix} 2D_1^c & D_1^c + D_2^c & \dots & D_1^c + D_n^c \\ D_2^c + D_1^c & 2D_2^c & \dots & D_2^c + D_n^c \\ \dots & \dots & \dots & \dots \\ D_n^c + D_1^c & D_n^c + D_2^c & \dots & 2D_n^c \end{bmatrix},$$

where the (ij)th entry is $D_i^c + D_j^c$ for $i, j = 1, \dots, n$. Since the sum of the out-degrees of all the vertices in $\mathbb{G}$ is equal to the sum of the in-degrees of all the vertices, we have $\sum_{i=1}^n D_i^c = 0$. The ith row-sum of the matrix $-(J\,L_{\mathbb{G}} + L_{\mathbb{G}}^T\, J)$ is then $nD_i^c + \sum_{i=1}^n D_i^c = nD_i^c$ for $i = 1, \dots, n$. Define the $n \times n$ matrix

$$\Delta \triangleq \operatorname{diag}\{nD_1^c, nD_2^c, \dots, nD_n^c\}.$$

Then it follows that the matrix $aL_{\mathbb{K}_n} + \frac{1}{2}\,(JL_{\mathbb{G}} + L_{\mathbb{G}}^T\, J) + \frac{1}{2}\,\Delta$ is symmetric and has zero row sums. Since the ith row-sum of the matrix $L_{\mathbb{G}} + L_{\mathbb{G}}^T$ is $-\sum_{k=1}^n \varepsilon_{ki} = -D_i^c$ for $i = 1, \dots, n$, we know that the matrix $\frac{n}{2}(L_{\mathbb{G}} + L_{\mathbb{G}}^T) + \frac{1}{2}\,\Delta$ is symmetric and has zero row sums and non-positive off-diagonal entries. Now we are ready to compare the two symmetric matrices $aL_{\mathbb{K}_n} + \frac{1}{2}\,(JL_{\mathbb{G}} + L_{\mathbb{G}}^T\, J) + \frac{1}{2}\,\Delta$ and $\frac{n}{2}(L_{\mathbb{G}} + L_{\mathbb{G}}^T) + \frac{1}{2}\,\Delta$. From (6.17), we have

$$\frac{1}{2}(L_{\mathbb{G}} + L_{\mathbb{G}}^T) + \frac{1}{2n}\,\Delta > \frac{a}{n}\left(L_{\mathbb{K}_n} + \frac{1}{2a}\,(JL_{\mathbb{G}} + L_{\mathbb{G}}^T\, J) + \frac{1}{2a}\,\Delta\right). \tag{6.18}$$

There are existing results providing sufficient conditions for the global synchronization of system (6.1). We list one such result below.

Theorem 6.9 (Belykh et al. 2006a) *Under Assumption 6.1, the synchronization manifold of system (6.1) is globally asymptotically stable if*

$$\sum_{i=1}^{n-1}\sum_{j>i}^{n}\left(\frac{\varepsilon_{ij}+\varepsilon_{ji}}{2}\right)(x_{i_k}-x_{j_k})^2 > \frac{a}{n}\sum_{i=1}^{n-1}\sum_{j>i}^{n} \times\left(1+\frac{D_i^c+D_j^c}{2a}\right)(x_{i_k}-x_{j_k})^2 \tag{6.19}$$

for $1 \leqslant k \leqslant d$.

One can easily check that the inequality (6.18) is equivalent to the inequality (6.19) in Theorem 6.9. Therefore, we have shown that Theorem 6.8 and Theorem 6.9 are in fact one and the same. Since Theorem 6.8 provides the synchronization criterion (6.18) in terms of graph comparison, it will be useful later on as we further develop spectral graph theoretic conditions in this section.

The spectral graph theory discussed in (Spielman 2004) mainly focuses on undirected graphs. It has been demonstrated in Section 6.3 that tools in spectral graph theory are powerful in utilizing flexibly topological features of a given network. However, the results developed in Section 6.3 can be applied only to undirected networks and are thus not general enough. Motivated by (Belykh et al. 2006a), what we propose to do in the next is to symmetrize the graph $\mathbb{G}$ first, and then construct synchronization criteria on the symmetrized graph using spectral graph theory. To be more specific, for any pair of unidirectionally coupled vertices i and j, we replace the directed edge between them by an undirected edge with the weight $\varepsilon_{ij}/2$ that is half of the original coupling strength; for any bi-directionally coupled pair of vertices i and j, we replace the two edges between them by an undirected edge with the coupling strength $(\varepsilon_{ij}+\varepsilon_{ji})/2$. Let $\mathbb{G}^s$ be the obtained symmetrized graph from $\mathbb{G}$. One can then check that the Laplacian matrix of $\mathbb{G}^s$ is $L_{\mathbb{G}^s} = \frac{1}{2}\left(L_{\mathbb{G}} + L_{\mathbb{G}}^T\right) + \frac{1}{2n}\Delta$.

For the symmetrized graph $\mathbb{G}^s$, consider a set of paths $\mathcal{P} = \{\mathcal{P}_{ij} | i, j = 1, \ldots, n, j > i\}$, one for each pair of distinct vertices i and j. Now we use Theorem 6.8 and (6.18) to construct graph theoretic conditions for the synchronization of network (6.1). We use $\mathcal{E}(\mathbb{G}^s)$ to denote the set of all the edges of $\mathbb{G}^s$ and assume that there are altogether m edges that are labeled by $1, \ldots, m$. In the following theorem, we show that lower bounds on the coupling strengths $\varepsilon_k, k = 1, \ldots, m$, can be constructed to guarantee that the inequality (6.18) holds.

Theorem 6.10 *Suppose that Assumption 6.1 holds, and the graph $\mathbb{G}$ contains a spanning directed tree. The synchronization manifold of network (6.1) is globally asymptotically stable*

if

$$\varepsilon_k > \frac{a}{n}\, b_k, \qquad \textit{for } k = 1, \ldots, m, \tag{6.20}$$

where $b_k = \sum_{j>i;k\in\mathcal{P}_{ij}} w(\mathcal{P}_{ij})$ *is the sum of the weighted lengths* $w(\mathcal{P}_{ij})$ *of all those paths* $\mathcal{P}_{ij}$ *in* $\mathcal{P}$ *that contain the edge* k *that belongs to the symmetrized graph* $\mathbb{G}^s$ *and the weighted path length* $w(\mathcal{P}_{ij})$ *is defined by*

$$w(\mathcal{P}_{ij}) \triangleq \begin{cases} |\mathcal{P}_{ij}|\,\chi\left(1+\frac{D_i^c+D_j^c}{2a}\right), & \textit{edge}(i,j)\notin\mathcal{E}(\mathbb{G}^s)\,; \\ 1+\frac{D_i^c+D_j^c}{2a}, & \textit{edge}(i,j)\in\mathcal{E}(\mathbb{G}^s)\,, \end{cases} \tag{6.21}$$

where for $z\in\mathbb{R}$, *the function* $\chi(z)=z$ *if* $z>0$, $\chi(z)=0$ *otherwise.*

Proof: Since the two matrices $L_{\mathbb{G}^s}$ and $\frac{a}{n}\left(L_{\mathbb{K}_n}+\frac{1}{2a}\left(JL_{\mathbb{G}}+L_{\mathbb{G}}^T J\right)+\frac{1}{2a}\Delta\right)$ are symmetric and have zero row and column sums, we can compare them as follows.

$$\begin{aligned}
&\frac{a}{n}\left(L_{\mathbb{K}_n}+\frac{1}{2a}\left(JL_{\mathbb{G}}+L_{\mathbb{G}}^T J\right)+\frac{1}{2a}\Delta\right)\\
&=\frac{a}{n}\sum_{j>i}\left(1+\frac{D_i^c+D_j^c}{2a}\right)L_{(i,j)}\\
&\preceq\frac{a}{n}\sum_{j>i;(i,j)\notin\mathcal{E}(\mathbb{G}^s)}\chi\left(1+\frac{D_i^c+D_j^c}{2a}\right)L_{(i,j)}+\frac{a}{n}\sum_{j>i;(i,j)\in\mathcal{E}(\mathbb{G}^s)}\left(1+\frac{D_i^c+D_j^c}{2a}\right)L_{(i,j)}
\end{aligned}$$

(For any pair of vertices i,j, if $(i,j)\in\mathcal{E}(\mathbb{G}^s)$, then we just keep the term $\left(1+\frac{D_i^c+D_j^c}{2a}\right)L_{(i,j)}$; if $(i,j)\notin\mathcal{E}(\mathbb{G}^s)$, we choose a path $\mathcal{P}_{ij}$ in $\mathbb{G}^s$. Using Lemma 6.4, we compare $L_{(i,j)}$ with the chosen path $\mathcal{P}_{ij}$.)

$$\begin{aligned}
&\preceq\frac{a}{n}\sum_{\substack{j>i;\\(i,j)\notin\mathcal{E}(\mathbb{G}^s)}}\left(|\mathcal{P}_{ij}|\chi\left(1+\frac{D_i^c+D_j^c}{2a}\right)\sum_{k\in\mathcal{P}_{ij};k\in\mathcal{E}(\mathbb{G}^s)}L_k\right)\\
&\quad+\frac{a}{n}\sum_{j>i;(i,j)\in\mathcal{E}(\mathbb{G}^s)}\left(1+\frac{D_i^c+D_j^c}{2a}\right)L_{(i,j)}
\end{aligned}$$

(We sum up all the weights for L_k where edge $k \in \mathcal{E}(\mathbb{G}^s)$.)

$$
\begin{aligned}
&= \frac{a}{n} \sum_{k=1}^{m} \left(\sum_{j>i;k\in P_{ij}} w(\mathcal{P}_{ij}) \right) L_k \\
&= \frac{a}{n} \sum_{k=1}^{m} b_k \, L_k \\
&< \sum_{k=1}^{m} \varepsilon_k \, L_k = L_{\mathbb{G}^s} \, ,
\end{aligned}
$$

where $b_k = \sum_{j>i;k\in\mathcal{P}_{ij}} w(\mathcal{P}_{ij})$ has been defined above. And the last inequality holds trivially when $\varepsilon_k > \frac{a}{n} b_k$ for each edge k. □

Remark 6.9 *Theorem 6.10 presents a coupling strength allocation strategy for the synchronization in a directed complex network. A similar result with slight differences in (6.21) has been achieved in (Belykh et al. 2006a). Using graph comparison, we have provided a different proof compared with those in (Belykh et al. 2006b, Belykh et al. 2006a). Our approach utilizes combinatorial features of the graphs associated with the networks, which results in a much simpler derivation.*

Remark 6.10 *If $\mathbb{G}$ is asymmetric but balanced, then $D_i^c = 0$ for $i = 1, \ldots, n$. From Theorem 6.10, it follows that network (6.1) can be asymptotically synchronized if $\varepsilon_k > \frac{b_k}{n} a$ for $k = 1, \ldots, m$, where $b_k = \sum_{j>i;k\in\mathcal{P}_{ij}} |\mathcal{P}_{ij}|$. The result then becomes the same as Theorem 1 in (Belykh et al. 2006b) in which the connection graph stability method on directed graphs with vertex balance is discussed.*

Theorem 6.10 can be used to find a set of coupling strengths to realize global synchronization in a network. We describe below an algorithm to achieve this goal.

Algorithm 6.1 Coupling strength allocation in a directed network.
Step 1. *Determine the vertex unbalance D_i^c for each vertex.*
Step 2. *Symmetrize $\mathbb{G}$ to obtain the undirected graph $\mathbb{G}^s$.*
Step 3. *Compare $\mathbb{G}^s$ with the corresponding complete graph $\mathbb{K}_n$. For any pair of vertices i, j, choose a path $\mathcal{P}_{ij}$ in $\mathbb{G}^s$. Here, we prefer to choose the shortest paths.*
Step 4. *For those paths $\mathcal{P}_{ij}$ whose lengths are greater than 1, assign the weight $1 + \frac{D_i^c + D_j^c}{2a}$ if $1 + \frac{D_i^c + D_j^c}{2a} > 0$, and zero otherwise. For those paths $\mathcal{P}_{ij}$ whose lengths equal 1, assign the weight $1 + \frac{D_i^c + D_j^c}{2a}$.*
Step 5. *For each edge k in $\mathbb{G}^s$ write down the inequality (6.20).*

Step 6. *Solve for the solutions to the obtained set of inequalities, which gives possible combinations of coupling strengths.*

Remark 6.11 *Similar ideas in this algorithm have been discussed in (Belykh et al. 2006a). The main differences lie in Steps 4 and 5 where we have used graph comparison techniques. Following (Belykh et al. 2006a), we call this algorithm the generalized connection graph method and use the abbreviation GCGM in the rest of the chapter.*

In the next subsection, we discuss in more detail a new systematic way to allocate coupling strengths for large networks with local structures.

6.4.2 Networks with local structures

Although GCGM uses the combinatorial features of graphs and sometimes greatly simplifies computation, it still has two shortcomings:
1) The computational complexity of counting paths grows exponentially as the size of the network inceases.
2) As the number of inequalities obtained in step 5 increases, it becomes more difficult, sometimes impossible, to find a solution in step 6.

To address these two shortcomings, we improve the results by looking more carefully at the networks' local structures and thus apply graph comparison only locally. To do so, we need to decompose graphs.

Definition 6.2 (Wu 2007) *The Frobenius normal form of the Laplacian matrix of a directed graph $\mathbb{G}$ is:*

$$L_{\mathbb{G}} = M \begin{bmatrix} B_1 & B_{12} & \dots & B_{1k} \\ & B_2 & \dots & B_{2k} \\ & & \ddots & \vdots \\ & & & B_k \end{bmatrix} M^T \tag{6.22}$$

where M is a permutation matrix and B_i are square irreducible matrices.

Lemma 6.7 (Wu 2007) *The matrices B_i in (6.22) are uniquely determined by $L_{\mathbb{G}}$ although their ordering can be arbitrary as long as they follow a partial order induced by $\lhd$ that is defined by $B_i \lhd B_j \Leftrightarrow B_{ij} \neq \mathbf{0}$.*

The uniqueness of the matrices B_i can be seen from the fact that these matrices correspond to the strongly connected components of graph $\mathbb{G}$. The decomposition of a

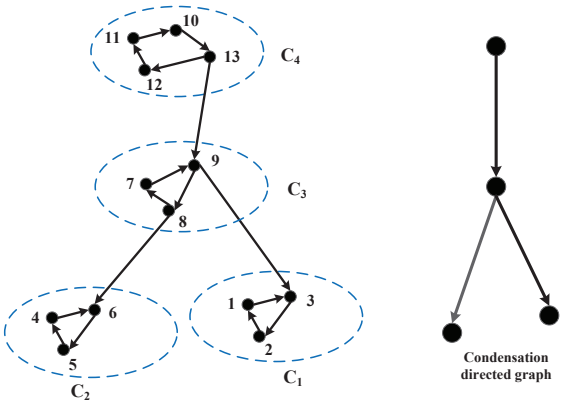

Figure 6.6: *A directed graph and its condensation directed graph.*

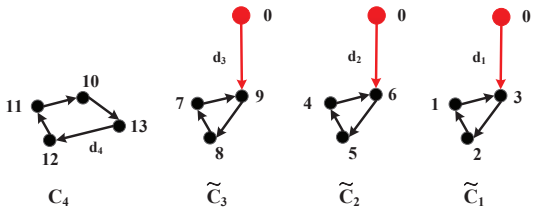

Figure 6.7: *Graph components.*

Laplacian matrix into its Frobenius normal form is thus equivalent to the decomposition of $\mathbb{G}$ into its strongly connected components. The partial order in Lemma 6.7 leads to the definition of condensation directed graphs as follows.

Definition 6.3 (Brualdi and Ryser 1991) *The condensation directed graph of a directed graph $\mathbb{G}$ is constructed by assigning a vertex to each strongly connected component of $\mathbb{G}$ and an edge between two vertices if there exists an edge of the same orientation between the corresponding strongly connected components of $\mathbb{G}$.*

The construction of condensation graphs can be done in linear time using standard graph searching algorithms (Tarjan 1972). We give an example of a directed graph and its corresponding condensation graph in Fig. 6.6. The condensation graph has the following property.

Lemma 6.8 (Wu 2007) *The condensation directed graph of $\mathbb{G}$ contains a spanning directed*

tree if and only if $\mathbb{G}$ contains a spanning directed tree.

The following synchronization criterion can be derived directly from Theorem 4.20 and Corollary 4.21 in (Wu 2007).

Lemma 6.9 (Wu 2007) *Under Assumption 6.1, if the graph $\mathbb{G}$ contains a spanning directed tree, then the network (6.1) synchronizes for sufficiently large coupling strength.*

The idea of graph decomposition motivates us to design the following algorithm to obtain the sets of coupling strengths for global synchronization using only local topological information. To avoid notational confusion and distinguish from the coupling strengths obtained by GCGM, we use d to denote the coupling strengths to be found using graph decomposition.

Algorithm 6.2 Coupling strength allocation in a decomposable directed network.
Step 1. *Decompose $\mathbb{G}$ into its k, $k \leqslant n$, strongly connected components $\mathbb{C}_1, \mathbb{C}_2, \ldots, \mathbb{C}_k$ and the partial ordering is given by Lemma 6.7.*
Step 2. *For $\mathbb{C}_k$, use the GCGM algorithm in the subsection 6.4.1 to obtain a lower bound of the coupling strength d_k to synchronize the systems corresponding to the vertices in $\mathbb{C}_k$.*
Step 3. *In descending order for $i = k-1, \ldots, 1$, treat $\mathbb{C}_i$ one by one. Replace all those vertices in $\mathbb{C}_{i+1}, \ldots, \mathbb{C}_k$, by a single vertex 0. And keep the edges between $\mathbb{C}_i$ and $\mathbb{C}_{i+1}, \ldots, \mathbb{C}_k$. Thus we arrive at an condensed component $\tilde{\mathbb{C}}_i$. Use the GCGM algorithm to obtain a lower bound of the coupling strength d_i for synchronization in $\tilde{\mathbb{C}}_i$.*
Step 4. *Combine d_i to get d.*

The theorem below guarantees the correctness of Algorithm 6.2.

Theorem 6.11 *Suppose that Assumption 6.1 holds, and the graph $\mathbb{G}$ contains a spanning directed tree. The synchronization manifold of network (6.1) is globally asymptotically stable if the coupling strengths for all the edges in $\mathbb{G}$ are allocated according to Algorithm 6.2.*

Proof: We need to prove the synchronization of network (6.1) under the coupling strength allocation according to Algorithm 6.2. Without loss of generality, we assume that M is an identity matrix in the Frobenius normal form of $L_{\mathbb{G}}$. Let $x \triangleq [x_1^T, x_2^T, \ldots, x_n^T]^T$. Let $\tilde{x}_i$ be the part of the state vector x corresponding to B_i for $i = 1, \ldots, k$. For vector $\tilde{x}_i = [\tilde{x}_{i1}^T, \ldots, \tilde{x}_{il}^T]^T$, we use $F(\tilde{x}_i)$ to denote

$$[f^T(\tilde{x}_{i1}), f^T(\tilde{x}_{i2}), \ldots, f^T(\tilde{x}_{il})]^T.$$

Then the dynamics of $(\tilde{x}_1^T, \ldots, \tilde{x}_{k-1}^T, \tilde{x}_k^T)$ can be written as (6.21). From (6.21), the

$$\begin{bmatrix} \dot{\tilde{x}}_1 \\ \dot{\tilde{x}}_2 \\ \vdots \\ \dot{\tilde{x}}_{k-1} \\ \dot{\tilde{x}}_k \end{bmatrix} = \begin{bmatrix} F(\tilde{x}_1) \\ F(\tilde{x}_2) \\ \vdots \\ F(\tilde{x}_{k-1}) \\ F(\tilde{x}_k) \end{bmatrix} + \begin{bmatrix} B_1 & B_{12} & \dots & B_{1k} \\ & B_2 & \dots & B_{2k} \\ & & \ddots & \vdots \\ & & B_{k-1} & B_{k-1,k} \\ & & & B_k \end{bmatrix} \otimes P \cdot \begin{bmatrix} \tilde{x}_1 \\ \tilde{x}_2 \\ \vdots \\ \tilde{x}_{k-1} \\ \tilde{x}_k \end{bmatrix} . \quad (6.21)$$

state equation for $\tilde{x}_k$ is

$$\dot{\tilde{x}}_k = F(\tilde{x}_k) + (B_k \otimes P)\tilde{x}_k \, ; \quad (6.24)$$

and the state equation for $\tilde{x}_{k-1}$ is

$$\dot{\tilde{x}}_{k-1} = F(\tilde{x}_{k-1}) + (B_{k-1} \otimes P)\tilde{x}_{k-1} + (B_{k-1,k} \otimes P)\tilde{x}_k \, . \quad (6.25)$$

For the component $\mathbb{C}_k$, we obtain a lower bound of the coupling strength d_k to synchronize the oscillators in (6.24) by GCGM. Suppose $x_s \in \mathbb{R}^d$ is the synchronous state for the oscillators in (6.24), and then the dynamics for x_s can be described by

$$\dot{x}_s = f(x_s) + \phi_s(t) \, , \quad (6.26)$$

where $\phi_s(t) \to \mathbf{0}$ as $t \to \infty$. Let $\mathbf{1}$ be the column vector of all ones with a proper dimension. Then we have $(\tilde{x}_k - \mathbf{1} \otimes x_s) \to \mathbf{0}$ as $t \to \infty$. Let $\phi_k(t) \triangleq (B_{k-1,k} \otimes P)(\tilde{x}_k - \mathbf{1} \otimes x_s)$. Then (6.25) can be rewritten as

$$\begin{aligned} \dot{\tilde{x}}_{k-1} = {} & F(\tilde{x}_{k-1}) + (B_{k-1} \otimes P)\tilde{x}_{k-1} \\ & + (B_{k-1,k} \otimes P)(\mathbf{1} \otimes x_s) + \phi_k(t) \, , \end{aligned} \quad (6.27)$$

where $\phi_k(t)$ satisfies $\lim_{t\to\infty} \phi_k(t) = \mathbf{0}$.
Now we replace all those vertices in $\mathbb{C}_k$ by a single vertex 0 and collect their dynamics into that of a single system whose state is x_s. Keeping the edges between $\mathbb{C}_k$ and $\mathbb{C}_{k-1}$, we arrive at a condensed component $\tilde{\mathbb{C}}_{k-1}$ whose vertex set consists of the vertex 0 and the vertices in the component $\mathbb{C}_{k-1}$. The dynamics of the condensed component $\tilde{\mathbb{C}}_{k-1}$ are described by (6.26) and

$$\dot{\tilde{x}}_{k-1} = F(\tilde{x}_{k-1}) + (B_{k-1} \otimes P)\tilde{x}_{k-1} + (B_{k-1,k} \otimes P)(\mathbf{1} \otimes x_s) \, . \quad (6.28)$$

According to the graph decomposition, there are edge(s) from the vertex 0 to the vertices in $\mathbb{C}_{k-1}$, but no edge in the opposite direction. Thus, the states of the oscillators in $\tilde{\mathbb{C}}_{k-1}$ will synchronize to x_s if the coupling strengths in $\tilde{\mathbb{C}}_{k-1}$ are big enough.

For the component $\tilde{\mathbb{C}}_{k-1}$, we can obtain a lower bound of coupling strength d_{k-1} by GCGM such that the oscillators in $\tilde{\mathbb{C}}_{k-1}$ synchronize. From the subsection 6.4.1, such coupling strength condition for graph $\tilde{\mathbb{C}}_{k-1}$ guarantees that $L_{\mathbb{K}} L_{\tilde{\mathbb{C}}_{k-1}} > aL_{\mathbb{K}}$, where $\mathbb{K}$ is the complete graph with the same vertex set of graph $\tilde{\mathbb{C}}_{k-1}$, which further guarantees that (6.2) in Lemma 6.1 holds. In addition, we have shown that $\lim_{t\to\infty} \phi_k(t) = \mathbf{0}$. Hence we are ready to use Theorem 4.4 in (Wu 2007). From it, one has that the oscillators coupled by the dynamics (6.26) and (6.27) synchronize; to be more specific, the states of those oscillators asymptotically converge to x_s. Now we can replace all those vertices in $\mathbb{C}_{k-1}, \mathbb{C}_k$ by a single vertex 0 and collect their dynamics into that of a single system whose state is x_s.
Then, we repeat the same operations for the components $\mathbb{C}_i$ for $i = k-2, \ldots, 1$ in descending order. We treat $\mathbb{C}_i$ one by one, replace all those vertices in $\mathbb{C}_{i+1}, \ldots, \mathbb{C}_k$, by a single vertex 0, and keep the edges between $\mathbb{C}_i$ and $\mathbb{C}_{i+1}, \ldots, \mathbb{C}_k$. Thus we arrive at a condensed component $\tilde{\mathbb{C}}_i$ whose vertex set consists of the vertex 0 and the vertices in $\mathbb{C}_i$. Using the GCGM algorithm to obtain a lower bound for the coupling strength d_i for synchronization in $\tilde{\mathbb{C}}_i$, we guarantee that the states of the oscillators in $\tilde{\mathbb{C}}_i$ asymptotically synchronize to x_s.
Finally, we get all the lower bounds $d_k, d_{k-1}, \ldots, d_1$ for the components $\mathbb{C}_k, \tilde{\mathbb{C}}_{k-1}$, $\ldots, \tilde{\mathbb{C}}_1$. Under these coupling strengths, the states of the oscillators of the whole network asymptotically synchronize. □

6.4.3 Numerical simulations

We use an example to show the effectiveness of the algorithm. We consider the directed network on the left of Fig. 6.6. For simplicity, we choose to use an identical coupling strength in the network. We follow all the four steps. First, we decompose $\mathbb{G}$ into $\mathbb{C}_1, \mathbb{C}_2, \mathbb{C}_3, \mathbb{C}_4$ as shown in Fig. 6.6. And thus we have the partial orderings $B_2 \lhd B_3 \lhd B_4$ and $B_1 \lhd B_3 \lhd B_4$. The condensation graph is shown on the right of Fig. 6.6. For $\mathbb{C}_4$, using the GCGM algorithm, we calculate that $d_4 > \frac{3}{2}\, a$. For $\mathbb{C}_3$, we obtain $\tilde{\mathbb{C}}_3$ shown in Fig. 6.7 and use the GCGM algorithm to obtain $d_3 > 3a$. Similarly, we get $d_2 > 3a$ for $\tilde{\mathbb{C}}_2$ and $d_1 > 3a$ for $\tilde{\mathbb{C}}_1$. Finally, taking the maximum over d_1 to d_4 together, we conclude that the global synchronization of the network associated with $\mathbb{G}$ can be realized under the coupling strength $d > 3a$.

6.5 Concluding remarks

In this chapter we have presented new ways to allocate coupling strengths using spectral graph theory in order to achieve synchronization in complex networks. The main idea is to bound the second-smallest eigenvalues of the Laplacian matrices associated with the given networks by comparing the corresponding network graphs to complete or other special graphs with the same vertex sets. The obtained results can simplify the computation and be applied to growing networks. We have also presented algorithms to allocate coupling strengths to achieve synchronization in directed complex networks using graph comparison. By exploiting the symmetrization operation, we have dealt with the challenge that the Laplacian matrices associated with directed graphs are not guaranteed to be positive semi-definite anymore. The obtained algorithms can be applied to large but decomposable networks.

Chapter 7

Conclusions

This final chapter summarizes the main results that have been presented in this thesis and provides recommendations for future research.

7.1 Conclusions

This thesis has discussed cooperative control of complex multi-agent networks facing information constraints. In particular, this thesis has taken into account the information constraints caused by quantized local information, uncertainties and heterogeneities in individual dynamics, and local knowledge on network topologies. The goal of this thesis has been to address the following three important issues in cooperative control: synchronization in multi-agent systems or complex dynamical networks, formation keeping of autonomous mobile agents, and trajectory tracking in complex multi-agent systems.

This thesis has first studied synchronizing a team of multi-agent systems under quantized communications. Chapter 3 has discussed how different quantizers affect the performances of consensus-type schemes for second-order dynamics to achieve synchronized collective motions. The performances of the logarithmic and uniform quantizers have been studied, respectively. Under the logarithmic quantizers and with symmetric neighbor relationships, it has been proven that the agents velocities and positions get synchronized asymptotically. Under the chosen symmetric uniform quantizers and with symmetric neighbor relationships, the agents velocities converge to the same value asymptotically while the differences of their positions converge to a bounded set. Moreover, undesirable system behaviors, e.g., oscillations or unbounded trajectories, may arise when asymmetric uniform quantizers or asymmetric neighbor relationships are adopted.

Chapter 4 has studied formation stabilization for teams of autonomous mobile agents when the agents' range measurements are coarse. A coarsely quantized control scheme based on the classical gradient-based formation-control strategies has

been proposed to stabilize three agents moving in a plane to the desired triangular formations. It has been proven that the expected convergence performance is almost global except the collinear initial positions of the three agents. Different from the existing stability results on triangular formations with precise range measurements, the convergence takes place within finite time and the settling time can be determined by the geometric information of the initial shape of the formation.

Chapter 5 has presented the trajectory tracking and output synchronization in a group of uncertain heterogeneous linear systems. We have tackled the problem of designing decentralized controllers able to track prescribed reference signals generated by exosystems under the restriction that not all the systems can access the information available at the exosystem. Under the assumption that each leader (exosystem) has a directed path to its follower systems, it has been shown that there exist decentralized controllers which achieve the desired regulation task in the presence of large but bounded uncertainties in the systems models.

Chapter 6 has discussed synchronizing a complex dynamical network by utilizing its flexibly topological features. Using spectral graph theory, new methodologies to allocate coupling strengths have been proposed to guarantee complete synchronization in complex networks. The main idea has been to bound the second-smallest eigenvalues of the Laplacian matrices associated with the given networks by comparing the corresponding network graphs to complete or other typical graphs with the same vertex sets. The obtained results can simplify the computation and be applied to growing networks. This chapter has also presented algorithms to allocate coupling strengths to achieve synchronization in directed complex networks using graph comparison. By exploiting the symmetrization operation, we have dealt with the challenge that the Laplacian matrices associated with directed graphs are not guaranteed to be positive semi-definite anymore. The obtained algorithms can be applied to large but decomposable networks.

7.2 Recommendations for future research

We identify three directions for subsequential research.

Consensus under communication constraints. This thesis has dealt with the limited bandwidth that is available for the communications among agents and analyzed quantization effects on cooperative control in multi-agent networks. More communication constraints will be taken into consideration in network models in future research, such as saturation of the transmitted signals, time-delay caused by finite transmission speeds, and random changes in network topologies. In addition, this

thesis has focused on the synchronization or consensus problem, under the condition that all the agents update their states synchronously. However, there might be no such a global clock in real applications. This motivates extending the study in this thesis to the case with asynchronous updates. That is to say, each agent can update its state disregarding other agents' updating times. It is a challenging problem if one considers a combination of different communication constraints.

Different formation patterns under coarse measurements. Chapter 4 has studied the cyclic triangular formations with coarse range measurements. The stabilization of acyclic triangular formations and formations through with angle and range measurements, can be further investigated when one considers limited sensing capabilities of the agents. Those elementary triangular formations will be carefully studied using the proposed schemes with coarse quantization. Based on rigid graph theory in (Krick et al. 2009), those schemes are applicable to larger rigid formations. Besides triangular formations, formation on circles or lines, which are inspired by intelligent transport systems, could be further studied using coarse measurements.

Application issues of synchronization criteria for complex dynamical networks. The current work in this thesis has focused on proposing new methodologies of coupling strength allocations to synchronize a network. It is of interest to use the constructed synchronization criteria to develop optimal or sub-optimal solutions for adding or deleting edges in a network to achieve better synchronizability. It should be further studied to apply the results to practical engineered complex networks, such as the synchronization of generators in electric power grids and data fusion for signal processing in sensor networks. For large scale complex networks, it is complicated to calculate the bounds for coupling strengths from graph comparison. Thus it is appealing to develop more efficient algorithms to perform the calculations. At last, the tools in spectral graph theory might be helpful to understand how the whole eigenvalue spectra of Laplacians affects synchronization behaviors or synchronization processes in dynamical complex networks.

Bibliography

Anderson, B. D. O., Yu, C., Fidan, B. and Hendrickx, J.: 2008, Rigid graph control architectures for autonomous formations, *IEEE Control Systems Magazine* **28**, 48–63.

Arcak, M.: 2007, Passivity as a design tool for group coordination, *IEEE Transactions on Automatic Control* **52**, 1380–1390.

Bacciotti, A. and Ceragioli, F.: 1999, Stability and stabilization of discontinuous systems and nonsmooth liapunov functions, *ESAIM: Control, Optimisation & Calculus of Variations* **4**, 361–376.

Bai, H., Arcak, M. and Wen, J.: 2011, *Cooperative Control Design: A Systematic, Passivity-Based Approach*, Springer, New York.

Bai, H., Arcak, M. and Wen, J. T.: 2009, Adaptive motion coordination: Using relative velocity feedback to track a reference velocity, *Automatica* **45**, 1020–1025.

Belykh, I., Belykh, V. and Hasler, M.: 2006a, Generalized connection graph method for synchronization in asymmetrical networks, *Physica D* **224**, 42–51.

Belykh, I., Belykh, V. and Hasler, M.: 2006b, Synchronization in asymmetrically coupled networks with node balance, *Chaos* **16**, 015102.

Belykh, V. N., Belykh, I. V. and Hasler, M.: 2004, Connection graph stability method for synchronized coupled chaotic systems, *Physica D* **195**, 159–187.

Bertsekas, D. P. and Tsitsiklis, J. N.: 1997, *Parallel and Distributed Computation*, Athena Scientific, Nashua.

Brualdi, R. A. and Ryser, H. J.: 1991, *Combinatorial Matrix Theory*, Cambridge University Press.

Bullo, F., Cortes, J. and Martinez, S.: 2009, *Distributed Control of Robotic Networks*, Princeton University Press, Princeton.

Cao, M. and Morse, A. S.: 2007, Station keeping in the plane with range-only measurements, *Proc. of the 2007 American Control Conference (ACC)*, pp. 5419–5424.

Cao, M. and Morse, A. S.: 2010, Dwell-time switching, *Systems and Control Letters* **59**, 57–65.

Cao, M. and Morse, A. S.: 2011, Maintaining a directed, triangular formation of mobile autonomous agents, *Communications in Information and Systems* **11**, 1–16.

Cao, M., Morse, A. S. and Anderson, B. D. O.: 2008, Reaching a consensus in a dynamically changing environment: A graphical approach, *SIAM Journal on Control and Optimization* **47**, 575–600.

Cao, M., Morse, A. S., Yu, C., Anderson, B. D. O. and Dasgupta, S.: 2007, Controlling a triangular formation of mobile autonomous agents, *Proc. of the 45th IEEE CDC*, pp. 3603–3608.

Cao, M., Yu, C. and Anderson, B. D. O.: 2011, Formation control using range-only measurements, *Automatica* **47**, 776–781.

Carli, R., Bullo, F. and Zampieri, S.: 2010, Quantized average consensus via dynamic coding/decoding schemes, *International Journal of Robust and Nonlinear Control* **20**, 156–175.

Ceragioli, F., De Persis, C. and Frasca, P.: 2011, Discontinuities and hysteresis in quantized average consensus, *Automatica* **47**, 1916–1928.

Chen, G., Lewis, F. L. and Xie, L.: 2011, Finite-time distributed consensus via binary control protocols, *Automatica* **47**, 1962–1968.

Chen, Y., Lü, J., Han, F. and Yu, X.: 2011, On the cluster consensus of discrete-time multi-agent systems, *Systems & Control Letters* **60**, 517–523.

Chung, S. and Slotine, J. E.: 2009, Cooperative robot control and concurrent synchronization of lagrangian systems, *IEEE Transactions on Robotics* **25**, 686–700.

Clarke, F. H.: 1983, *Optimization and Nonsmooth Analysis*, Wiely, New York.

Cortés, J.: 2006, Finite-time convergent gradient flows with applications to network consensus, *Automatica* **42**, 1993–2000.

Cortés, J.: 2008a, Discontinuous dynamical systems, *IEEE Control Systems Magazine* **28**, 36–73.

Cortés, J.: 2008b, Distributed algorithms for reaching consensus on general functions, *Automatica* **44**, 726–737.

Couzin, I. D., Krause, J., Franks, N. R. and Levin, S. A.: 2005, Effective leadership and decision making in animal groups on the move, *Nature* **434**, 513–516.

de Abreu, N. M. M.: 2007, Old and new results on algebraic connectivity of graphs, *Linear Algebra and its Applications* **423**, 53–73.

De Persis, C.: 2011, On the passivity approach to quantized coordination problems, *Proc. of the 50th IEEE Conference on Decision and Control and European Control Conference*, pp. 1086–1091. Full version available at `http://arxiv.org/pdf/1108.4216v2`.

De Persis, C. and Jayawardhana, B.: 2012, Coordination of passive systems under quantized measurements, *SIAM Journal on Control and Optimization* **50(6)**, 3155–3177.

De Persis, C., Liu, H. and Cao, M.: 2010, Control of one-dimensional guided formations using coarsely quantized information, *Proc. of the 49th IEEE Conference on Decision and Control (CDC)*, pp. 2257–2262.

De Persis, C., Liu, H. and Cao, M.: 2012, Robust decentralized output regulation for uncertain heterogeneous systems, *Proc. of 2012 American Control Conference*, pp. 5214–5219.

Dimarogonas, D. V. and Johansson, K. H.: 2010, Stability analysis for multi-agent systems using the incidence matrix: Quantized communication and formation control, *Automatica* **46**, 695–700.

Dong, W.: 2011, On consensus algorithms of multiple uncertain mechanical systems with a reference trajectory, *Automatica* **47**, 2023–2028.

Fink, J., Ribeiro, A. and Kumar, V.: 2013, Robust control of mobility and communications in autonomous robot teams, *Access, IEEE* **1**, 290–309.

Frasca, P., Carli, R., Fagnani, F. and Zampieri, S.: 2009, Average consensus on networks with quantized communication, *International Journal of Robust and Nonlinear Control* **19**, 1787–1816.

Gazi, V.: 2005, Formation control of a multi-agent system using non-linear servomechanism., *International Journal of Control* **78(8)**, 554–565.

Gazi, V. and Passino, K. M.: 2006, Decentralized output regulation of a class of nonlinear systems, *International Journal of Control* **79**, 1512–1522.

Godsil, C. and Royle, G.: 2001, *Algebraic Graph Theory*, Springer-Verlag, New York.

Grocholsky, B., Stump, E., Shiroma, P. M. and Kumar, V.: 2008, Control for localization of targets using range-only sensors, *Experimental Robotics* **39**, 191–200.

Guattery, S., Leighton, T. and Miller, G. L.: 1999, The path resistance method for bounding the smallest nontrivial eigenvalue of a laplacian, *Combinatorics, Probability and Computing* **8**, 441–460.

Guattery, S. and Miller, G. L.: 2000, Graph embeddings and laplacian eigenvalues, *SIAM J. Matrix Anal. Appl.* **21(3)**, 703–723.

Gul, E. and Gazi, V.: 2010, Adaptive internal model based formation control of a class of multi-agent systems, *Proc. of 2010 American Control Conference*, pp. 4800–4805.

Guo, J. H., Su, K. L., Wang, C. C. and Wu, C. J.: 2009, Laser range finder applying in motion control system of mobile robots, *Fourth International Conference on Innovative Computing, Information and Control*, pp. 536–539.

Hegselmann, R. and Krause, U.: 2002, Opinion dynamics and bounded confidence: Models, analysis and simulation, *Journal of Artificial Societies and Social Simulation* **5**, 1–24.

Hokayem, P. F., Stipanovic, D. M. and Spong, M. W.: 2009, Semiautonomous control of multiple networked Lagrangian systems, *International Journal of Robust and Nonlinear Control* **19**, 2040–2055.

Hong, Y., Wang, X. and Jiang, Z. P.: 2011, Distributed output regulation of leader-follower multi-agent systems, *International Journal of Robust and Nonlinear Control* . Published online in Wiley Online Library (wileyonlinelibrary.com). DOI: 10.1002/rnc.1814.

Horn, R. A. and Johnson, C. R.: 1985, *Matrix Analysis*, Cambridge University Press, Cambridge, U.K.

Isidori, A., Marconi, L. and Serrani, A.: 2003, *Robust Autonomous Guidance: An Internal Model Approach (Advances in Industrial Control)*, Springer.

Jadbabaie, A., Lin, J. and Morse, A. S.: 2003, Coordination of groups of mobile autonomous agents using nearest neighbor rules, *IEEE Transactions on Automatic Control* **48**, 985–1001.

Johansson, K. H., Speranzon, A. and Zampieri, S.: 2005, On quantization and communication topologies in multi-vehicle rendezvous, *Proc. of the 16th IFAC World Congress*.

Kahale, N.: 1998, A semidefinite bound for mixing rates of markov chains, *Random structurs and Algorithms* **11**, 299–313.

Kashyap, A., Basar, T. and Srikant, R.: 2007, Quantized consensus, *Automatica* **43**, 1192–1203.

Kim, H., Shim, H. and Seo, J. H.: 2011, Output consensus of heterogeneous uncertain linear multi-agent systems, *IEEE Transactions on Automatic Control* **56**, 200–206.

Krick, L., Broucke, M. E. and Francis, B. A.: 2009, Stabilization of infinitesimally rigid formations of multi-robot networks, *International Journal of Control* **82**, 423–439.

Kumar, V., Leonard, N. E. and Morse, A. S.: 2005, *Cooperative Control*, Springer-Verlag, New York.

Kurths, J., Boccaletti, S., Grebogi, C. and Lai, Y. C.: 2003, Focus issue: Control and synchronization in chaotic dynamical systems, *Chaos* **13**, 126.

Lin, Z., Francis, B. and Brouche, M.: 2004, Local control strategies for groups of mobile autonomous agents, *IEEE Transactions on Automatic Control* **49**, 622–629.

Liu, H., Cao, M. and De Persis, C.: 2011, Quantization effects on synchronization of mobile agents with second-order dynamics, *Proc. of the 18th IFAC World Congress*, pp. 2376–2381.

Liu, H., Cao, M. and De Persis, C.: 2012, Quantization effects on synchronized motion of teams of mobile agents with second-order dynamics, *Systems and Control Letters* **12**, 1157–1167.

Liu, H., Cao, M. and Wu, C. W.: 2013a, Coupling strength allocation for synchronization in complex networks using spectral graph theory, *IEEE Transactions on Circuits and Systems-I, regular paper* .

Liu, H., Cao, M. and Wu, C. W.: 2013b, Graph comparison and its application in network synchronization, *Proc. of the 12th European Control Conference*, pp. 3809–3814.

Liu, H., Cao, M. and Wu, C. W.: 2013c, New spectral graph theoretic conditions for synchronization in directed complex networks, *Proc. of the 2013 IEEE International Symposium on Circuits and Systems*, pp. 2307–2310.

Liu, H., de Marina, H. G. and Cao, M.: n.d., Controlling triangular formation of autonomous agents in finite-time using coarse measurements, *Proc. of 2014 IEEE International Conference on Robotics and Automation*. Submitted.

Liu, H., De Persis, C. and Cao, M.: 2013, Robust decentralized output regulation with single or multiple reference signals for uncertain heterogeneous systems, *International Journal of Robust and Nonlinear Control* .

Liu, H., Lu, J., Lü, J. and Hill, D. J.: 2009, Structure identification of uncertain general complex dynamical networks with time delay, *Automatica* **8**, 1799–1807.

Lü, J., Yu, X. and Chen, G.: 2004, Chaos synchronization of general complex dynamical networks, *Physica A* **334**, 281–302.

Lü, J., Yu, X., Chen, G. and Cheng, D.: 2004, Characterizing the synchronizability of small-world dynamical networks, *IEEE Transactions on circuits and systems-I* **51(4)**, 787–796.

Mei, J., Ren, W. and Ma, G.: 2011, Distributed coordinated tracking with a dynamic leader for multiple Euler-Lagrange systems, *IEEE Transactions on Automatic Control* **56**, 1415–1421.

Mei, S., Zhang, X. and Cao, M.: 2011, *Power Grid Complexity*, Springer-Verlag, Berlin.

Mohar, B.: 1991, Eigenvalues, diameter, and mean distance in graphs, *Graphs and Combinatories* **7**, 53–64.

Mondada, F., Bonani, M., Raemy, X., Pugh, J., Cianci, C., Klaptocz, A., Magnenat, S., Zufferey, J.-C., Floreano, D. and Martinoli, A.: 2009, The e-puck, a robot designed for education in engineering, *Proceedings of the 9th Conference on Autonomous Robot Systems and Competitions*, pp. 59–65.

Moulay, E. and Perruquetti, W.: 2005, Finite time stability of differential inclusions, *IMA Journal of Mathematical Control and Information* **22**, 465–475.

Nedic, A., Olshevsky, A., Ozdaglar, A. and Tsitsiklis, J. N.: 2009, On distributed averaging algorithms and quantization effects, *IEEE Transactions on Automatic Control* **54**, 2506–2517.

Newman, M. E. J.: 2010, *Networks: An introduction*, Oxford University Press.

Nuno, E., Ortega, R., Basanez, L. and Hill, D.: 2011, Synchronization of networks of nonidentical Euler-Lagrange systems with uncertain parameters and communication delays, *IEEE Transactions on Automatic Control* **56**, 935–941.

Olfati-Saber, R., Fax, J. A. and Murray, R. M.: 2007, Consensus and cooperation in networked multi-agent systems, *Proceedings of the IEEE* **95**, 215–233.

Pecora, L. M. and Carroll, T. L.: 1998, Master stability functions for synchronized coupled systems, *Physical Review Letters* **80**, 2019–2112.

Quigley, M., Stavens, D., Coates, A. and Thrun, S.: 2010, Sub-meter indoor localization in unmodified environments with inexpensive sensors, *IEEE/RSJ International Conference on Intelligent Robots and Systems*, pp. 2039–2046.

Rad, A. A., Jalili, M. and Hasler, M.: 2011, A lower bound for algebraic connectivity based on the connection-graph-stability method, *Linear Algebra and its Applications* **435**, 186–192.

Ren, W.: 2008, On consensus algorithms for double-integrator dynamics, *IEEE Transactions on Automatic Control* **53**, 1503–1509.

Ren, W. and Beard, R.: 2008, *Distributed consensus in Multi-Vehicle Cooperative Control*, Springer-Verlag New York, Inc.

Rodriguez-Angeles, A. and Nijmeijer, H.: 2004, Mutual synchronization of robots via estimated state feedback: A cooperative approach, *IEEE Transactions on Control Systems Technology* **12**, 542–554.

Scardovi, L. and Sepulchre, R.: 2009, Synchronization in networks of identical linear systems, *Automatica* **45**, 2557–2562.

Shamma, J.: 2007, *Cooperative control of distributed multi-agent systems*, John Wiley & Sons Inc., England.

Shevitz, D. and Paden, B.: 1994, Lyapunov stability theory of nonsmooth systems, *IEEE Transactions on Automatic Control* **39**, 1910–1914.

Smith, S. L., Broucke, M. E. and Francis, B. A.: 2006, Stabilizing a multi-agent system to an equilibrium polygon formation, *Proc. of the 17th MTNS*, pp. 2415–2424.

Spielman, D. A.: 2004, *Spectral graph theory and its applications*. Lecture Notes. Available online, http://www.cs.yale.edu/homes/spielman/eigs/.

Spielman, D. A.: 2012, Spectral graph theory, *in* U. Naumann and O. Schenk (eds), *Combinatorial Scientific Computing*, CRC Press.

Strogatz, S. H.: 2003, *SYNC: The emerging science of spontaneous order*, Hyperion, New York.

Stump, E., Kumar, V., Grocholsky, B. and Shiroma, P. M.: 2009, Control for localization of targets using range-only sensors, *International Journal of Robotics Research* **28**, 743–757.

Su, Y. and Huang, J.: 2012a, Cooperative output regulation of linear multi-agent systems, *IEEE Transactions on Automatic Control* **57(4)**, 1062–1066.

Su, Y. and Huang, J.: 2012b, Cooperative output regulation of linear multi-agent systems by output feedback, *Systems & Control Letters* **61**, 1248–1253.

Tang, L., Lu, J., Lü, J. and Yu, X.: 2012, Bifurcation analysis of synchronized regions in complex dynamical networks, *International Journal of Bifurcation and Chaos* **22**, 1250282.

Tarjan, R. E.: 1972, Depth-first search and linear graph algorithms, *SIAM Journal on Computing* **1,2**, 146–160.

Turpin, M., Michael, N. and Kumar, V.: 2012, Decentralized formation control with variable shapes for aerial robots, *Proc. of the IEEE Int. Conf. on Robotics and Automation*, pp. 23–30.

Wang, C., Cao, M. and Xie, G.: 2011, Antiphase formation swimming for autonomous robotic fish, *Proc. of the 18th IFAC World Congress*, pp. 7830–7835.

Wang, X. and Chen, G.: 2002, Synchronization in scale-free dynamical networks: Robustness and fragility, *IEEE Transactions on circuits and systems-I* **49**, 54–62.

Wang, X., Hong, Y., Huang, J. and Jiang, Z. P.: 2010, A distributed control approach to a robust output regulation problem for multi-agent linear systems, *IEEE Transactions on Automatic Control* **55**, 2891–2895.

Wieland, P.: 2011, *From static to dynamic couplings in consensus and synchronization among identical and non-identical systems*, Ph.D thesis, University of Stuttgart.

Wieland, P., Sepulchre, R. and Allgower, F.: 2011, An internal model principle is necessary and sufficient for linear output synchronization, *Automatica* **47**, 1068–1074.

Wu, C. W.: 2003, Perturbation of coupling matrices and its effect on the synchronizability in arrays of coupled chaotic systems, *Physics Letters A* **319**, 495–503.

Wu, C. W.: 2007, *Synchronization in complex networks of nonlinear dynamical systems*, World Scientific.

Wu, C. W. and Chua, L. O.: 1994, A unified framework for synchronization and control of dynamical systems, *International Journal of Bifurcation and Chaos* **4**, 979–998.

Wu, C. W. and Chua, L. O.: 1995, Synchronization in an array of linearly coupled dynamical systems, *IEEE Transactions on Circuits and Systems I* **42**, 430–447.

Wu, W., Zhou, W. and Chen, T.: 2009, Cluster synchronization of linearly coupled complex networks under pinning control, *IEEE Transactions on Circuits and Systems I* **56**, 829–839.

Xia, W. and Cao, M.: 2011, Clustering in diffusively coupled networks, *Automatica* **47**, 2395–2405.

You, K. and Xie, L.: 2011, Network topology and communication data rate for consensusability of discrete-time multi-agent systems, *IEEE Transactions on Automatic Control* **56**, 2262–2275.

Yu, W., Chen, G. and Cao, M.: 2010a, Distributed leader-follower flocking control for multi-agent dynamical systems with time-varying vecocities, *Systems & Control Letters* **59**, 543–552.

Yu, W., Chen, G. and Cao, M.: 2010b, Some necessary and sufficient conditions for second-order consensus in multi-agent dynamical systems, *Automatica* **46**, 1089–1095.

Summary

In the past two decades, cooperative control of complex multi-agent networks has been a hot topic in many disciplines, including engineering, biology, social science, and so on. A central topic is to coordinate in a distributed fashion the agents in the whole network only using local information that is available to each agent. The adjustments of each agent's individual behavior in response to their neighbors' may lead to desired collective behaviors at the network level. Along this line, the focus of this thesis is cooperative control of complex multi-agent networks facing information constraints.

We first study how quantized information affects collective behaviors in a network. We study quantization effects on the performances of consensus-type algorithms for second-order multi-agent systems. The performances under the logarithmic and uniform quantizers are investigated. Under the logarithmic quantizers and with symmetric neighbor relationships, it is proven that the agents velocities and positions get synchronized asymptotically. Under the chosen symmetric uniform quantizers and with symmetric neighbor relationships, the agents velocities converge to the same value asymptotically while the differences of their positions converge to a bounded set. Moreover, undesirable system behaviors, e.g., oscillations or unbounded trajectories, may happen when asymmetric uniform quantizers or asymmetric neighbor relationships are adopted.

In addition, we study coarse quantization effects on the performances of the classical gradient-based formation-control strategies for teams of autonomous mobile agents. We focus on the formation problem when the agents' range measurements are coarse. Similar to the existing stability results for triangular formations with precise range measurements, it is proven that under coarse range measurements, the convergence to the desired formation is almost global except for initially collinearly positioned formations. More importantly, we are able to make stronger statements that the convergence takes place within finite time and that the settling time can be

determined by the geometric information of the initial shape of the formation.

We study how to overcome heterogeneities of agents to synchronize a network in which the individuals are associated with different uncertainties. We consider the problem in which multiple coupled agents described by heterogeneous uncertain linear systems aim at tracking one or more reference signals generated by given exosystems. We consider information constraints that not all the agents can get direct access to the exosystems. To tackle this problem, the reference signals are reconstructed via local interaction among the agents themselves and between agents and the exosystems in accordance with the given communication graph. Then decentralized robust controllers that use the reconstructed reference signals are designed and are shown to result in a closed loop tracking the prescribed reference signals.

In the end we study how to allocate coupling strengths for interactions only using local network topological information to guarantee the global synchronization in a network given the pairwise synchronizability of any two coupled agents. Using spectral graph theory, new methodologies to allocate coupling strengths are proposed to guarantee complete synchronization in complex networks. The key step is that all the eigenvalues of the Laplacian matrix associated with a given network can be estimated by flexibly utilizing topological features of the network. The proposed methodologies enable the construction of different coupling-strength combinations in response to different knowledge about sub-networks. We also present algorithms to allocate coupling strengths, using graph comparison, to achieve synchronization in directed complex networks. For large directed networks that can be decomposed into a set of smaller strongly connected components, we apply the methodology at the local level to improve computational efficiency.

Samenvatting

In de afgelopen twee decennia is coöperatief regelen van complexe multi-agent netwerken een actueel onderwerp geweest in veel disciplines, waaronder techniek, biologie, sociale wetenschappen, enzovoort. Het centrale onderwerp is het coördineren van de agenten op een gedistribueerde manier met alleen gebruik makend van informatie dat lokaal beschikbaar is voor elke agent. Aanpassingen van het individuele gedrag van elke agent als reactie op hun buren zou kunnen leiden tot gewenst collectief gedrag op netwerk niveau. Soortgelijk, is de focus van dit proefschrift het coöperatief regelen van complexe multi-agent netwerken met informatie restricties.

We onderzoeken eerst hoe gekwantificeerde informatie het collectieve gedrag in een netwerk beïnvloedt. We bestuderen kwantisatie effecten op de prestaties van consensus-type algoritmes voor tweede-orde multi-agent systemen. De prestaties onder de logaritmische en uniforme kwantisatoren zijn onderzocht. Onder de logaritmische kwantisatoren met symmetrische buurrelaties is het bewezen dat de snelheden en posities van de agenten asymptotisch synchroniseren. Onder de gekozen symmetrische uniforme kwantisatoren en met symmetrische buurrelaties convergeren de snelheden van de agenten asymptotisch naar dezelfde waarde terwijl de verschillen van hun posities convergeren naar een begrensde verzameling. Bovendien kan ongewenst systeemgedrag, zoals oscillaties of onbegrensde trajecten, optreden wanneer asymmetrische uniforme kwantisatoren of asymmetrische buurrelaties worden aangenomen.

Daarnaast bestuderen we grove kwantisatie effecten op de prestaties van de klassieke gradiënt-gebaseerde strategieën voor formatieregeling van teams van autonome mobiele agenten. Wij richten ons op het formatie probleem wanneer de afstandsmetingen van de agenten grof zijn. Vergelijkbaar met de bestaande stabiliteitsresultaten voor driehoekige formaties met precieze afstandsmetingen, is het bewezen dat onder grove afstandsmetingen de convergentie naar de gewenste for-

matie vrijwel globaal is, behalve voor initiële collineaire gepositioneerde formaties. Belangrijker, we zijn in staat sterkere statements te maken dat de convergentie plaatsvindt binnen eindige tijd en dat de convergentietijd bepaald kan worden door de geometrische informatie over de initiële vorm van de formatie.

Verder onderzoeken we hoe we de heterogeniteit van de agenten kunnen overwinnen wanneer we een netwerk synchroniseren waarin de individuen worden geassocieerd met verschillende onzekerheden. We beschouwen het probleem waarbij meerdere gekoppelde agenten, beschreven door heterogene onzeker lineaire systemen, zijn gericht op het volgen van één of meer referentiesignalen gegenereerd door gegeven exogene systemen. We beschouwen de informatie restricties dat niet alle agenten rechtstreeks toegang tot de exogene systemen kunnen krijgen. Om dit probleem aan te pakken zijn de referentiesignalen gereconstrueerd via lokale interactie tussen de agenten onderling en tussen agenten en de exogene systemen in overeenstemming met de gegeven communicatie graaf. Gedecentraliseerde robuuste regelaars die de gereconstrueerde referentiesignalen gebruiken zijn ontworpen en er wordt aangetoond dat ze resulteren in het volgen van de voorgeschreven referentiesignalen in gesloten lus.

Op het einde bestuderen we hoe we de koppelingssterktes kunnen bepalen voor interacties, enkel gebruik makend van topologische informatie van het lokale netwerk, zodat globale synchronisatie gegarandeerd wordt in een netwerk gegeven de paarsgewijze synchronisatie van iedere twee gekoppelde agenten. Met behulp van spectrale grafentheorie zijn nieuwe methodieken voorgesteld om koppelingssterktes te verdelen die volledige synchronisatie garanderen in complexe netwerken. De belangrijkste stap is dat alle eigenwaardes van de Laplaciaanse matrix gekoppeld aan een gegeven netwerk kunnen worden geschat door flexibel gebruik te maken van topologische eigenschappen van het netwerk. De voorgestelde methodiek maakt de constructie van verschillende combinaties van koppelingssterktes mogelijk, afhankelijk van de verschillende kennis over de subnetwerken. We presenteren algoritmes, gebruik makend van graaf vergelijkingen, om koppelingssterktes toe te wijzen die synchronisatie in gerichte complexe netwerken bereiken. Voor grote gerichte netwerken die kunnen worden ontbonden in een verzameling kleinere sterk verbonden componenten passen we de methodiek op lokaal niveau toe om de computationele efficiëntie te verbeteren.